Analysis of spatial dynamics and time delays in epidemic models

By

Muhammad Abdullahi Yau

Thesis submitted for the degree of Doctor of Philosophy

January 2014

Declaration

I hereby declare that this thesis has not been and will not be submitted in whole or in part to another University for the award of any other degree.

Signature:

Muhammad Abdullahi Yau

Dedication

To my father, who pointed the way, and to my mother, who helped me along it.

Acknowledgements

First and foremost, I will like to thank my supervisors Dr. Konstantin Blyuss and Dr. Omar Lakkis for providing me with the conducive atmosphere where this work was carried out, for their patience, assistance and guidance through out this research, and from whom I acquired a great deal of skills and knowledge. Their contributions towards the completion of this thesis are unmeasurable. I will forever remain indebted to them.

To other members of the Sussex faculty including (but not limited to) Drs. Anotida Madzvamuse, Istvan Kiss, Yuliya N. Kyrychko, I thank them for their useful ideas and helps.

Also, I am indebted to my postgraduate colleagues whom include Hussaini Salihu Ndakwo, Oshungade Stephen Ayodele, Rahman Bootan, Aminu Murtala, Abubakar Kagu, Abinbola Abolarinwa, Konstantinos Blazakis, Andy Chung, Elham Khairi, Neofytou Giannis, Maryam Asghar, Oke-Oghene Philomena for their useful comments and friendship.

Finally, to my family, especially my mother and father, wife and daughter, brothers and sisters for providing me with all the support I needed.

Abstract

Reaction-diffusion systems and delay differential equations have been extensively used over the years to model and study the dynamics of infectious diseases. In this thesis we consider two aspects of disease dynamics: spatial dynamics in a reaction-diffusion epidemic model with nonlinear incidence rate, and a delayed epidemic model with combined effects of latency and temporary immunity. The first part of the thesis is devoted to the analysis of stability and pattern formation in an SIS-type epidemic model with nonlinear incidence rate. By considering the dynamics without spatial component, conditions for local asymptotic stability are obtained for general values of the powers of nonlinearity. We prove positivity, boundedness, invariant principle and permanence of our model. The next generation matrix method is used to derive the corresponding basic reproductive number $\mathcal{R}_0$, and the Routh-Hurwitz criterion is used to show that for $\mathcal{R}_0 \leq 1$, the disease-free equilibrium is found to be locally asymptotically stable, for $\mathcal{R}_0 > 1$, a unique endemic steady state exists and is found to be locally asymptotically stable. In the presence of diffusion, Turing instability conditions are established in terms of system parameters. Numerical simulations are performed to identify the spatial regions for spots, stripes and labyrinthine patterns in the parameter space. Numerical simulations show that the system has complex and rich dynamics and can exhibit complex patterns, depending on the recovery rate r and the transmission rate β. We have discovered that whenever the transmission rate exceeds the recovery rate the system exhibits stripe patterns which correspond to a disease outbreak, and in the opposite case the system settles on spot patterns which imply the absence of disease outbreaks. Also, we find that increasing the power q can lead to epidemic outbreak even at lower values

of the transmission rate β. All numerical simulations use an Implicit-Explicit (IMEX) Euler's method, which computes diffusion terms in Fourier space and reaction terms in the real space. Numerical approximation of the model is benchmarked to prove stability of the numerical scheme, and the method is shown to converge with the correct order. Experimental order of convergence (EOC) and estimates for the error in both L^2, H^1 and maximum norms have also been computed. Also, we compare our results to those on infectious diseases and our model shows good predictions.

In the second part of this thesis, we derive and analyse a delayed SIR model with bilinear incidence rate and two time delays which represent latency τ_1 and temporary immunity τ_2 periods. We prove both local and global stability of the system equilibria in the case when there are no time delays, i.e. both the latency and temporary immunity periods are set to zero. For the case when there is only latency ($\tau_1 > 1, \tau_2 = 0$) and the case when the two time delays are identical ($\tau_1 = \tau_2 = \tau$), we show that the endemic steady state is always stable for any parameter values. For the case when there is only temporary immunity ($\tau_2 > 0, \tau_1 = 0$) and the case when there are both latency and temporary immunity in the system ($\tau_1 > 0, \tau_2 > 0$), we prove the existence of periodic solutions arising from the Hopf bifurcation. The endemic steady state undergoes Hopf bifurcation giving rise to stable periodic solutions. For the last two cases, we show interesting regions of (in)stability of the endemic steady state in the different parameter regimes. We find that by varying the transmission rate β, the natural death rate γ and the disease-induced death rate μ increase the regions of (in)stability. Also, we find that the dynamics of the system is richer when we have the two time delays in the model. Analytical results are supported by extensive numerical simulations, illustrating temporal behaviour of the system in different dynamical regimes. Finally, we relate our results to modelling infectious diseases and our results show good predictions of safety and epidemic outbreak.

Contents

List of Tables

List of Figures

Chapter 1

Introduction

Mathematical models have been extensively used to study the dynamics of epidemics and diseases. They aim to capture the major factors that are responsible for the progression of diseases, and can forecast how diseases spread in both time and space. Infectious diseases affect human in many ways, causing significant health problems and loss of life to millions of people annually. Since the pioneering work of Kermack and McKendrick [ker27], epidemic models have been employed for studying the spread and control of infectious diseases both qualitatively and quantitatively. This was stimulated by the early work by Ross [Ros11] on malaria. The research results obtained from these models are useful in predicting how infectious diseases develop and spread in their ecological environment. Also, they help determine the factors responsible for epidemics spread and to develop the best strategies of controlling and preventing the spread of infectious diseases [Wei12], [Ma09]. This thesis focuses on two areas of mathematical epidemiology; the first part deals with pattern formation and the spatial aspect of disease spread. The second part is concerned with the interaction between latency and temporary immunity.

Analytical and numerical studies of ODE models in epidemiology have uncovered a number of interesting dynamical patterns including stable steady states, limit cycles and chaos [Ma09], [Wei12]. The aim of epidemic models is to quantify the interactions between and within species and their ecological environment, and to investigate the temporal

changes of cohorts of individuals. It is important to note that the environmental factors and species distributions in ODE models are assumed to be homogeneous. In many epidemic models, all processes are assumed to take place instantaneously and uniformly in space. However, inclusion of spatial diffusion is known to provide a more realistic description of the spread of epidemics [Oku01].

Mathematical models can be used as tools to analyse how infectious diseases spread, and also to develop appropriate control measures. We know that individual populations are distributed in space and interact in their spatial environment with other populations. It has been established for long that the spatial component of the ecosystem is an important factor in determining how the ecosystem is functioning and shaped, but still understanding the role the space plays in the ecological communities is very challenging empirically and also theoretically. Many researchers have emphasised the need to include the spatial component when formulating realistic mathematical models of biological systems.

In the last two decades significant progress has been made in studying and understanding different mechanisms for epidemic spread and control. A large number of existing mathematical models of epidemics are based on ODEs which do not take into account time lags. However, including time lags explicitly in the models allows one to make them more practical and more realistic. The spread of infectious diseases is characterised by a number of factors including the mode of transmission, infectious agents, infectious periods, incubation periods, resistance, and susceptibility [Tak10]. Including time delays in the models provides a way to capture the effects of these factors (temporary immunity, latent, incubation periods e.t.c), [Col07], [Col06], [Yon09], [Zha10], [Kyr05], [Yan93], [Wei11].

The inclusion of spatial dynamics and time delays in epidemic models makes them more challenging both analytically and numerically. But, the addition of these components makes these models more realistic. Therefore, the need to include space and time delays in modelling infectious diseases is very important even though it makes the analysis more complicated. Unlike ODE models, when one considers delay differential

equation (DDE) models, linearisation about steady states result in a transcendental or quasi-polynomial characteristic equations which are difficult to analyse. However, these two components (space and time delays) of the ecological system cannot be ignored because of their roles in epidemics spread and control. Therefore, for the epidemic models to be more realistic and to capture the underlying ecological and biological processes, space and/or time delays must be included in the models formulation.

These and some other challenges stimulated me to propose two mathematical models of infectious diseases: a spatial SIS epidemic model and a delayed SIR epidemic model. These models will be analysed both analytically and numerically and to study the stability and different types of dynamical behaviour depending on model parameters. I will also discuss the implications of the analysis of these models for understanding of the epidemic spread and control.

1.1 Literature review

In this section we review some related literature to our work and present some of the methodologies and results from previous works. In the past two decades, significant progress has been made in the studies of disease transmission and control using epidemic models. Mathematical models are currently being used to project how infectious diseases progress in both time and space to show the possibility of a likely outcome of an epidemic, and are also used to better inform public health interventions. Epidemic models rely on some basic assumptions to identify the most important parameters for various infectious diseases, and these parameters are used to determine the effects of possible interventions. These models ranges from ODEs and DDEs to PDEs, deterministic to stochastic, discrete to continuum. The choice of what type of model to be used depends on the nature of the problem. Here, we review only some of these models that are related to the models we will derive and analyse in this thesis.

1.1.1 SIR epidemic models

Kermack and McKendrick [ker27], the pioneers in the studies of epidemic models, derived the simple classical SIR model in 1927. Their work was stimulated by the earlier work of Ross [Ros11]. They used this model to predict temporal dynamics of the spread of infectious diseases. Since that early work the epidemic models have been studied extensively by many researchers. In this section, we present some mathematical models, in particular, the SIS and SIR epidemic models. These models can be found in biomathematics and epidemiology. Their applications in studying disease transmission and control have received significant attention and have been applied in a number of distinct contexts.

The SIR model can be written.

$$\begin{aligned} \frac{dS}{dt} &= -\beta SI, \\ \frac{dI}{dt} &= \beta SI - \gamma I, \\ \frac{dR}{dt} &= \gamma I, \end{aligned}$$

where β is the transmission rate, γ is the natural clearance or death rate.

If one assumes that individuals give birth at a rate b, and all individuals die from natural death at a rate μ, then we obtain the following modified model.

$$\begin{aligned} \frac{dS}{dt} &= bN - \beta SI - \mu S, \\ \frac{dI}{dt} &= \beta SI - \gamma I - \mu I, \\ \frac{dR}{dt} &= \gamma I - \mu R. \end{aligned}$$

SIR epidemic models with diffusion (or the reaction-diffusion epidemic models) are derived from the standard epidemic models by assuming that the individual populations can move in space. This means that individuals are spatially distributed and interact in their physical environment. Adding diffusion to the three equations of the above SIR

model gives the following SIR reaction-diffusion system:

$$\begin{aligned}\frac{\partial S}{\partial t} &= d_1\nabla^2 S - \beta SI + \mu(N-S),\\ \frac{\partial I}{\partial t} &= d_2\nabla^2 I + \beta SI - \gamma I - \mu I,\\ \frac{\partial R}{\partial t} &= d_3\nabla^2 R + \gamma I - \mu R,\end{aligned}$$

where $d_1,\ d_2,\ d_3$ are the diffusion rates for the susceptible, infected and recovered individuals respectively.

Recently, many researchers showed that spatial epidemic models are appropriate tools for studying the fundamental mechanism of complex spatiotemporal epidemic dynamics. Space play an important role in determining how populations live and interact in their physical environment, [Oku01],[Neu01],[Mur03],[Hol94]. The importance of adding spatial component in deriving more realistic mathematical models of infectious disease has also been recently recognised [Ras03]. A number of papers, for instance, [Hos95], [Cru99], [Fer01], [Gre01], [He03], [Llo04], [Bal04], [Fil04], [Fun05], [Pas05], [Fes07], [Mul07], [Hil07], [Wan07], [Wan08], [Wan09], [Mal08] and references therein, showed that spatial epidemic models are more appropriate for studying the fundamental spatiotemporal mechanism of epidemic dynamics.

Sun (2012) [Sun12(a)] considered pattern formation in an epidemic model with diffusion and nonlinear incidence rate of the form $\beta S^p I^q$ with $p = 1$ and $q = 2$. He found the conditions for period dynamics and Turing instability. Numerically, he showed that the transmission rate β played an important role in the spatial pattern formation, more specifically, different spatial patterns emerge as β increases. In another paper, Sun et al (2012) [Sun12(b)] considered a Holling-Tanner predator-prey model with cross-diffusion which means the prey individuals have self-defence mechanism to protect them from the attack of the predator. They obtained conditions on parameters that give rise to Hopf and Turing bifurcations. Their numerical experiments revealed that typical dynamics of population density variation is the formation of isolated groups, such as spot, stripe-like, or labyrinthine patterns. Also, they confirmed that cross-diffusion can lead to station-

ary patterns, which can enrich the finding of pattern formation in a typical ecosystem. Weiming et al (2012) [Wei12] have studied complex dynamics of an SI reaction-diffusion epidemic model incorporating epidemiological processes and demography. They used Lyapunov approach to establish the stability of the steady states in the model and also derived Turing instability conditions and identified Turing space depending on system parameters. This system has been demonstrated to have rich dynamics of patterns.

Hosono et al [Hos95] proved the existence of travelling waves in an SI epidemic model. Cruickshank et al in [Cru99] derived a highly efficient numerical method for finding the principal characteristics for spatial invasions described by the reaction-diffusion epidemic model and the dynamics included the Allee effect. Ferguson et al in [Fer01] the authors derived and analysed a model of a foot-and-mouth disease in the UK within the first two months of the outbreak. They studied the pathogen's net transmission potential and estimated the increasing impact of control measures over the course of the epidemic outbreak. Grenfell et al in [Gre01] reported recurrent epidemic travelling waves for measles in an exhaustive spatiotemporal data set in the UK. Filipe et al in [Fil04] used numerical simulations to study the effects of spatial dispersal mechanisms on the spatio-temporal of disease dynamics using a stochastic SI epidemic model. Mulone et al in [Mul07], they derived an SIR epidemic model with diffusion of individuals influenced by the effect of intraspecific competition pressure. Wang et al [Wan07], [Wan08], and Xu et al in [Xu09] investigated the complex dynamics of a spatial HBV model.

The study of pattern formation in spatial epidemic models has intensified over the past two decades. Turing's original work [Tur52] demonstrated that passive diffusion can interact with the chemical reaction in such a manner that even when the reaction itself has no symmetry breaking capabilities, the diffusion could destabilise the symmetry and the system with diffusion can be driven unstable. Liu and Jin [Liu06] studied the effects of population diffusion on the formation of spatial patterns from Turing mechanisms. They found striking formation of spot patterns in the process. In a modified version of this model, Sun et al [Sun07] considered a spatial SIS epidemic model and nonlinear incidence rate, they obtained spots, stripes and stripe-spot patterns. Jin et al in [Jin08] investigated

how population diffusion can affect the formation of the spatial patterns in the spatial epidemic model using Turing mechanisms. Li et al in [Li08] proved that chaotic patterns can also be found in epidemic models. Cai et al [Cai11] studied a reaction-diffusion epidemic model and proved that the model behaviour has diffusion-controlled pattern formation. They found spots, stripes, spots-stripes, spots-holes, stripes-holes and pattern replication. Also, they showed that as the diffusion of the infected individuals increases, the rate of the disease spread also increases. Bendahmane et al [Ben11] presented global existence of solutions of a reaction-diffusion epidemic model and showed by numerical computations the Turing patterns.

Spatial modelling today is an active research area aimed at understanding disease transmission in space [Wei12]. We want to use spatial epidemic models to investigate the dynamical behaviour of complex physical systems with relation to epidemic spread [Sun07]. In modelling the dynamics of infectious diseases a particular important role is played by correct identification of the precise mechanism for a disease transmission [Liu06].

1.1.2 Delay SIR models

Almost all systems that involve a feedback control result in time delays. Time delays occur due to the fact that in some systems a finite time is needed to obtain information and to take action. One example of time delays is observed when a pilot tries to control their aircraft by operating many functions at the same time which can result in what is known as pilot-induced oscillations (PIO) [Tho09]. Models of many physical systems are based on the assumption that all processes take place instantaneously. This means the present and future states of these systems do not depend on their past histories. In reality, however, this assumption can be violated. A more realistic approach is to add some of the past history of the system in the models [Yan93]. The best way to model such processes is by incorporating time delays into the models. The DDE systems differ from the ODE systems because the evolution of a state variable in the present and in the future depends not only on the current value but also on past history. In the past two

decades, there have been a huge increase in the applications of DDE models in physics, engineering, epidemiology and biology [Tho09].

Minorsky in 1942 [Min42] was the first to study DDE in the contexts of stabilisation and automatic steering ships. He pointed out the need to add delays in the feedback control mechanism. His idea stimulated interest in problems with times delays and provided a Major contribution to the theory of differential equations that depend on their past history [Yan93]. Solutions of DDEs are determined by the initial conditions that have to be specified on an interval which has the same length as the time delay. This means, one is required to set an infinite dimensional initial states $t \in [t_0 - \tau, t_0]$. Therefore, DDEs are infinite dimensional systems even for a single linear DDE [Tho09].

Delay differential equations (DDEs) are almost identical in appearance to ordinary differential equations (ODEs), however, they have many characteristic features that make their analysis very challenging. To highlight some of the features we consider as an example a DDE of the form:

$$\dot{\nu}(t) = f(\nu(t), \nu(t-\tau)). \tag{1.1}$$

For ODE systems, a unique solution is found by an initial point in the Euclidean space at a start time t_0. On the other hand, for a DDE system, we need more information on the whole domain $[t_0 - \tau, t_0]$. Therefore, to find the derivative at time t_0, we require $\nu(t_0)$, $\nu(t_0 - \tau)$, and for $\nu(t_0 + \epsilon)$, we require to have $\nu(t_0 + \epsilon)$ and $\nu(t_0 + \epsilon - \tau)$. That is, for the initial value problem to be meaningful, we require to have an initial data or previous history, the value of $\nu(t)$ for the interval $[t_0 - \tau, t_0]$. For every choice of past history, one can find a unique solution for the DDE. If we require the initial data to be continuous, this means the space of the solutions have the same dimension as $C([t_0 - \tau, t_0], \mathbb{R})$, that is, we will have an infinite-dimensional space. The infinite-dimensional nature of DDEs is noticeable in the study of linear systems. For ODE systems, looking for exponential solutions, leads to polynomial equations. On the other hand, for DDE systems, the

characteristic equation, takes the form of a transcendental polynomial

$$\mathcal{P}_0(\lambda) + \mathcal{P}_1(\lambda)e^{-\lambda\tau} = 0, \tag{1.2}$$

where $\mathcal{P}_0$ and $\mathcal{P}_1$ are both polynomials in λ. The transcendental equation 1.2 has infinitely many solutions, corresponding to an infinite family of independent solutions to the linear differential equation [Els73]. Therefore, linear stability analysis for these differential equations is more difficult.

Now we discuss how the location of the roots of the transcendental characteristic equation is related to the behaviour of solutions of the associated linear system. In particular, we shall show the equivalence between the stability of the zero solution and the location of all polynomial roots in the right complex half-plane. Consider a first-order DDE as follows:

$$\dot{\nu}(t) = \sum_{j=1}^{m} B_j \nu(t - \tau_j), \tag{1.3}$$

where B_j is an $n \times n$ constant matrix for all j, and $0 \leq \tau_j \leq \tau$ for all j and some fixed τ. Note that, higher-order linear systems are equivalent to 1.3 by adding more dummy variables. The characteristic equation has the form

$$\det\left(\lambda I - \sum_{j=1}^{m} B_j e^{-\lambda\tau_j}\right) = 0. \tag{1.4}$$

We state and sketch the proof of the following results from [Dri70], [Jon05]

Theorem 1.1 *If ρ is any real number, the characteristic equation 1.4 has at most a finite number of roots λ such that $Re(\lambda) \geq \rho$.*

Proof:

Note that equation 1.4 has the form

$$\lambda^n + p_{n-1}(e^{-\lambda\tau_1}, ..., e^{-\lambda\tau_m}) + ... + p_0(e^{-\lambda\tau_1}, ..., e^{-\lambda\tau_m}) = 0, \tag{1.5}$$

where each of the $p_{n-1}, ..., p_0$ is a polynomial in $e^{-\lambda\tau_1}, ..., e^{-\lambda\tau_m}$.
Now let ρ be a given real number and assume $Re(\lambda) \geq \rho$. Then

$$|e^{-\lambda\tau_j}| = e^{-Re(\lambda)\tau_j} \leq e^{-\rho\lambda\tau_j}, \tag{1.6}$$

so that

$$|p_k(e^{-\lambda\tau_1}, ..., e^{-\lambda\tau_m})| \leq A_k \tag{1.7}$$

for some constant A_k (depending on ρ) for $k = 0, ..., n-1$.
Next we choose a positive number R so large that

$$\frac{A_{n-1}}{R} + ... + \frac{A_0}{R^n} < 1. \tag{1.8}$$

Equation 1.5 can have no roots with $Re(\lambda) \geq 0$ and $|\lambda| \geq R$, since then we can have

$$|\lambda|^n > A_{n-1}|\lambda|^{n-1} + ... + A_0, \tag{1.9}$$

contradicting 1.5. So all roots with $Re(\lambda) \geq \rho$ must have $|\lambda| < R$. But an analytical function which is not identically zero cannot have more than a finite number of zeros in any bounded set in the complex plane. Hence, equation 1.5 cannot have infinitely many roots with $Re\lambda \geq \rho$. ■

Theorem 1.2 *If $Re(\lambda) < \rho$ for every solution of the characteristic polynomial 1.4, there exists a positive constant M, such that for each $\phi \in C([t_0 - r, t_0], \mathbb{R})$, the solutions of 1.3 satisfy*

$$||x(t;\phi)|| \leq M||\phi||e^{\rho(t-t_0)}. \tag{1.10}$$

This means that the behaviour of linear DDEs has an upper bound by the location of the root with the largest real part. From the above two theorems, one can derive the

following lemma, which forms the basis for our linear stability analysis.

Lemma 1.1 *If $Re(\lambda) < 0$ for every solution of the characteristic polynomial 1.4, there exist positive constants M, γ, such that for each $\phi \in C([t_0 - r, t_0], \mathbb{R})$, the solutions of 1.3 satisfy*

$$||x(t;\phi)|| \leq M||\phi||e^{-\gamma(t-t_0)}. \tag{1.11}$$

In other words, if all of the eigenvalues have negative real part, then solutions to the linear delay differential equation decay exponentially to 0, exactly as is the case of ordinary differential equations [Jon05].

In recent years, the use of delay differential equations to model infectious diseases has greatly increased. Hethcote and Van den Driessche [Het95] considered a delayed SIS epidemic model with varying population size. The delay in their model represents infectious period. They proved the existence of periodic solutions arising from a Hopf bifurcation of an endemic steady state for certain parameter values. Beretta et al [Ber01] considered the global stability for an SIR epidemic model with time delay that accounts for a period of times after which individuals can lose their infectiousness. To prove global stability of both the trivial and non-trivial steady states the authors used the Lyapunov method. Arino et al [Ari04] considered a delayed epidemic model with vaccine, whose effectiveness wanes with time according to a general distribution function. They proved the existence of backward bifurcation and multi-stability for certain parameter values, with an important implication for the design of cost-effective vaccination policies. Cooke et al [Coo99] found stability switches from stable to unstable back to stable as τ increases from zero. More recently Beretta et al [Ber02] gave a detailed analysis of delayed models with the time delay incorporated in the coefficients. Detailed analysis of epidemic models with time delay models can be found in for instance, Arino and van den Driessche (2006) [Ari06], see also references therein.

Many authors have considered stability boundaries and identified regions of stability for epidemic models with time delays. For analysis of scalar systems with two time delays

see Hale and Huang [Hal93] and references therein. Gu and Niculescu [Gu05] considered a geometric approach of analysis of a two time delay problem. Louisell [Lou01] investigated a multi-dimensional system with a single time delay. Also, Chen et al [Che95] studied the stability region for the case of commensurate delays that is, when the time delays are integer multiples of each other. Niculescu et al [Nic05] extended Chen's idea by deriving a method of obtaining the stability switching direction. There is a considerable number of papers devoted to finding the conservative bounds of the stability region, for instance a detailed description was presented in Niculescu [Nic01] and also in Gu et al [Gu03] with detailed descriptions of the methods of stability analysis for such systems.

Several authors have analysed the stability and bifurcation for delayed SIR epidemic models with discrete and/or distributed delays. For stability and bifurcation analysis for models with discrete delays, see for instance [Takeuchi et al [Tak10], Wei et al [Wei08], Cooke et al [Coo82], [Coo97]]. For models with distributed delays see [[Rua04], [Zhu07], [Coo82]]. For global stability of SIR models with delays using Lyapunov function approach see for instance [Cruz [Cru09], Enatsu [Ena12], Hale et al [Hal93]]. Time delays in epidemic models can represent temporary immunity [Kyrychko et al [Kyr05], Blyuss et al [Bly10]], latent or infectious periods [Zha10]], and Takeuchi et al [[Tak10]]. For models with delay and diffusion see for instance, Weiming et al [[Wei11]] and references therein. Finally, some work has been done on models with two time delays see [Cooke et al [Coo96], Ruan et al [Rua01], [Rua99], Gu et al [Gu05]] and for models with multiple delays see [Gu et al [Gu03], Ruan et al [Rua04]] for instance.

1.2 Error analysis

Numerical approximations of mathematical models of physical and biological phenomena often have to rely on some kind of discretisation. For instance, in finite difference schemes, the differential equations are approximated by difference equations, and these difference equations cannot solve the original problem exactly, that is the discrete solutions will always come with errors from the discretisation process. Therefore, numerical

solutions of mathematical models are subject to uncertainties, and hence it is important to understand these errors and how to analyse them. It may never be possible to approximate these models exactly, as no matter how small the errors are made, they are always there. In order to draw valid conclusions about numerical approximation of a model, the error must be indicated and properly taken into account.

Error analysis is an important aspect of numerical analysis of differential equations. It provides means to study how far the discrete solution deviates from the exact solution. We know that as the error gets smaller, that is, as the difference of the discrete and exact solutions tend to zero then, the approximate solution converges to the exact solution. Comparing the discrete solution with a known exact solution, one can then tell whether the method used in the numerical computation converges or not, thus indicating whether the numerical method actually solves the problem at hand. From the magnitude of the error it is possible to tell if there is a need to improve the regularity of the discrete solution.

It is, therefore, imperative to understand the behaviour of the error of numerical approximation to see how far is discrete solutions from the exact solutions of the models we will be analysing. When the system is expected to reach a spatially inhomogeneous steady state, a suitable stopping criterion can be chosen to be a measure of the error (e_h) from the exact solution which is given by

$$e_h = |u_h - \Xi| \leq \epsilon \tag{1.12}$$

for some small number ϵ, where u_h is the approximate solution, Ξ is the exact solution and h is the timestep. We compute the experimental order of convergence (EOC) by the formula

$$\text{EOC} \approx \frac{\log e(h_j) - \log e(h_{j-1})}{\log(h_j) - \log(h_{j-1})}, \tag{1.13}$$

where $j = 2, 3, ..., N$ is the time loop.

The EOC is important because it tells whether the method converges with correct order

or not. Also, it tells how correctly the method used has solved the problem under consideration. There are no known analytical or closed form solutions to the system we will study in this thesis. Therefore, it is not possible to check directly how well our numerical experiments compare with the exact solutions. So, we need to construct a solution that will satisfy a modified version of the original system we will study from which we can indirectly check the stability and performance of our numerical methods and the code itself. We will compute the error in various norms, including the L^2, H^1 and the maximum norms. Computing the error in various norms will give more insights into the behaviour of the error and how close the discrete solution is to the true solution. This will allow us to draw conclusions on the stability and convergence of our method and how good the discrete solution is. The various errors are defined as follows: the error in L^2 norm is given by:

$$L^2 = \sqrt{\sum_j |e_j|^2}, \tag{1.14}$$

the error in H^1 norm is:

$$H^1 = \sqrt{\sum_j |\nabla e_j|^2 + \sum_j |e_j|^2}, \tag{1.15}$$

and for the error in L^∞ norm we have thus:

$$L^\infty = \max_j |e_j|. \tag{1.16}$$

We will be using these quantities in Chapter 3 to show the stability and convergence of our numerical methods.

1.3 Motivation

The motivation behind this research lies in the challenges facing epidemiologists and medical personnel today in our societies. The increasing complexity of dynamics of

diseases transmission poses a challenge to both medics and mathematicians. The need for new models and methods that capture different scenarios are continuously growing. Pattern formation due to diffusion-driven instability provides one possible way to explain the spread and control of epidemics. Also, temporal delays are inherent in most of these problems. Adding time delays explicitly in the models is often a way of simplification or idealisation that is introduced because in most cases a detailed description of the underlying processes may be too complicated to be modelled mathematically , and in some cases the details of the underlying epidemiological processes are unknown [Coo82]. The research in this thesis addresses the following two major themes:

- Analysis of spatio-temporal dynamics in an SIS model with nonlinear incidence rate
- Study of the interactions between latency and temporary immunity as modelled by time delays.

The significant of the results from this research are many, for instance the results can be used to better understand the effects of space and time delays in disease spread, the results can be used to identify areas of safety and areas of epidemic outbreak etc.

1.4 Thesis outline

We consider a spatial pattern formation on the example of an SIS reaction-diffusion model with nonlinear incidence rate and spatial diffusion. First, we analyse the stability of disease-free and the endemic equilibrium states of the model, and then derive the general conditions for Turing instability. Numerical experiments are performed to illustrate how these patterns evolve over time with random initial perturbations around the steady states as the disease transmission rate is varied. In the numerical computations, we will use a fast and reliable method called the Implicit-Explicit (IMEX) method. We will derive a delayed SIR epidemic model with two time delays representing latency and temporary immunity. For this time-delayed model, we are interested in periodic solutions from a

Hopf bifurcation when the time delays are varied.

Chapters 2 and 3 are based on the following paper:

- K. Blyuss, and M.A Yau (2014) *Pattern formation in epidemic models*

This draft of this paper is ready to be sent for publication.

Chapter 4 is based on the paper:

- K. Blyuss, and M.A Yau (2014) *Stability and bifurcation analysis in a SIRS epidemic model with two time delays*

whose draft is also ready to be sent for publication.

Chapter 2 : This chapter is concerned with stability and bifurcation analysis for the non-spatial SIS model. The chapter starts with a brief introduction to linear stability analysis and summary of the chapter. In section 2.1, we derive the non-spatial SIS model with nonlinear incidence rate. Section 2.2 presents stability and bifurcation analysis for the system equilibria. In subsection 2.2.1, we find the threshold conditions for the steady states of the system. In section 2.2.2, we present the basic reproduction ratio $\mathcal{R}_0$ and derive and explicit expression for $\mathcal{R}_0$ using the famous *next generation method*. Subsections 2.2.3 and 2.2.4 present the stability analysis of the disease free and the endemic steady state solutions respectively. Section 2.3 presents some numerical simulations in one dimensional space. Finally, we present a summary and conclusion for this chapter in section 2.4.

Chapter 3 : This chapter is concerned with the spatial dynamics of the SIS model derived in section 3.1. First in section 3.2 we describe and derive the methods we will use in the numerical computation section. In subsection 3.2.1 we describe the methods and subsection 3.2.2 we present the implicit-explicit (IMEX) methods. In subsection 3.2.3 we benchmark the model by taking an exact solution to a modified version of our model and compute some quantities like the EOC and the error in L^2, H^1 and L^∞ norms in space. For each we show the loglog plot of the error versus the modes. In section 3.3, we derive and present the Turing instability conditions for the spatial model derive in section 3.1 and then we present the necessary and sufficient conditions for Turing instability to

occur for our model. In section 3.4 we present some numerical experimentations. In subsection 3.4.1, we perform some numerical experiments for our model by fixing all other parameters and vary the transmission rate β and the treatment r to numerically study the dynamical behaviour of the system in certain parameter regimes. Finally, in section 3.5 we discuss the results from the chapter and draw conclusions by on the results.

Chapter 4: Here we derive a delayed SIR epidemic model with two time delays (latency and temporary immunity) and a bilinear incidence rate. In section 4.1, we derive the model and prove the positivity of all quantities in section 4.1.1. Section 4.2 presents linear stability analysis without time delays. Subsections 4.2.1 & 4.2.2 present global stability of the system steady state solutions using the idea of Lyaponuv direct method. Section 4.3 presents the stability and bifurcation analysis with time delays. Subsection 4.3.1 presents the system with only latency and prove the existence of stable solutions any parameter values. In subsection 4.3.2, the system with temporary only immunity is presented and prove for existence of periodic solutions from Hopf bifurcation is also presented. In subsection 4.3.4, the system with both latency and temporary immunity is presented and the proof for existence of Hopf bifurcation is also presented. Also, in section 4.4 an extensive numerical experiments are presented in the parameter regime. Finally, a summary and conclusion for the chapter is presented in section 4.5.

Chapter 5: presents a general summary and conclusion for the thesis.

Chapter 2

The SIS model with nonlinear incidence rate

In this chapter, we derive and analyse a non-spatial SIS epidemic model with nonlinear incidence rate. Both quantitative and qualitative techniques will be applied to gain insights into the dynamical behaviour of the system and to determine the essential epidemiological threshold parameters that characterise disease prevalence and transmission in the absence and in the presence of the disease. We shall start by deriving the model and finding its steady states. We will derive an explicit expression for the basic reproduction rate $\mathcal{R}_0$ using the *next generation matrix method*. Then, we will prove local and global stability of the system's equilibria. Also, we will attempt to prove global stability of the system steady state solutions using the Lyapunov principle. We will also present some numerical results for the non-spatial or ODE model.

2.1 Model derivation

We begin this section with the following quotations from [Liu86], [Liu87] and [Het91]: Liu et al [Liu86] *"When the traditional assumption that the incidence rate is proportional to the product of the numbers of infectives and susceptibles is dropped, the SIRS model can exhibit qualitatively different dynamical behaviours, including Hopf bifurcations, saddle-node bifurcations, and homoclinic loop bifurcations."* In a second paper Liu et al [Liu87] *"Epidemiological models with nonlinear incidence rates $\lambda I^P S^q$ show a much wider range of dynamical behaviours than do those with bilinear incidence rates λIS. These behaviours are determined mainly by p and λ, and secondarily by q. For such models, there may exist multiple attractive basins in phase space; thus whether or not the disease will eventually die out may depend not only upon the parameters, but also upon the initial conditions."* Hethcote et al [Het91] *"Epidemiological models with nonlinear incidence rates can have very different dynamical behaviours than those with bilinear incidence rate."*

In mathematical modelling of infectious diseases, it is natural to subdivide the total population N into compartments or classes, where each compartment comprises of cohorts of individuals which are assumed to have the same characteristic features. In this model, we will subdivide the total population into groups according to their disease status, that is, susceptible to the disease or infected with the disease. This type of compartmental models is called the susceptible-infected-susceptible SIS because it is assumed that as soon as the infected individuals recover they immediately become susceptible. Now, if the number of susceptible individuals at time t is S and the number of infected individuals at time t is I, then the total population is $N = S + I$. It is assumed in this model the recruitment into the population occurs only through natural birth in the S-compartment at a constant rate R. All the new recruitments (newborns) are assumed to be susceptible. There is a natural death rate γ in all the compartments and a disease-induced death in the I-compartment. Also, infected individuals recover at a constant rate r.

In many epidemiological models, the incidence rate is bilinear in the infective I and the susceptible S individuals. Such models can have an asymptotic stable trivial state

corresponding to the disease-free equilibrium, or an asymptotic stable endemic steady state corresponding to the positive nontrivial state depending on parameter values. Liu et al [Liu87] observed that if the restriction on bilinear incidence rates is removed, the models can have a much wider range of dynamical behaviours. They studied the dynamical behaviour of epidemiological models with nonlinear incidence rate of the form $\lambda S^p I^q$ and found they have different qualitative dynamics than those with bilinear incidence rate. These behaviours include Hopf bifurcations, saddle-node bifurcations, and homoclinic loop bifurcations. They concluded that the bilinear mass action incidence rate due to saturation before infection can lead to a nonlinear incidence rate of the form $\lambda I^q S^p$ which accounts for multiple exposures and high contagious effects of some diseases like influenza. Also, Hethcote and van den Driessche [Het91] showed that epidemiological models with nonlinear incidence rates can have very different dynamical behaviours than those with the usual bilinear incidence rate. They showed that the qualitative dynamical behaviour of epidemiological models with nonlinear incidence rate can be different from those with bilinear incidence rate. They concluded that the dynamical behaviour is mainly determined by the parameters λ and q. Therefore, we assumed that the incidence rate is nonlinear be given by $\beta S^p I^q$ without a periodic forcing, which we now know has much wider range of dynamical behaviours in comparison to bilinear incidence rate. Here β is the rate of transmission, and p and q are phenomenological exponents, $(p, q \in \mathbb{Z}^+)$. It is worth nothing that unlike in [Liu86], [Liu87] and [Het91] who concluded that the dynamical behaviour of the system is mainly determined by β and q, here we will show that the dynamical behaviour also depend on the recovery r. Examples of diseases that fit into this kind of models are chlamydia infection, influenza, Tuberculosis etc.

Here we assume that the population is well-mixed. That is, every infected individual has a probability of contacting any susceptible individual. This is often the most problematic assumption, but is easily relaxed in more complex models. In simple epidemic models like ours, this can be true but in reality or in general this may not be true. The assumption simply means that any pair of individuals is equally likely to interact with each other during a given time interval [Mur75]. Perhaps the best way of extending

the model to account for spatial structure is to subdivide the population into two or more classes, representing, for example, different disease status. It is typically assumed that these classes are well-mixed and that there is some level of mixing between different classes. An alternative way to describe spatial structure assumes that individuals are distributed continuously across space and that infection spreads as individuals move about the spatial domain, for details on well-mixed assumption of population models see [Wod13], [Nob74], [Bol96], [Mur75].

Based on the above-mentioned assumptions we consider the following SIS epidemic model. The rate of change of susceptible and infected individuals are governed by the following two equations.

$$\begin{aligned} \frac{dS}{dt} &= R - \beta S^p I^q - \gamma S + rI, \\ \frac{dI}{dt} &= \beta S^p I^q - (\gamma + r + \mu)I, \end{aligned} \tag{2.1}$$

where R the natural birth rate, β the transmission rate, γ the natural death rate, r the recovery rate, μ the disease-induced death rate and $S(t)$ and $I(t)$ the number of susceptible and infected individuals at time t, respectively. In this chapter, we will study this model rigorously both analytically and numerically. We will perform linear stability analysis in the absence of diffusion. In the next Chapter, we will perform linear stability analysis in the presence of diffusion. For linear stability and bifurcation analysis, we will use this model to establish the conditions that will tell us when the steady states can be stable or unstable. We start the chapter by deriving the *basic reproduction ratio* ($\mathcal{R}_0$) using the *next generation operator method*. Then, we find the steady states of the model and prove their local and global stability. Here, we present local stability of system's equilibria for the general phenomenological exponents p and q. The cases for $p + q = 1$ and $p = 1,\ q = 2$ have been considered in [Sun07] and [Sun12(a)] respectively.

2.2 Stability and Bifurcation Analysis

This section presents both local stability analysis of the steady states for the model 2.1. We first analyse the local stability of the trivial steady state and then analyse the local stability of non-trivial solution of model 3.32. First, we find the equilibria for the non-spatial model 2.1 and establish their stability. The model 2.1 has two equilibria; a disease free and an endemic states as follows.

2.2.1 Threshold conditions of the model steady states

Let $E_i = (S_i, I_i)$ be arbitrary non-negative equilibria of the system 2.1 that satisfy the following algebraic equations

$$\begin{aligned} R - \beta S^p I^q - \gamma S + rI &= 0, \\ \beta S^p I^q - (\gamma + r + \mu) I &= 0. \end{aligned} \tag{2.2}$$

Obviously, one of the solutions of the system 2.1 is the disease-free or uninfected steady state E^0 given by:

$$E^0 = (S^0,\ I^0) = \left(\frac{R}{\gamma},\ 0\right).$$

Besides the disease-free steady state E^0, a non-trivial endemic state can exist which is characterised by the non-zero values of both S and I. In the following we prove that the non-trivial or endemic state exists and is unique in the following remark.

Remark 2.1

If $\mathcal{R}_0 > 1$, the endemic steady state E^* exists and is unique.

Proof:

Solving system 2.1 for S and I we have the following:

From the second equation in 2.1 we have

$$\beta S^p I^q - (\mu + r + \gamma)I = 0$$
$$S = \left(\frac{(\mu + r + \gamma)}{\beta}\right)^{1/p} I^\alpha$$

where $\alpha = (q-1)/p,\ q > 1$.

From the first equation in 2.1 it follows that

$$R - \beta S^p I^q - \gamma S + rI = 0,$$
$$(r - \beta S^p I^{q-1})I = \gamma S - R.$$

But we know from above

$$\beta S^p I^{q-1} = (\mu + r + \gamma)$$
$$\implies (r - (\mu + r + \gamma))I = \gamma S - R$$
$$I^* = \frac{R - \gamma S^*}{(\mu + \gamma)}$$
$$= \frac{R - \gamma\left(\frac{(\mu+r+\gamma)}{\beta}\right)^{\frac{1}{p}} I^{*\alpha}}{(\mu + \gamma)}$$

Therefore,

$$I^* = \frac{R}{(\mu + \gamma)} - \frac{\gamma}{(\mu + \gamma)}\left(\frac{\gamma + r + \mu}{\beta}\right)^{\frac{1}{p}} I^{*\alpha} \tag{2.3}$$

Hence, $E^* = (S^*, I^*)$.

Now, we prove the uniqueness of E^*. Now we let $f(I^*) = I^*$ in 2.3, to show that E^* is unique, it is sufficient to show that $f(I^*)$ is monotone (decreasing/increasing). That is, for any parameter in the expression 2.3 there will be only one point of intersection.

To check for monotonicity, we differentiate $f(I^*)$ with respect to I^* as follows:

$$\frac{df(I^*)}{dI^*} = -\alpha\left(\frac{\gamma}{\gamma+\mu}\right)\left(\frac{\gamma+r+\mu}{\beta}\right)^{1/p} I^{\alpha-1} < 0, \quad \forall I^* > 0. \tag{2.4}$$

Since $f^{'}(I^*) < 0$, this means I^* is monotonically decreasing and in the $(f(I^*), I^*)$-plane there is only one point of intersection. Therefore, for a positive root of $f(I^*) = 0$ to exist, $f(I^*)$ has to satisfy $f(I^*) > 0$, i.e.

$$f(0) = \frac{R}{\gamma+\mu} > 0.$$

Hence, E^* exists and is unique. Also, we can show this numerically by plotting the expression for $f(I^*)$ versus I^*. See below the graph of $f(I^*)$ against I^* showing the one point intersection.

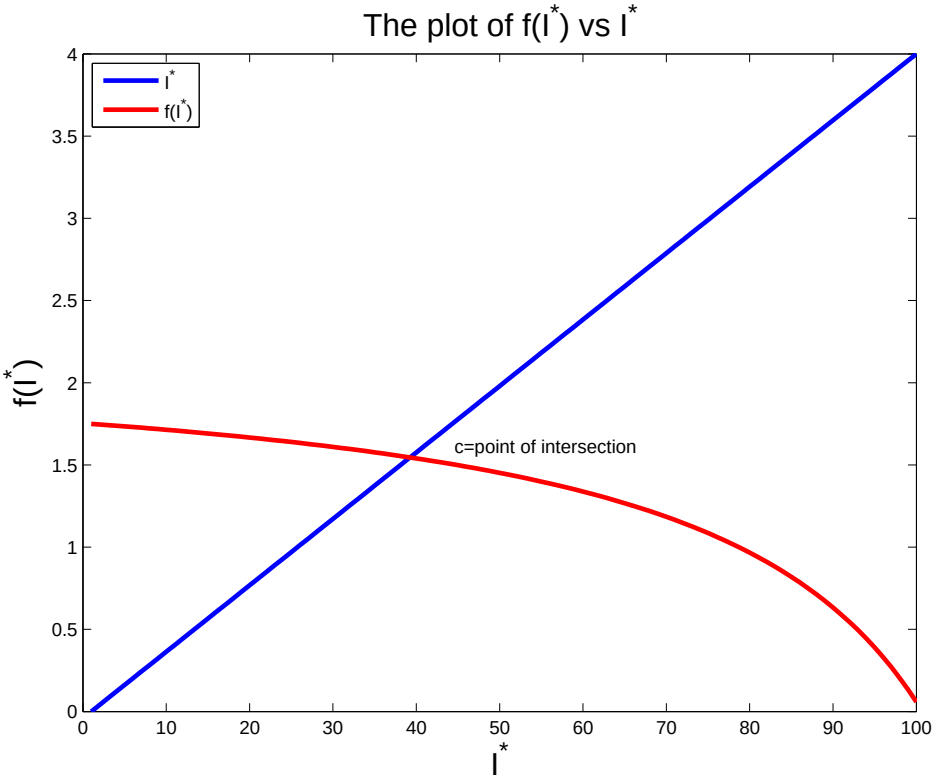

Figure 2.1: This figure shows the uniqueness of the endemic steady state, $\beta = 0.5, R = 0.35, \gamma = 0.1, r = 0.5, \mu = 0.1, p = 2, q = 2$.

■

2.2.2 The basic reproduction number $\mathcal{R}_0$

In epidemiology, the basic reproduction number $\mathcal{R}_0$, is an important threshold quantity which tells how epidemics grow in a population of completely susceptible individuals when a single infected individual is introduced into the population. For simple models $\mathcal{R}_0$ is the mean number of secondary cases obtain from a single primary infection when introduced into a population that is completely susceptible [Dri02]. There are many ways to derive an explicit expression for $\mathcal{R}_0$ for the model 2.1 but here we will use the so-called next generation matrix operator in the following subsection.

Derivation of the basic reproduction ratio using the next generation matrix operator

We will derive an explicit expression for $\mathcal{R}_0$ by the next generation matrix method. According to this method the basic reproduction number is the largest eigenvalue of the next generation matrix, that is, the spectral radius of the next generation matrix Ψ defined as follows:

$\Psi = -FV^{-1}$,

where F and V are the transmission and transition matrices respectively [Dri02]. F and V are the derivatives of the right hand sides of 2.1 with respect to the state variables. F is obtained from the terms that give rise to infection, which only occurs in the second equation of 2.1 with respect to the second variable I (i.e. transmission only occurs in the I-class with respect to the infective. While, V is obtained from the derivative of transition terms with respect to state variables. From the model 2.1 taking the derivatives with respect to the state variables for the the transmission and transition terms, the matrices F and V can be found as

$$F = \left[\frac{\partial F_i(E_0)}{\partial x_j}\right] \tag{2.5}$$

$$V = \left[\frac{\partial V_i(E_0)}{\partial x_j}\right] \tag{2.6}$$

The F_i are the new infections (transmission), while the V_i are the transfers of infections

(transition) from one compartment to another. E_0 is the disease-free steady state. For system 2.1 F_i and V_i are given below

$$F = \begin{pmatrix} 0 & 0 \\ 0 & \beta(\frac{R}{\gamma})^p \end{pmatrix}, \tag{2.7}$$

and

$$V = \begin{pmatrix} -\gamma & r \\ 0 & -(\mu + r + \gamma) \end{pmatrix} \tag{2.8}$$

$$V^{-1} = \begin{pmatrix} \frac{1}{\gamma} & \frac{r}{\gamma(\mu+r+\gamma)} \\ 0 & \frac{1}{(\gamma+r+\mu)} \end{pmatrix} \tag{2.9}$$

$$\Psi = \begin{pmatrix} 0 & 0 \\ 0 & \beta(\frac{R}{\gamma})^p \end{pmatrix} \begin{pmatrix} \frac{1}{\gamma} & \frac{r}{\gamma(\mu+r+\gamma)} \\ 0 & \frac{1}{(\mu+r+\gamma)} \end{pmatrix} = \begin{pmatrix} 0 & 0 \\ 0 & \frac{\beta}{(\mu+r+\gamma)}(\frac{R}{\gamma})^p \end{pmatrix}$$

$$\begin{aligned} \mathcal{R}_0 &= \rho(\Psi) = \frac{\text{trace}(\Psi) \pm \sqrt{\text{trace}(\Psi)^2 - 4\text{det}(\Psi)}}{2} \\ &= \frac{\frac{\beta}{(\mu+r+\gamma)}(\frac{R}{\gamma})^p \pm \sqrt{\left(\frac{\beta}{(\mu+r+\gamma)}(\frac{R}{\gamma})^p\right)^2 - 0}}{2}. \end{aligned}$$

It follows that the eigenvalues of the next generation matrix Ψ are

$$\lambda_1 = \left(\frac{\beta}{\gamma + r + \mu}\right)\left(\frac{R}{\gamma}\right)^p, \quad \lambda_2 = 0,$$

and therefore,

$$\mathcal{R}_0 \;=\; \left(\frac{\beta}{\gamma+r+\mu}\right)\left(\frac{R}{\gamma}\right)^p. \tag{2.10}$$

This approach is valid for even higher dimenssion systems.

Remark 2.2

If the determinant of the next generation matrix is zero, then the spectral radius (which is $\mathcal{R}_0$) of this matrix is the sum of its diagonal elements.

2.2.3 Stability analysis of the disease-free equilibrium state

Let f and g be the right hand sides of the first and second equations of the system 2.1, respectively, linearise the system 2.1 near the disease-free steady state as follows.

The Jacobian matrix J of linearisation of the system 2.1 near its steady state $E^0 = (S^0, I^0)$ is given by

$$J \;=\; \begin{pmatrix} -\beta p S_0^{(p-1)} I_0^q - \gamma & -\beta q S_0^p I_0^{(q-1)} + r \\ \\ \beta p S_0^{(p-1)} I_0^q & \beta q S_0^p I_0^{(q-1)} \;-\; (\gamma+r+\mu) \end{pmatrix}.$$

The characteristic equation of the linearised system near the disease-free steady state for $q > 1$ is therefore

$$\lambda^2 + \lambda(2\gamma + r + \mu) + \gamma(\gamma + r + \mu) = 0. \tag{2.11}$$

The characteristic polynomial 2.11 is a quadratic with two roots (eigenvalues) both being negative:

$$\lambda_1 = -\gamma \quad \text{and} \quad \lambda_2 = -(\gamma + r + \mu). \tag{2.12}$$

We can observe from the above that E_0 for $q > 1$ is stable because the eigenvalues are both real and negative. Also, the determinant is positive and the trace is negative. Hence by Routh-Hurwitz stability criterion, the disease-free steady state E_0 is locally asymptotically stable.

For $q = 1$ the conditions of stability for the disease-free steady state are different. In this case the Jacobian matrix is

$$J_{E_0\,|_{q=1}} = \begin{pmatrix} -\gamma & -\beta\left(\frac{R}{\gamma}\right)^p + r \\ \\ 0 & \beta\left(\frac{R}{\gamma}\right)^p - (\gamma + r + \mu) \end{pmatrix} \tag{2.13}$$

The characteristic equation now takes the form

$$\lambda^2 + \lambda\left[(\mu + r + 2\gamma) - \beta\left(\frac{R}{\gamma}\right)^p\right] + \gamma(\mu + r + \gamma) - \beta\left(\frac{R}{\gamma}\right)^p = 0. \tag{2.14}$$

Rewriting the characteristic equation 2.14 above in terms of the basic reproduction ratio $\mathcal{R}_0$ we have the following.

$$\lambda^2 + \lambda\left[(1 - \mathcal{R}_0) + \gamma\right] + \gamma(1 - \mathcal{R}_0) = 0. \tag{2.15}$$

The equation 2.15 have two roots with negative real parts whenever $\mathcal{R}_0 < 1$, that is $\lambda_1 = -\gamma < 0$ and $\lambda_2 = -(1 - \mathcal{R}_0) < 0$ (since $\mathcal{R}_0 < 1$). For $\mathcal{R}_0 > 1$, it will have one negative root $\lambda_1 = -\gamma$ and one positive root $\lambda_1 = -(1 - \mathcal{R}_0) > 0$ (because $\mathcal{R}_0 > 1$), and for $\mathcal{R}_0 = 1$, then $\lambda_1 = -\gamma$ and $\lambda_2 = 0$ which means the steady state is neutrally-stable at $\mathcal{R}_0 = 1$. The following remark contains the summary of the above analysis.

Lemma 2.1

The disease-free steady state E_0 of model 2.1 is locally asymptotically stable when $\mathcal{R}_0 < 1$, neutrally-stable when $\mathcal{R}_0 = 1$, and unstable when $\mathcal{R}_0 > 1$.

Next, we state and prove an important Theorem on a positive invariant region $\mathbb{D}$ for our

model.

Theorem 2.1

There exists a positive invariant region

$$\mathbb{D} = \left\{ (S, I) \in \mathbb{R}^2 : S > 0,\ I > 0,\ S + I \leq \frac{R}{\gamma} \right\}. \tag{2.16}$$

Proof:

We show that the region $\mathbb{D}$ defined above is an invariant region. We use the idea of [Bel89] to show that the inner product of the vector field defined by right hand sides 2.1 with the inward normal to $\mathbb{D}$ is non-negative. But before that, we will prove the positivity and boundedness of model 2.1 in the following lemma.

Lemma 2.2

The solution $(S(t),\ I(t))$ *of 2.1 is non-negative for* $t \geq 0$ *and*

$$\lim_{t \to +\infty} \sup N(t) \leq \frac{R}{\gamma}. \tag{2.17}$$

$S(0) > 0,\ I(0) \geq 0.$

Proof:

A detailed proof can be found in [Li00], [Zha08]. The proof proceeds by contradiction. First, we assume there exists the first time t_1 when $S(t_1)I(t_1) = 0$. If we assume that $S(t_1) = 0$, this gives $I(t) \geq 0$, $\forall t \in [0; t_1]$. We have by the S equation of model (2.1) thus:

$$\left.\frac{dS(t)}{dt}\right|_{t_1} = \underbrace{R}_{>0} - \underbrace{\beta S^p(t_1) I^q(t_1)}_{=0} - \underbrace{\gamma S(t_1)}_{=0} + \underbrace{r I(t_1)}_{>0} > 0. \tag{2.18}$$

And since $S(0) > 0$ for $S(t_1) = 0$, we require

$$\frac{dS(t)}{dt}\Big|_{t=t_1} < 0,$$

which contradicts 2.18. Following the same logic, we can also show that $I(t)$ is also non-negative.

Therefore, $S(t) > 0,\ I(t) > 0$ for all $t \in [0, \alpha)$, where $0 < \alpha \leq +\infty$. Also,

$$\dot{N}(t) \;=\; R - \gamma S - (\gamma + \mu)I = R - \gamma N - \mu I \leq R - \gamma N. \tag{2.19}$$

which implies that

$$N(t) \leq N(0)e^{-\gamma t} + \frac{R}{\gamma}(1 - e^{-\gamma t}) \leq N(0) + \frac{R}{\gamma}. \tag{2.20}$$

This implies that $(S(t), I(t))$ is bounded on $[0, \infty)$ [Zha08]. Hence, by 2.19 and by comparison theorem for differential inequalities (see appendix 5.2 for details) it implies that

$$\lim_{t \to +\infty} \sup N(t) \leq \frac{R}{\gamma}. \tag{2.21}$$

This completes the proof of Lemma 2.2. ■

Next we prove that $\mathbb{D}$ is positive invariant as follows. Let f and g denote the right hand sides of 2.1. The inward normal to the I-axis is $(1, 0)$, therefore,

$$\begin{aligned}(1,0)\begin{pmatrix} f \\ g \end{pmatrix} = f \;&=\; (R - \beta S^p I^q - \gamma S + rI) \\ &=\; (R + rI) > 0 \quad \text{(because } S = 0 \text{ on this axis).}\end{aligned}$$

Next the inward normal to the S-axis is $(0, 1)$ then,

$$(0,1)\begin{pmatrix} f \\ g \end{pmatrix} = g = (\beta S^p I^q - (\gamma + r + \mu)I) = 0 \ \text{ (since } I = 0 \text{ on this axis).}$$

Finally, on the line $S + I = N$, we know that N is not constant, but again, we know that $S + I \leq N$ and $\lim_{t\to+\infty} \sup(S + I) \leq \lim_{t\to+\infty} \sup N(t) \leq \frac{R}{\gamma}$. Now, we know at boundary of our invariant region $S + I = N = \frac{R}{\gamma}$ then $dN/dt = -\mu I < 0$ since $I > 0$. Therefore, if we wait long enough the total population will become a constant, that is, there exists $T > 0$ such that for all $t > T$ we have the following on the line $S + I = \frac{R}{\gamma}$.

$$\begin{aligned}
\frac{1}{\sqrt{2}}(-1,-1)\begin{pmatrix} f \\ g \end{pmatrix} &= -\frac{1}{\sqrt{2}}[f + g] \\
&= -\frac{1}{\sqrt{2}}[R - \beta S^p I^q - \gamma S + rI + \beta S^p I^q - (\mu + r + \gamma)I] \\
&= -\frac{1}{\sqrt{2}}[R - \gamma S - (\mu + \gamma)I] \\
&= \frac{1}{\sqrt{2}}[\gamma S + (\mu + \gamma)I - R] \\
&= \frac{1}{\sqrt{2}}[\gamma N + \mu I - R] \\
&= \frac{1}{\sqrt{2}}\mu I > 0
\end{aligned}$$

the last inequality holds because $N = R/\gamma$ on the boundary of the invariant region $\mathbb{R}$. Thus we have shown that the region $\mathbb{D}$ is positive invariant. ■

As a next step in the analysis, we concentrate on the non-trivial state E^* of the system 2.1, that is, when both susceptibles and infecteds coexist. This is a situation when the disease is present in the population. In the next subsection, we will carefully study the steady state (E^*) for the model 2.1. We will derive conditions for local stability analysis.

2.2.4 Stability of the endemic equilibrium

To study the stability of the endemic equilibrium state, we use the same approach as in subsection 2.2.3 above and assume that $\mathcal{R}_0 > 1$ throughout this subsection. The Jacobian matrix at the endemic state is given below for the general phenomenological exponents p and q:

$$J_{E_*} = \begin{pmatrix} -(\beta p S_*^{p-1} I_*^q + \gamma) & -\beta q S_*^p I_*^{q-1} + r \\ \\ \beta p S_*^{p-1} I_*^q & \beta q S_*^p I_*^{q-1} - (\gamma + r + \mu) \end{pmatrix}$$

The trace and the determinant of this matrix are, respectively,

$$\begin{aligned} \text{trace}(J_{E^*}) &= -(\beta p S_*^{p-1} I_*^q + \gamma) + \beta q S_*^p I_*^{q-1} - (\gamma + r + \mu) \\ &= \beta S_*^{p-1} I_*^{q-1} [q S_* - p I_*] - (2\gamma + r + \mu) \end{aligned}$$

$$\begin{aligned} \det(J_{E^*}) &= -[\beta p S_*^{p-1} I_*^q + \gamma] \times [\beta q S_*^p I_*^{q-1} - (\gamma + r + \mu)] - [\beta p S_*^{p-1} I_*^q] \times [-\beta q S_*^p I_*^{q-1} + r] \\ &= -\beta^2 pq S_*^{2p-1} I_*^{2q-1} + \beta p(\gamma + r + \mu) S_*^{p-1} I_*^q - \beta\gamma q S_*^p I_*^{q-1} + \gamma(\gamma + r + \mu) + \\ &\quad \beta^2 pq S_*^{2p-1} I_*^{2q-1} - \beta p r S_*^{p-1} I_*^q \\ &= \beta p(\gamma + \mu) S_*^{p-1} I_*^q - \beta\gamma q S_*^p I_*^{q-1} + \gamma(\gamma + r + \mu) \\ &= \beta S_*^{p-1} I_*^{q-1} [p(\gamma + \mu) I_* - q\gamma S_*] + \gamma(\gamma + r + \mu) \\ &= \beta p \mu S_*^{p-1} I_*^q + \gamma(\gamma + r + \mu) + \beta\gamma S_*^{p-1} I_*^{q-1} [p I_* - q S_*]. \end{aligned}$$

The endemic steady state E^* is stable if the trace is negative and the determinant is positive for any $p, q \in \mathbb{Z}^+$. One such possibility is when $pI_* > qS_*$.

Remark 2.3

We note here that actually there are more than one explicit possibility to ensure that the trace is less than zero and the determinant is greater than zero.

2.3 Numerical solution for the non-spatial model

The non-spatial model tracks the numbers of susceptible and infected individuals during an infection with the help of ordinary differential equations. We will simulate the model and plot and interpret the results. We will use the simulation to verify some analytical results. We will plot time evolution and phase diagrams. Here, we present the numerical solutions to system 2.1. This is the non-spatial or ODE model. We will show the progression of the infection over the course of time and the solutions in phase space. The reason for the solution of the non-spatial model is to see the interaction and behaviour of susceptible and infective populations as time evolves. Here, we do not care about the effects of space because we are in the ODE case, though we know space plays an important role in disease transmission but here we ignore it. Later in the next Chapter we shall show Turing patterns in two space dimensions and use them to study disease transmission. In the figures below, we will only vary β and all other parameters will be kept fixed with the following values $R = 0.35,\ \gamma = 0.1,\ r = 0.05,\ \mu = 0.1$.

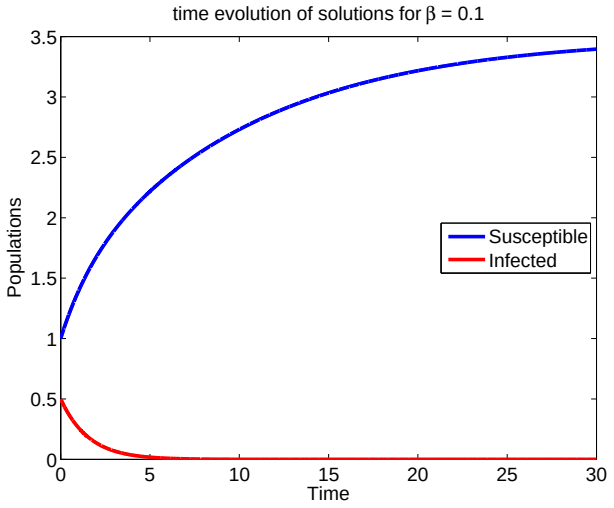

(a)

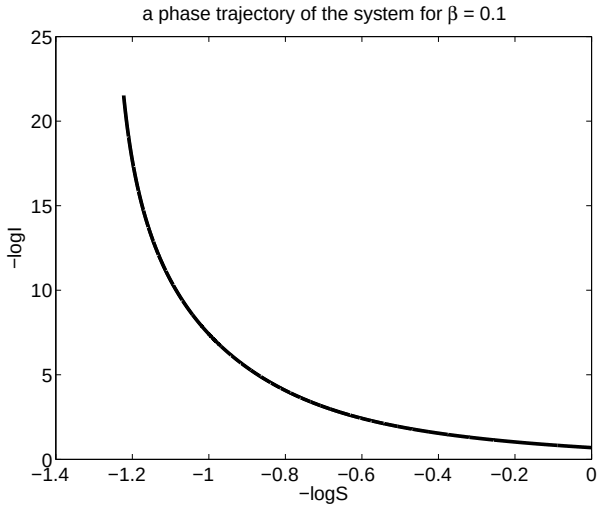

(b)

Figure 2.2: In the first figure, we have the time series solutions for $\beta = 0.1, R = 0.35, \gamma = 0.1, \mu = 0.1, r = 0.5, p = q = 2$, this shows how the susceptible and the infective grow over time. The second figure shows the solutions phase space for the two populations.

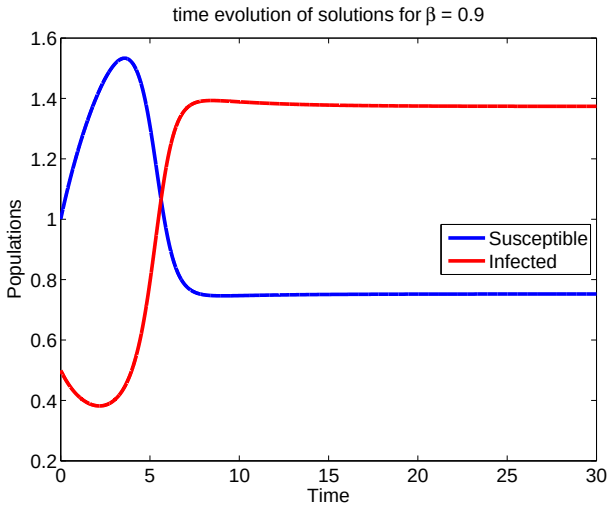

(a)

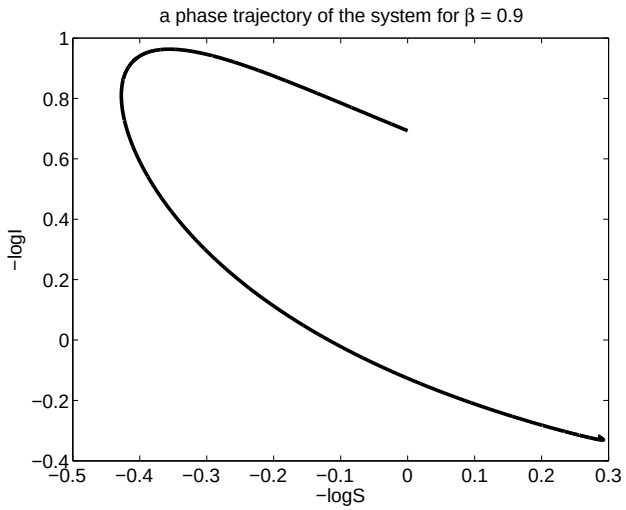

(b)

Figure 2.3: In the first figure, we have the time series solutions for $\beta = 0.9, R = 0.35, \gamma = 0.1, \mu = 0.1, r = 0.5, p = q = 2$, this shows how the susceptible and the infective grow over time. The second figure shows the solutions phase space for the two populations.

In figures 2.2 and 2.3 above, we considered an instance of a disease with the following parameter estimates, a recruitment rate of 0.35, a natural death rate of 0.1, a disease-

induced death rate of 0.1, and a recovery rate of 0.5. Also, we fixed the exponents $p = 2,\ q = 2$, and varied the transmission rate β. In the first figure (2.2), the transmission rate is taken to have a small value of 0.1, which is equal to the natural death constant γ and is less than the recovery rate r. We observed that the number of susceptible individuals kept on growing, and the number of infected individuals decayed to zero. At about $t = 5$, the number of infected individuals approached zero. This is because the treatment rate r is high, and the transmission rate β and the natural death rate γ are small and equal. This means almost everyone who is infected gets treated or recovered, and immediately returns to the susceptible class. In the second figure (2.3), we increased the value of β to 0.9, which means high transmission rate. Since fewer people get treated than get infected, we observed that initially the number of susceptible individuals increased, and the number of infected individuals decreased, then after about $t = 4$ the number of susceptibles started declining as the infection started to invade the population. Then at about $t = 7$, the two sub-populations remained constant. This may be due to development of resistance by the susceptible individuals, and it is worth noting that some diseases naturally have this kind of dynamics after some period of time.

2.4 Conclusion

In this chapter, we have derived an SIS non-spatial epidemic model with nonlinear incidence rate that describes the interactions of the susceptible and infected individuals. The model is derived in such a way that it can describe the behaviours of many communicable diseases. We established local stability of the system equilibria. We found that the trivial steady state E^0 is always stable for the general values of the phenomenological exponents p and q. But when $q = 1$, the disease-free steady state E^0 is locally asymptotically stable if $\mathcal{R}_0 < 1$, unstable if $\mathcal{R}_0 > 1$ and neutrally stable if $\mathcal{R}_0 = 1$. For $\mathcal{R}_0 > 1$, we proved that there exists a unique non-trivial state E^* which is locally asymptotically stable if $pI_* > qS_*$ for all $p, q \in \mathbb{Z}^+$. Also, we proved positivity, boundedness, permanence of the model 2.1 and showed that the region $\mathbb{D}$ is positively invariant for the case when

the total population N is not a constant. Finally, we presented some useful numerical results for the non-spatial model to show the interactions between the susceptible and infected individuals for a fixed value of the transmission rate β.

In general, in this chapter, we have proved stability of the system's endemic equilibrium for the general exponents p and q, this has not been done before. We have generalised the proofs and results in the papers [Sun07], [Sun12(a)]. Our results are different from those in [Sun07] and [Sun12(a)] because in the former the authors fixed the exponents $p + q = 1$, and in the latter the author fixed the exponents $p = 1$ and $q = 2$, while in our case we generalised the results in the two papers by proving the stability of the system's equilibrium for any $p, q \in \mathbb{Z}^+$. This showed that it is possible to have wider dynamics than what was found in those papers, and we will discuss further differences in the case of the spatial model in the next Chapter. Unlike [Sun07] and [Sun12(a)], in our case we found that at $q = 1$ we have conditional stability for the disease-free steady state E^0. Also, we have proved the permanence and invariance principle for the case when N is not a constant which was not done in the aforementioned papers. In [Sun07], [Cai11], [Sun12(a)] and most of the papers on pattern formation, the authors assumed positivity, boundedness, permanence and invariance but in our case we proved all these. In all the papers we have seen so far on pattern formation in epidemic models, no one had attempted to prove permanence and invariance principle for a non-constant N. Most authors assume N to be constant, and in reality N may not be constant in models with births and deaths. SIS epidemic models are known to be helpful in studying the dynamics of many bacterial diseases (e.g. meningitis), as well as for numerous sexually transmitted infections (e.g. chlamydia infection). In general, our model can be applicable in many communicable diseases. We will extend this model in the next Chapter to incorporate space and to study the spatiotemporal dynamics of the model.

Chapter 3

Spatial dynamics

In chapter 1, we have seen from the literature the role of spatial models in epidemic control and why the spatial models are preferred to the ODE models. The classical ODE models assumed that both the susceptible and the infective individuals experience the same homogeneous environment. But in reality, this is not the case since individuals are distributed in space and naturally interact with each other. Most parts of the ecological setting such as climatic conditions, food can differ from place to place. There are other ecological and biological phenomena like invasions by foreign species, which are intrinsically spatial in nature and can affect the dynamics of populations and the structure of the ecosystem [Can03]. Therefore, the need to include space in modelling epidemics is vital to make the models more realistic and more practical.

Therefore, this chapter is concerned with analysis of spatial dynamics for the SIS model that we will derive in the next section. First, we derive the model, then present the methods we will use in the numerical simulation section. We will prove the stability of the method. To do this, we will benchmark the spatial model and compute the error in various norms such as L^2, H^1 and L^∞. Also, we will compute the experimental order of convergence (EOC) which tells if the method converges with the correct order. We will derive the conditions for our model that will guarantee Turing instability in the parameter regime. These conditions will guide us through the numerical experimentation

section. Finally, we will perform some numerical simulations for the spatial model using the methods we will derive in the next section.

3.1 Model derivation

In the previous Chapter, we derived and analysed a non-spatial SIS model which represents the interaction between susceptible and infected populations. All the assumptions we made in the derivation of the non-spatial model 2.1 are also assumed for the spatial model. One of the main assumptions of this model is that the population consists subpopulations: the healthy individuals that is, susceptible S to the infection and the infected (sick) individuals I that is, those that can transmit the disease to the susceptible individuals. Both populations are functions of time and space. In this thesis we assume that reproduction is only through natural birth from the susceptible individuals at a constant rate R and there is a natural constant death rate γ in all compartments. In the absence of infection in the population, the susceptible individuals are represented by the following equation:

$$\frac{dS}{dt} = R - \gamma S. \tag{3.1}$$

In the presence of the disease, there is an additional disease-induced death rate μ in the infected class. The infected individuals recover at a constant rate r and immediately return to the susceptible class. Liu et al [Liu87] concluded that the bilinear mass action incidence rate due to saturation before infection can lead to a nonlinear incidence rate $\lambda I^q S^p$ which accounts for multiple exposures. Therefore the incidence rate is assumed to be nonlinear, $\beta S^p I^q$ without a periodic forcing, which has much wider range of dynamical urs in comparison to the case of a bilinear incidence rate. Here β is the rate of transmission and p and q are phenomenological exponents, $(p, q \in \mathbb{Z}^+)$. From the assumptions, the

model describing the interaction between susceptible and infected individuals is

$$\begin{aligned} \frac{dS}{dt} &= R - \beta S^p I^q - \gamma S + rI, \\ \frac{dI}{dt} &= \beta S^p I^q - (\gamma + r + \mu) I. \end{aligned} \tag{3.2}$$

Assume Fick's law holds for the reason that individuals are distributed randomly and can move freely in space according to Brownian motion (see [Hol94], [Sun07] for details). The diffusion coefficients for the susceptible and infected individuals are d_1 and d_2 respectively. We also assume that the diffusion coefficients are distinct and that $d_1 > d_2$. The reason for $d_1 > d_2$ is because we assume that the susceptible (healthy individuals) move faster and infected (sick individuals) move slower. Let $S(\boldsymbol{x}, t)$ and $I(\boldsymbol{x}, t)$ be the densities of the susceptible and infected individuals at time t and position $\boldsymbol{x}$ respectively. This leads to flux terms be given by

$$\begin{aligned} \frac{\partial S}{\partial t} &= d_1 \nabla^2 S, \\ \frac{\partial I}{\partial t} &= d_2 \nabla^2 I, \end{aligned} \tag{3.3}$$

where $\nabla^2 = \dfrac{\partial^2}{\partial x^2} + \dfrac{\partial^2}{\partial y^2}$ is the normal Laplacian operator in 2-dimension space.

Given $\boldsymbol{x} \in \Omega^2 = [0, L]^2$, $t \in [t_0, T]$, where L is the length of the domain, and t_0 and T are the initial and final time respectively. Furthermore, we assumed no-flux Newmann boundary conditions in both compartments, which biologically represents the fact that the population is geographically isolated, i.e. individuals cannot enter or leave through the boundary Ω. Combining the systems 3.2 and 3.3, we derive the model describing the

interaction of the susceptible and infected populations as follows:

$$
\begin{aligned}
&\frac{\partial S}{\partial t} = d_1 \Delta S \; - \; \beta S^p I^q \; - \; \gamma S \; + \; R \; + \; rI, \qquad \boldsymbol{x} \; \in \; \Omega \\
&\frac{\partial I}{\partial t} = d_2 \Delta I \; + \; \beta S^p I^q \; - (\gamma \; + \; r \; + \; \mu) I, \qquad \boldsymbol{x} \; \in \; \Omega \\
&S(\boldsymbol{x}, t_0) = S_0(\boldsymbol{x}) \qquad \text{in } \; \Omega, \quad t_0 = 0 \\
&I(\boldsymbol{x}, t_0) = I_0(\boldsymbol{x}) \qquad \text{in } \; \Omega, \quad t_0 = 0 \\
&n.\nabla S = 0 \qquad\quad \text{on } \; \partial\Omega, \quad t > 0 \\
&n.\nabla I = 0 \qquad\quad \text{on } \; \partial\Omega, \quad t > 0
\end{aligned}
\tag{3.4}
$$

where $S_0(\mathbf{x})$ and $I_0(\mathbf{x})$ represent the initial data.

In this Chapter, we will study this model rigorously both analytically and numerically. We will perform linear stability analysis in the presence of diffusion.

3.2 The method and benchmarking

In this section, we present the methods we will use in the numerical simulations section and prove their stability. First, we will show how to derive these methods. Then, we benchmark the system 3.4, that is, we take an exact solution and compare it with the discrete solution and compute the errors in L^2, H^1 and L^∞ in space and also to compute the Experimental Order of Convergence (EOC). But since there are no known closed form solutions to the system 3.4, therefore, we will take an exact solution to a modified version of the model. This is a way to ascertain that the method can be a good solver for the system 3.4. Computing the error in various norms can tell how close the approximate (discrete) is to the true (exact) solution.

3.2.1 The Method

The method we will introduce here is known as the Implicit-Explicit (IMEX) or splitting method. This method has been studied and used extensively for solving nonlinear PDEs, see [Jia09], [Cra06], [Han09], [Zoh13] and the references therein. The method is similar to the semi-implicit pseudo-spectral methods and the predictor-corrector method. In the IMEX method, the diffusion terms (linear part) are computed implicitly in the Fourier space, and all other terms are computed explicitly (nonlinear part) in real space. Applying one integration formula to the different parts of the reaction diffusion equations is generally inefficient. For example, using a single implicit integration formula for the whole problem will lead to a large nonlinear algebraic system. The idea behind splitting is to break down a complicated problem into smaller parts and then treat each part with a suitable integration formula. For more details see, [Sai12] and the references therein.

3.2.2 Implicit-Explicit (IMEX) Splitting Methods

We will discuss splitting methods with an improved treatment of the explicit terms in this section. These methods involve a mixture of implicit and explicit schemes, for example, using an explicit scheme such as the Euler's scheme to advance the nonlinear part and an implicit scheme such as backward Euler or Crank-Nicolson schemes, to advance the linear part. We consider here the IMEX-θ methods (which is the same as the classical θ-method), see [Nag07], [Han09], [Alf12], [Zoh13] for details. The classical θ-method is the general way of writing the forward Euler, backward Euler and Crank-Nicolson schemes in a compact form which we will explain below. Now rewrite the system 3.4 as follows:

$$\begin{aligned} \partial_t S &= d_1 \Delta S + f(S, I) \\ \partial_t I &= d_2 \Delta I + g(S, I) \end{aligned} \tag{3.5}$$

The θ-scheme, see [Nag07], for the system 3.5 gives

$$\begin{aligned} \mathbf{M}\frac{\mathbf{S}_h^{n+1}-\mathbf{S}_h^n}{\Delta t} &= \theta\mathbf{F}(\mathbf{S}_h^{n+1}) + (1-\theta)\mathbf{F}(\mathbf{S}_h^n) \\ \mathbf{M}\frac{\mathbf{I}_h^{n+1}-\mathbf{I}_h^n}{\Delta t} &= \theta\mathbf{F}(\mathbf{I}_h^{n+1}) + (1-\theta)\mathbf{F}(I_h^n) \end{aligned} \tag{3.6}$$

where M is a mass matrix (mass matrix is obtained from the time derivative of the state variables), F are the reaction terms, S_h^n, I_h^n are the approximate solutions at time n, θ determines the method (Forward Euler, Backward Euler or Crank-Nicolson).

Note: The formula 3.6 is the general way of representing the explicit Euler (forward Euler), implicit Euler (backward Euler) and the Crank-Nicolson schemes. For instance, if $\theta = 0$, we have the explicit Euler's scheme; if $\theta = 1$, we recover the implicit (backward) Euler which is first order accurate in time; if $\theta = \frac{1}{2}$, we obtain the Crank-Nicolson scheme which is second order accurate in time. Now the question is, which of these schemes can be used for reaction-diffusion systems or in general for a given ODEs/PDEs. For stability reasons, one may prefer the implicit schemes, which are more accurate and allow one to take larger time steps. At the same time, these schemes are expensive to implement due to the fact that at every time step one has to approximate system of equations, and with the nonlinearity we have this is not cost effective. Explicit schemes are cheaper to implement but are only conditionally stable, which means that in some instances, one might need to take small time steps to achieve the desired accuracy. We will now derive the so-called IMEX splitting θ-method for the system 3.5. For the diffusion terms we take $\theta = 1$ and for the reaction terms we take $\theta = 0$. We treat the diffusion terms implicitly in Fourier space and the reaction terms explicitly in real space as follows:

From the system 3.5, we have:

$$\begin{aligned} S^{j+1} - S^j &= \Delta t \underline{\mathrm{L}} S^{j+1} + \Delta t f(S^j, I^j), \\ I^{j+1} - I^j &= \Delta t \underline{\mathrm{L}} I^{j+1} + \Delta t g(S^j, I^j), \end{aligned} \tag{3.7}$$

where $\underline{\mathrm{L}} = -d\Delta$,
Now, the diffusion parts (linear part) first in Fourier space as follows

$$\begin{aligned} \widehat{S}^{j+1} &= (\underline{\mathrm{l}} + \Delta t d_1 \underline{\mathrm{L}})^{-1}, \\ \widehat{I}^{j+1} &= (\underline{\mathrm{l}} + \Delta t d_2 \underline{\mathrm{L}})^{-1}, \end{aligned} \tag{3.8}$$

where $\underline{\mathrm{l}}$ is an identity matrix and $\widehat{S}$ and $\widehat{I}$ are the Fourier transforms of S and I for the Laplacian (diffusion) terms respectively. Hence, our $(j+1)$ solutions are thus:

$$\begin{aligned} S^{j+1} &= \widehat{S}^{j+1} + \Delta t f(\widehat{S}^{j+1}, \widehat{I}^{j+1}) \\ I^{j+1} &= \widehat{I}^{j+1} + \Delta t g(\widehat{S}^{j+1}, \widehat{I}^{j+1}) \end{aligned} \tag{3.9}$$

We can observe that system 3.8 is the predictor and system 3.9 is the corrector.

3.2.3 Benchmarking

First we check the stability of the method, that is, whether the scheme 3.9, to be used for numerically solving the system 3.4 will converge with correct order. Since this is an IMEX Euler's method, we expect to have a convergence of order one. Since there is no known analytical or closed form solutions to the system 3.4, it is not possible to check directly how well the numerical solutions compare with the exact solutions. Hence,

one needs to construct a solution that would satisfy a modified version of the system 3.4 from which it should be possible to indirectly check the stability and performance of the numerical scheme and the code itself. In order to provide numerical verification of the convergence rate, we insert a source term such that the exact solution of the system 3.4 is:

$$\Xi(x, y, t) = (\sin(x) + \cos(y)) \exp(-t) \tag{3.10}$$

For simplicity we take, $S = I = \Xi$ which does not satisfy the model 3.4, but it is the exact solution to the modified model below. To obtain the modified model, we find the time and spatial derivatives of S and I, and substitute these quantities into 3.4 and compute the remainders as follows.

$$\begin{aligned} S_t = I_t &= -(\sin x + \cos y)e^{-t}, \\ S_{xx} = I_{xx} &= -(\sin x)e^{-t}, \\ S_{yy} = I_{yy} &= -(\cos x)e^{-t}. \end{aligned} \tag{3.11}$$

Subtituting these quantities into 3.4, we have the reminders F_1 and F_2 as follows:

$$\begin{aligned} F_1 &= (1 - d_1 + \gamma + r) - \beta\Xi^{p+q-1} + \tfrac{R}{\Xi}, \\ F_2 &= (1 - d_2 - \gamma - r - \mu) - \beta\Xi^{p+a-1}. \end{aligned} \tag{3.12}$$

Adding F_1 and F_2 to the right hand sides of model 3.4, we obtain the modified model below.

$$\begin{aligned} \partial_t S &= d_1 \Delta S - \beta S^p I^q - \gamma S + R + rI + F_1 \\ \partial_t I &= d_2 \Delta I + \beta S^p I^q - (\gamma + r + \mu)I + F_2. \end{aligned} \tag{3.13}$$

The exact solution 3.10 now satisfies the above modified model. Therefore, we will use the modified model to test the method we described above and the code we will use in the numerical simulation. We now solve 3.13 using the IMEX method and compute

the error from the exact solution 3.10. We consider a numerical approximation of the exact value Ξ. A measure of the error (e_h) from the exact solution is given by

$$e_h = |u_h - \Xi| \leq Ch^p \tag{3.14}$$

where u_h is the approximate solution and Ξ is the exact solution, C is a constant, h is the time step and p is the order of the method. We are often faced with the problem of how to determine the order of convergence p given a sequence of approximations $u_1, u_2, ...$ This can be a good check that a method is correctly implemented (if p is known) and also a way to get a feeling for the credibility of an approximation u_h. We can either be in the situation that the exact value Ξ is known or more commonly, that Ξ is unknown. The standard way to get a precise number for p is to halve the time step h and look at the ratios of the errors $|u_{h_1} - \Xi|$ and $|u_{h_2} - \Xi|$ i.e.

$$p \approx \frac{\log e(h_1) - \log e(h_2)}{\log(h_1) - \log(h_2)}$$

Here p is called the Experimental Order of Convergence (EOC). Therefore, in general the Experimental Order of Convergence (EOC) is given by

$$\text{EOC}_{j-1} \approx \frac{\log e(h_j) - \log e(h_{j-1})}{\log(h_j) - \log(h_{j-1})}, \tag{3.15}$$

where h is the time step and $j = 2, 3, ..., N$ is the time loop. This means, for each h_j we re-compute our discrete solution and compare it with the exact solution to re-compute the error. We do this computation j-times and plot the results in the same figure. This way we can see how the error behaves as we refine or make our solution smoother.

Since we are using IMEX Euler's method, we expect the EOC to be around one or exactly one. Now, we compute the error in various norms, including L^2, H^1 and L^∞ norms and for each of these quantities we compute their experimental order of convergence. First, we will present these on a loglog plot and summarise the results in tabular form as follows. In figure 3.1 and table (3.1) below, we take the loglog plot of the errors as

functions of time against the time step h. Note that the L^2-error, the H^1-error and the max-error are the discrete errors in L^2, H^1 and maximum norms in time.

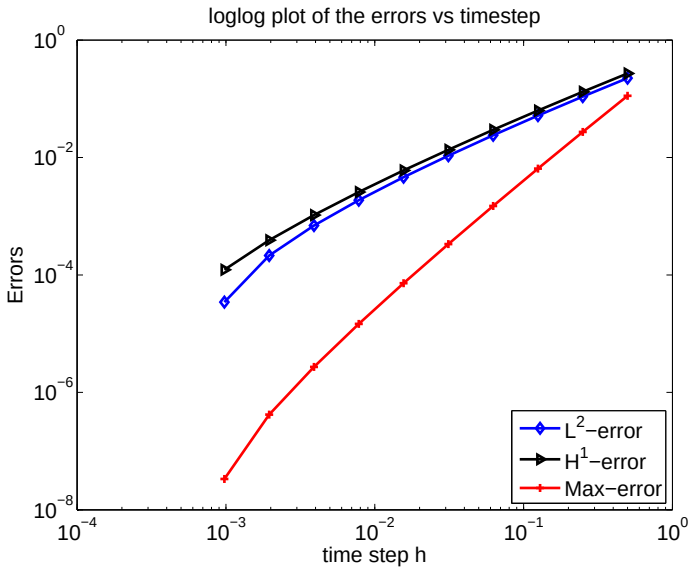

Figure 3.1: errors for $\beta = 0.1$, $R = 0.35, \gamma = 0.1, r = 0.5, \mu = 0.1, d_1 = 10, d_2 = 1, p = 2, q = 2$

j	h	L^2-Error	L^2-EOC	H^1-Error	H^1-EOC	Max-Error	Max-EOC
1.00000	0.50000	2.25086e-01	1.02329	2.70004e-01	1.02116	1.12543e-01	0.93329
2.00000	0.25000	1.09179e-01	1.04157	1.31637e-01	1.03748	2.72948e-02	0.95157
3.00000	0.12500	5.17796e-02	1.06077	6.30086e-02	1.05449	6.47244e-03	0.97077
4.00000	0.06250	2.39366e-02	1.08148	2.95515e-02	1.07263	1.49604e-03	0.99148
5.00000	0.03125	1.07278e-02	1.10437	1.35357e-02	1.09232	3.35244e-04	1.01437
6.00000	0.01562	4.61824e-03	1.13051	6.02251e-03	1.11430	7.21600e-05	1.04051
7.00000	0.00781	1.87737e-03	1.16146	2.57977e-03	1.13953	1.46669e-05	1.07146
8.00000	0.00391	6.95563e-04	1.19987	1.04698e-03	1.16964	2.71704e-06	1.10987
9.00000	0.00195	2.13815e-04	1.25026	3.89688e-04	1.20714	4.17608e-07	1.16026

Table 3.1: The L^2, H^1, L^∞ errors and their EOCs for $h/20$ and $\beta = 0.9$

In the above subsection, we have presented benchmark results for the modified model 3.13. We computed the EOC and the error in three different norms that is, L^2, H^1 and

L^∞. As we can observed from figure 3.1 and the table (3.1) above, the error behaved well and the EOC confirmed the method converged with the order of one. Also, we observed that as we refined the discrete solutions, the errors get better. The maximum error is better compare to the L^2 and H^1 errors and this agrees well with theory in error analysis. This showed that the method actually solved our model. Also, from the errors we have seen that as we refined our discrete solution the errors got better. The main reasons for the above section are to test our codes and the IMEX method described above to be sure if the codes and the method actually solved our model. From the error analysis and the EOC, we are now certain that our codes and method actually solved our model perfectly. Therefore, we will use this method in the numerical simulation section. Also, this means that the IMEX-schemes are appropriate for reaction-diffusion models compare to finite differences which we used initially and were very slow for large computational time. Our convergence results in figure 3.1 and table (3.1) above are comparable to the results in for instance [Tri10] and [Nag07].

3.3 Turing instability

The formal study of pattern formation mechanisms in the life sciences owes much to Alan Turing's seminal paper [Tur52] on a mathematical model for a pattern-generating chemical reaction. The motivation behind the model was to investigate the symmetry-breaking and differentiation mechanisms in biological organisms. Turing's work presented a simple mechanism that can generate patterns from an initially homogeneous medium. By performing linear stability analysis, he showed it is possible to determine conditions for the existence of stable spatially-inhomogeneous solutions. In physical terms this means that under some conditions, a two-component chemical reaction can evolve into a stable non-trivial pattern. This new concept took many years to be accepted, despite early experimental evidence Ignacio [Ign12]. Alan Turing research work concluded that the process of diffusion alone can cause symmetry breaking. We now perform the linear stability analysis of uniform solutions of the two component reaction-diffusion system

3.4. Turing's surprising and important discovery was that there exist conditions under which the spatially uniform steady state is stable in the absence of diffusion and can become unstable to non-uniform perturbations because of diffusion. One can choose perturbations that consist of Fourier modes and some kinds of randomness around the equilibrium states S^* and I^* but this is a crude way to the stability of the system. The more standard way to perform stability analysis and to determine Turing conditions of the system 3.4 is to linearise the system around the steady state and diagonalise the resulting Jacobian. We will find the Turing space which is the region of (in)stability in the parameter regime.

3.3.1 Derivation of the Turing instability conditions

By linearising the model 3.4 near the steady state, we obtain the following linear system:

$$\frac{\partial W}{\partial t} = d\nabla^2 W + J_0 W \tag{3.16}$$

where:

$$W = \begin{pmatrix} W_1 \\ W_2 \end{pmatrix} = \begin{pmatrix} S - S^* \\ I - I^* \end{pmatrix},$$

$$d = \begin{pmatrix} d_1 & 0 \\ 0 & d_2 \end{pmatrix},$$

$$J_0 = \begin{pmatrix} \frac{\partial f}{\partial S} & \frac{\partial f}{\partial I} \\ \frac{\partial g}{\partial S} & \frac{\partial g}{\partial I} \end{pmatrix}_{(S^*, I^*)} = \begin{pmatrix} f_S & f_I \\ g_S & g_I \end{pmatrix}.$$

Here J_0 is community matrix.

In order to solve a linear system of the form 3.16, it is instructive to necessary to first define a solution which is time-independent for the Laplacian operator ∇^2 as $\varphi_m(r)$:

$$\nabla^2 \varphi_m(r) = -k^2 \varphi_m(r), \quad \varphi_m(r) = 0 \quad \text{on} \quad \partial\Omega \tag{3.17}$$

$\partial\Omega$ is a closed boundary in the domain $\Omega \in [0, L]^2$. If we solve 3.17 satisfying $\varphi_n(r)$ vanishing at $r = 0$ and $r = L$ the general solution is given by:

$$\varphi_m(r) = c_1 \cos(\frac{m_1 \pi r_x}{L}) + c_2 \sin(\frac{m_2 \pi r_y}{L}) \tag{3.18}$$

Applying the boundary conditions at $r = 0$ and $r = L$ we obtain the following simplified solution:

$$\varphi_m(r) = c_2 \sin(\frac{m\pi r}{L}) \tag{3.19}$$

where the eigenvalue

$$k = \frac{m\pi}{L} \tag{3.20}$$

is refered to as the *wavenumber* which is inversely proportional to the *wavelength* [Rob94] given by

$$\varpi = \frac{2\pi}{k} \tag{3.21}$$

and the typical eigenfunction is then:

$$\varphi_m(r) \propto \sin\left(\frac{m\pi r}{L}\right). \tag{3.22}$$

Now let us return to our system 3.16. Since the system is linear, the solution $W(r, t)$ can be written as the sum of eigenfunctions

$$W(r, t) = \sum_j a_j e^{\lambda t} \varphi_j(r) \tag{3.23}$$

or more explicitly,

$$\begin{pmatrix} S \\ I \end{pmatrix} = \begin{pmatrix} a_1 \\ a_2 \end{pmatrix} \sum_j e^{\lambda t} \sin\left(\frac{k\pi r}{L}\right) \tag{3.24}$$

Now, substituting 3.24 into 3.16 the $\lambda' s$ are obtained from the roots of the characteristic polynomial:

$$\begin{aligned} \lambda W(r,t) &= J_0 W(r,t) - dk^2 W(r,t) \\ \lambda I_0 &= J_0 - dk^2 \\ J_0 &- dk^2 - \lambda I_0 = 0 \\ |J_0 &- dk^2 - \lambda I_0| = 0 \end{aligned} \tag{3.25}$$

where I_0 is an identity matrix and

$$d = \begin{pmatrix} d_1 & 0 \\ 0 & d_2 \end{pmatrix} \tag{3.26}$$

is a diagonal matrix. Therefore, the matrix J_k is thus

$$\begin{aligned} J_k &= J_0 - dk^2 \\ &= \begin{pmatrix} f_S - d_1 k^2 & f_I \\ g_S & g_I - d_2 k^2 \end{pmatrix} \end{aligned} \tag{3.27}$$

This leads to the relation

$$\lambda^2 - \lambda[\text{trace} J_0 - k^2(d_1 + d_2)] + h(k^2) = 0 \tag{3.28}$$

where

$$h(k^2) = \det J_0 - k^2(d_2 f_S + d_1 g_I) + d_1 d_2 k^4. \tag{3.29}$$

The eigenvalues are therefore given by

$$\lambda_{1,2}(k) = \frac{\text{trace}J_k \pm \sqrt{(\text{trace}J_k)^2 - 4\det J_k}}{2}. \tag{3.30}$$

From the expression 3.30, it follows that for both eigenvalues to be non-positive, the trace must be negative and the determinant must be positive. For the matrix 3.27 the criteria for stability take the form

$$\text{trace}(J_k) = f_S + g_I - k^2(d_1 + d_2) < 0 \tag{3.31a}$$

$$\det(J_k) = (f_S - d_1 k^2)(g_I - d_2 k^2) - f_I g_S > 0 \tag{3.31b}$$

If these two conditions hold for all wave numbers k, then the steady state is linearly stable with respect to any small pertubations.

Now we derive conditions under which the model 3.4 will have Turing instability and consequently will exhibit stationary space-inhomogeneous patterns in terms of parameters. Turing's idea was that diffusion of substances (chemicals) may somehow cause diffusion-driven and a pattern forming instabilities. The first step in the analysis of Turing instability is to assume that the diffusion is absent. In this case from inequalities 3.31a and 3.31b we obtain the conditions for stability of the steady state in the absence of diffusion from the non-spatial model 2.1 as follows:

- $f_S + g_I < 0$
- $f_S g_I - f_I g_S > 0$

If these two conditions hold, it means that the system 2.1 in absence of diffusion (non-spatial model) will be stable. Considering the case when the diffusion is present, we have

$$\text{trace}(J_k) = f_S + g_I - k^2(d_1 + d_2) < f_S + g_I. \tag{3.32}$$

This means the trace of J_k is always negative. Therefore, the only possible way to have Turing instability is for the sign in the second inequality 3.31b to be reversed so that the determinant of J_k will be negative. Now the problem is to find the values of parameters for which the determinant of J_k is negative. The inequality 3.31b shows that the determinant of J_k is a parabola in the wave number k^2 and hence linear instability will occur when the minimum value of this parabola first becomes negative. To obtain this minimum value for the wave number k denoted by k_m we take the derivative of the determinant of J_k with respect to k as follows:

$$\begin{aligned}
\frac{d(\det J_k)}{dk} &= (-2d_2k)(f_S - d_1k^2) + (-2d_1k)(g_I - d_2k^2) \\
&= -2k[(d_2f_S + d_1g_I) - 2d_1d_2k^2] \\
4d_1d_2k^3 &= 2k(d_2f_S + d_1g_I) \\
&\text{hence} \\
k_m^2 &= \frac{d_2f_S + d_1g_I}{2d_1d_2}
\end{aligned} \tag{3.33}$$

The value of $\det J_k$ at this minimum is obtained by substituting 3.33 into 3.27 which gives

$$\det J_k = f_Sg_I - f_Ig_S - \frac{(d_2f_S + d_1g_I)^2}{4d_1d_2}. \tag{3.34}$$

The expression 3.34 is negative if

$$(d_2f_S + d_1g_I)^2 > 4d_1d_2(f_Sg_I - f_Ig_S). \tag{3.35}$$

The RHS of 3.35 is positive due to 3.32 and the LHS is also positive. It follows that either f_S or g_I must be negative for this condition to be satisfied. Therefore, it is wise to choose $f_S < 0$ from 3.4. We also require that f_I and g_S to have opposite signs.
In figure 3.2 below, we plot the largest eigenvalue as function of the modes k^2 for the inqualities 3.31a and 3.31b.

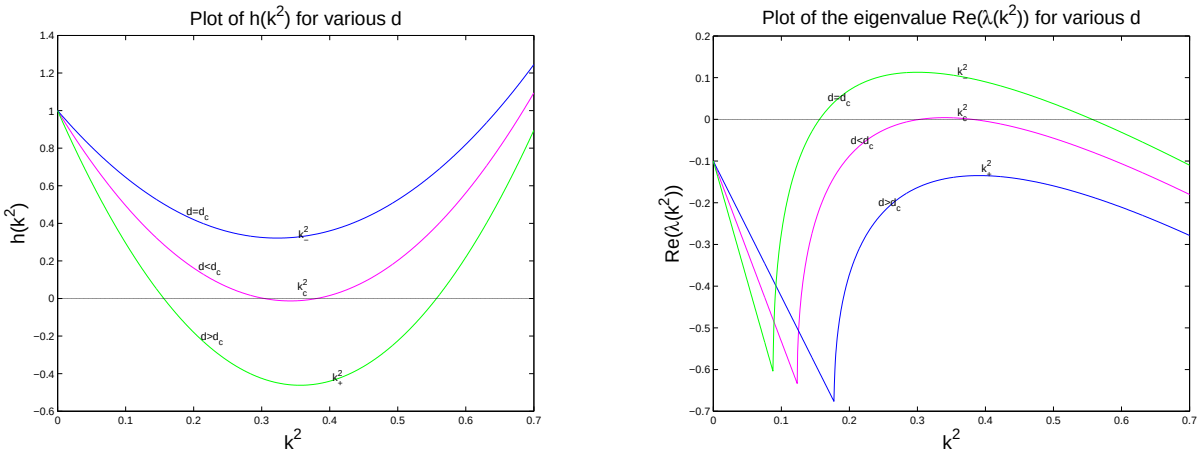

(a) (b)

Figure 3.2: (a) This shows how h varies as a function of k^2, (b) this shows the largest eigenvalue as a function of k^2, parameter values are $\beta = 0.5, R = 0.35,\ r = 0.5,\ \mu = 0.1,\ d_1 = 10,\ d_2 = 1, p = q = 2$

In figure 3.2 above, (a) shows h as a function of the modes k^2, here $h(k^2)$ is the determinant of J_k i.e the community matrix in the presence of diffusion. This expression is important for Turing analysis because from the above analysis we know trace of $J_k < 0$, therefore, the only way to have Turing is for $h(k^2) < 0$. From the figure in (a) above, we obtain Turing instability when $d > d_c$ for a finite range of wavenumbers k^2 creating unstable modes where the real part of the largest eigenvalue becomes positive. Figure (3.2(b)) shows the real part of the largest eigenvalue as functions of the modes k. We see that when $d < d_c$ we have finite range of linear stable modes and for $d > d_c$, we have finitely many linearly unstable modes.

So far we have the necessary and sufficient conditions for Turing instability which can be summarised as follows.

Summary of the necessary and sufficient Turing instability conditions

The conditions below are one of my main results.

$$\begin{aligned} &\bullet f_S + g_I < 0 \\ \Rightarrow\ &\beta S^{p-1} I^{q-1}[qS - pI] - (2\gamma + r + \mu) < 0 \end{aligned} \tag{3.36}$$

$$\begin{aligned} &\bullet f_S g_I - f_I g_S > 0 \\ \Rightarrow\ &\beta S^{p-1} I^{q-1}[(\gamma + \mu)pI - \gamma qS] + \gamma(\gamma + r + \mu) > 0 \end{aligned} \tag{3.37}$$

$$\begin{aligned} &\bullet d_2 f_S + d_1 g_I > 0 \\ \Rightarrow\ &\beta S^{p-1} I^{q-1}[d_1 qS - d_2 pI] - [\gamma(d_1 + d_2) + r + \mu] > 0 \end{aligned} \tag{3.38}$$

$$\begin{aligned} &\bullet (d_2 f_S + d_1 g_I)^2 > 4 d_1 d_2 (f_S g_I - f_I g_S) \\ \Rightarrow\ &[\beta S^{p-1} I^{q-1}(d_1 qS - d_2 pI) - (\gamma(d_1 + d_2) + r + \mu)]^2 > 4 d_1 d_2 [\beta S^{p-1} I^{q-1}[(\gamma + \mu)pI - \gamma qS] + \gamma(\gamma + r + \mu)] \end{aligned} \tag{3.39}$$

In the above four conditions, S and I denote steady state values of the state variables. We now compute the Turing space for the model 3.4, that is, we identify a region in the (γ, β) parameter plane where the endemic steady state undergoes Turing stability/instability. In the figures below we have the regions of boundary of stability. In figure 3.3.1 below, we show the Turing space for the system 3.4 satisfying the above four conditions.

Figure 3.3: The Turing space in the (γ, β) plane showing the regions of (in)stability for $R = 0.35,\ r = 0.5,\ \mu = 0.1,\ d_1 = 10,\ d_2 = 1, p = 2,\ q = 2$, the *blue region* corresponds to stable endemic steady state", and *red region* corresponds to unstable endemic steady state.

The figure above shows regions of Turing instability for the endemic steady state in the two parameter space (γ, β). This figure will guide us in the next section during the numerical simulation.

Two of the necessary and sufficient conditions of Turing instability as shown in the above analysis are
(i) $f_S < 0$,
(ii) f_I and g_S must have opposite signs.
For the model 3.4, we have:

$$f_S = -(\beta p S_*^{p-1} I_*^q + \gamma) < 0,$$

since both the state variables and the parameters are non-negative, hence the first condition is satisfied. For the second condition one has to check whether f_I and g_S have opposite signs as follows:

$$f_I = -\beta q S_*^p I_*^{q-1} + r = -[q(\gamma+\mu) + r(q-1)] < 0, \quad \text{because } q \geq 1 \tag{3.40}$$

and

$$g_S = \beta p S_*^{p-1} I_*^q > 0. \tag{3.41}$$

From equations 3.40 and 3.41, it follows that the second condition is also satisfied, and hence Turing instability will occur provided system parameters satisfy the four conditions above and this can be seen in figure 3.3.1 above.

3.4 Numerical experimentation

Initially we used finite differences to numerically approximate the solutions of system 3.4 but these methods converge slowly, especially for large computational time, and

another problem is the restriction on the time steps for the explicit schemes. While the implicit schemes are faster, one needs to invert matrices which is very costly for large computational time. Hence, the need for another method that is both fast and accurate becomes important. One of such methods that have been tested and proven to be fast and accurate is the *Implicit-Explicit (IMEX) method* introduced in section 3.2 earlier which computes diffusion terms implicitly in Fourier space, while interactions are evaluated explicitly in real space. The reason for using this method is because the nonlinearity usually cannot be handled implicitly in an easy way, therefore, the linear part is treated implicitly, and the nonlinearity and the reaction terms explicitly. For details of these methods see [Han09], [Alf12], [Zoh13].

3.4.1 Numerical experiments

This subsection presents results of numerical simulation of the system 3.4 with the method described in section 3.2. Now we will numerically study the dynamics of the system 3.4 as the bifurcation parameter (β) is varied. And the parameters are located in the Turing space (cf., Figure 3.3.1), the region where Turing instability occurs. Initial conditions for the simulations were taken to be perturbations around the endemic steady state. In 1D, these perturbations quickly settle on a stable stationary spatially periodic solution (figures 3.6 and 3.9) with a wavelength close to the one prescribed by the linear analysis from the previous section. In two spatial dimensions, however, the situation is different. The numerical results in two spatial dimensions are presented in the figures (3.4, 3.5, 3.7, 3.8, 3.10, 3.11, 3.12) below for different values of the bifurcation parameter β. After a short time, the system picks up the spatial period of the Turing pattern, and initial perturbations grow. At a later stage of the evolution, this growth is damped by the nonlinearities in the equations, and as a result the system finally reaches stable patterns (e.g. spots, stripes, spot-stripe mixtures, spot-holes), as shown in figures 3.4−3.12 below.

For the first five numerical experiments (figures 3.4, 3.5, 3.7, 3.8, 3.10) we fix all parameters and vary β to observe the dynamics and patterns that evolve from this as time progresses. We choose β as the control parameter in this model, since the transmission

rate is the crucial parameter that controls the rate of new infections. First, we take a small value of $\beta = 0.1$ and observe the evolution of patterns in this case. Thereafter, we take higher values of β and at each stage repeat the experiments at different times. While, figure 3.11, we test the effects of the recovered rate r on the dynamics of the system and finally, in figure 3.12, we check the effects of higher values of the exponent q on the dynamical behaviour of the system.

In order to illustrate the application of our results to real world situations, we estimate our parameter's values to be close to real data of some infectious diseases whose dynamics can be described by system 3.4. We did not use real data from any particular disease because from the beginning we wanted our model to be more general but not to focus on only one disease in the entire research. With our parameter's estimates in the Turing space (3.3.1), we hope our results can describe the dynamics of some diseases like influenza, chlamydia infection, not from reality but from view point of dynamical asymptotic behaviour. Also, the SIS models are known to be adequate for many bacterial diseases (e.g. meningitis), as well as for numerous sexually transmitted infections. For instance, influenza is known to be extremely contagious and this can fit well in our model and can be described by the nonlinear incidence rate $\beta S^p I^q$ which is an alternative to introducing multiple contacts as a multiplier in a disease transmission term. The influenza infection lasts for about a week, affects annually $5-15\%$ of the population, and causes between 250000 and 500000 deaths every year around the world [Who03]. Even though in the industrialised world influenza is rather harmless and its deaths are mostly associated with elderly of 65 years of age and over, in tropics the influenza outbreaks tend to have high attack and case-fatality rates. For example, in summer 2002 in Madagascar 30000 cases of influenza were reported and 800 deaths occurred despite rapid intervention [Wer02]. We assume the following estimates for our model parameters which are not real data. The recruitment rate is taken to be $R = 0.35$, transmission rate β can be estimated to be in the interval $(0, 1]$, the recovery rate is $r \in (0, 1)$ (with 5 being the average length of infection). Finally, the natural death rate is taken to be $\gamma = 0.1$, and the disease-induced death rate is assumed to be $\mu = 0.1$. We take the powers p and q as $p = 2$

and $q = 2$, respectively. Again, we assume that if healthy individuals can walk (say) 10km, then we assume sick individuals can only walk (say) 1km. Therefore, the diffusion coefficients of the healthy and sick individuals are $d_1 = 10$ and $d_2 = 1$.

In the experiment below, we take a very small β with value 0.1 which corresponds to low transmission rate in the I-class. We want to observe the kind of patterns we can get from this as time progresses. As initial conditions, we will choose some random perturbations about the steady state of the system. This first numerical experiment is to test the effect of β at different values on the dynamics of the system as time increases. In figure 3.4 below we observe the evolution of patterns at four different times. At time $t = 0$, we have small random perturbation of the homogeneous steady state solution. In figure 3.4(b), which correspond to $t = 1000$, one observes sparsely spoted patterns which are scattered in the domain. Figure 3.4(c) corresponds to $t = 10000$, we now see clusters of spoted patterns scattered in the domain. Figure 3.4(d) corresponds to $t = 100000$ where spot pattern fills the whole domain and is settled.

In the numerical simulations below, we observed different types of dynamical behaviours for the system 3.4 in the Turing space. We have found that the distributions of susceptible and infected individuals are always of the same type. Therefore, we will restrict our numerical analysis of the pattern formation to one distribution. In this section, we show the distribution of only the infected individuals I. For details on each figure and its application (biologically/epidemiological) to epidemic spread and control see the next section on discussion.

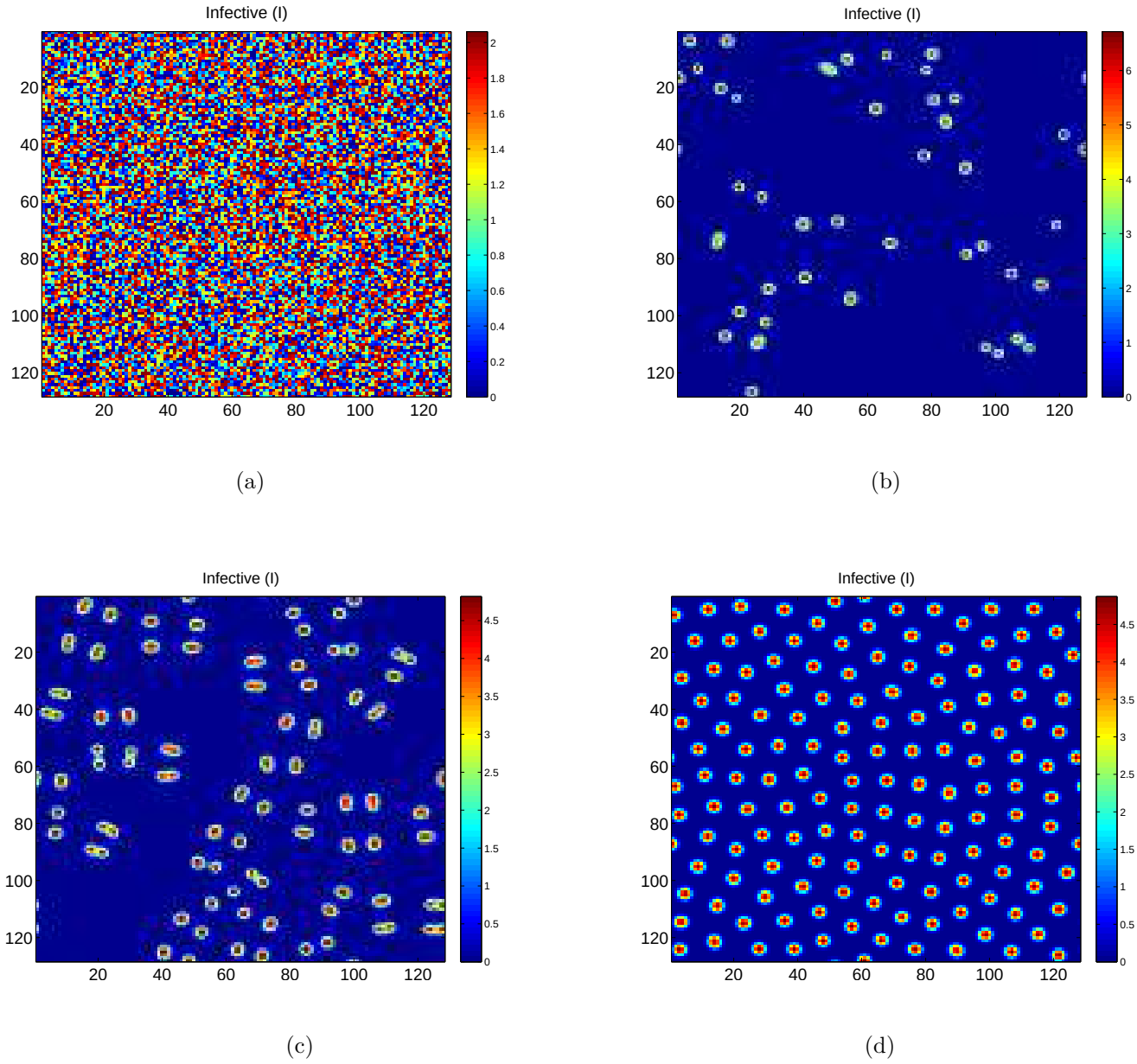

(a) (b)

(c) (d)

Figure 3.4: Time evolution corresponding to $\beta = 0.1$: (a) this is the initial solutions of 3.4 for $t = 0$. We can see that initially we have some random pertubations about the steady state for the I individual populations, (b) $t = 1000$, (c) clusters of spot patterns of 3.4 for $t = 10000$ and (d) fully matured and stable spots of 3.4 for $t = 100000$. Other parameters are: $R = 0.35,\ \gamma = 0.1,\ r = 0.5,\ \mu = 0.1,\ d_1 = 10,\ d_2 = 1,\ p = 2,\ q = 2$.

In the above figure, we can see that initially we have random pertubations, gradually sparsely distributed spots begin to emerge and at the later stage of the simulation these structures settled on stable spots. We have hot or red spots (maximum density of I) on

a blue background (minimum density of I). The infectious are isolated zones with high densities and the other region which has low densities is larger, this region is safe.

In this experiment, we increase the value of β to 0.3 and observe the dynamical behaviour of the system.

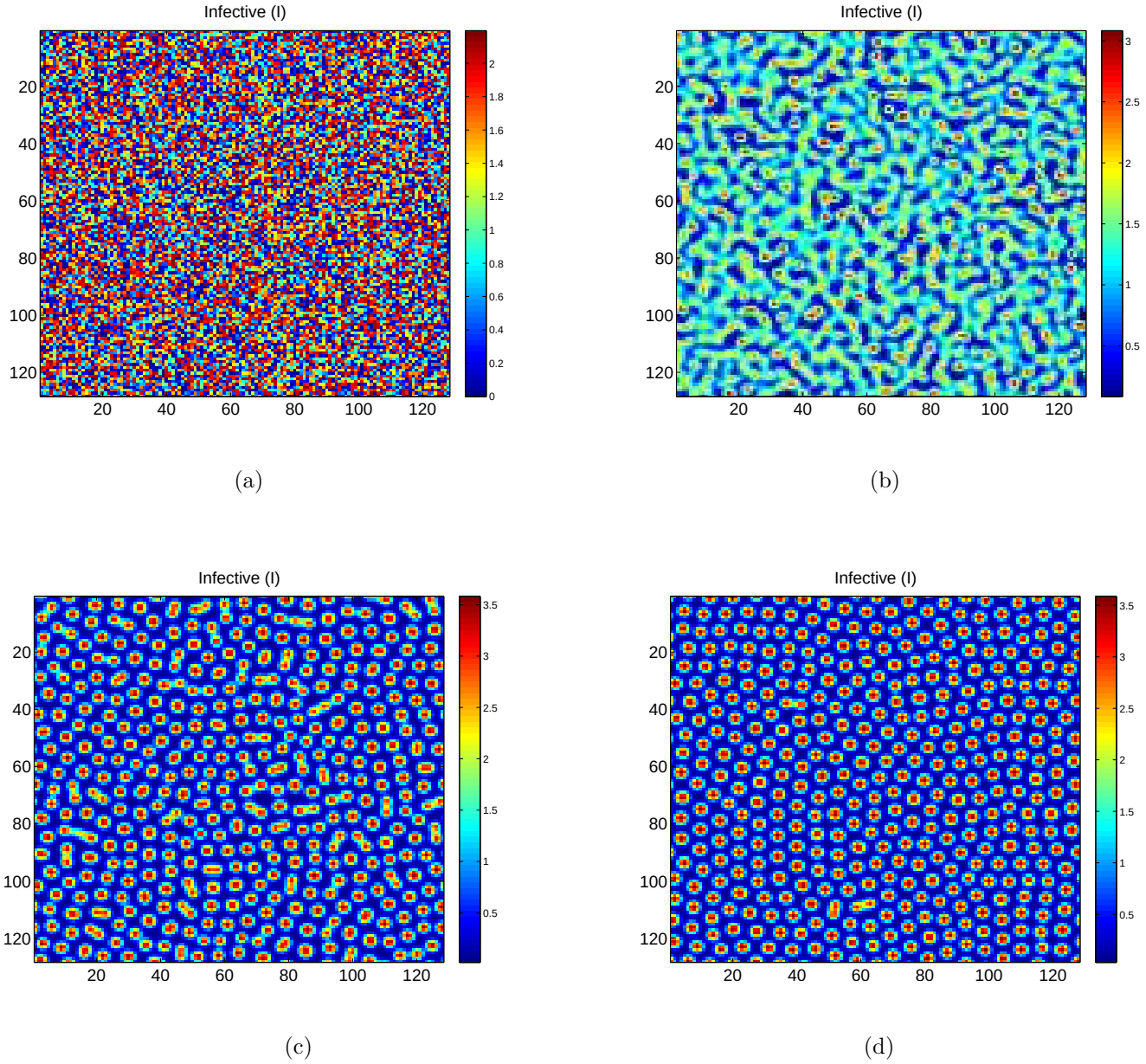

(a) (b)

(c) (d)

Figure 3.5: Time evolution corresponding to $\beta = 0.3$, (a), this is the initial solutions of 3.4 for $t = 0$, (b) is for $t = 1000$, (c) is for $t = 10000$ and (d) is for $t = 100000$. Other parameters are: $R = 0.35,\ \gamma = 0.1,\ r = 0.5,\ \mu = 0.1,\ d_1 = 10,\ d_2 = 1,\ p = 2,\ q = 2$.

In figure 3.5 above, initially we have a small pertubation of the homogeneous solution for

$t = 0$ (figure 3.5(a)) and immediately the system picks up an irregular patterns; choatic type of pattern (figure 3.5(b)) that later settles on a fully spot pattern at $t = 10000$ (figure 3.5(c)). And in figure (figure 3.5(d)), we have fully stable spot patterns. The two figures above (figures 3.4 and 3.5), we have low transmission rates and the system settled on stable spot patterns at the later stage of the simulations. The spots are red hexagons (maximum density of I) on a blue region or background (minimum density of I) which we called red-holes. The infectious are isolated zones with high population densities and are disconnected. The remainder regions are of low densities which are larger than the red-holes areas. From epidemic point of view, this means there is no epidemic outbreak in the area. Therefore, this area is safe.

In the experiment below, we show the solution profiles or I-cross section for $\beta = 0.3$ for the system 3.4.

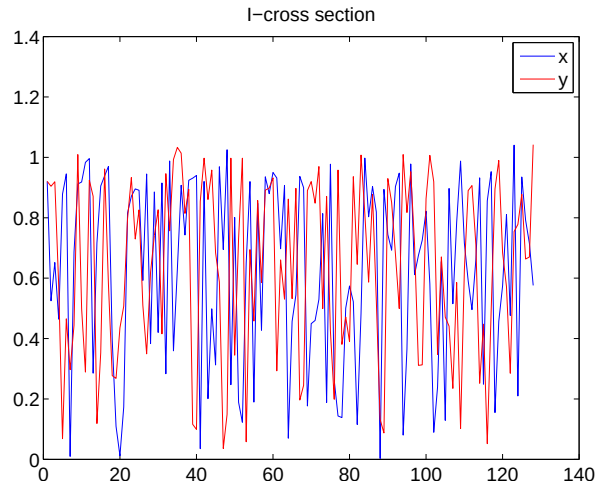

(a)

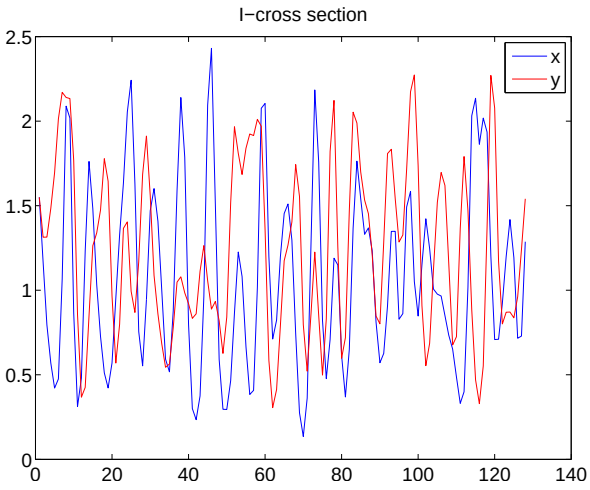

(b)

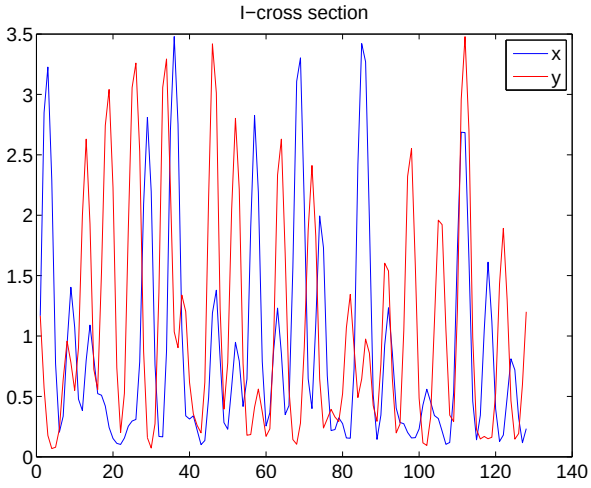

(c)

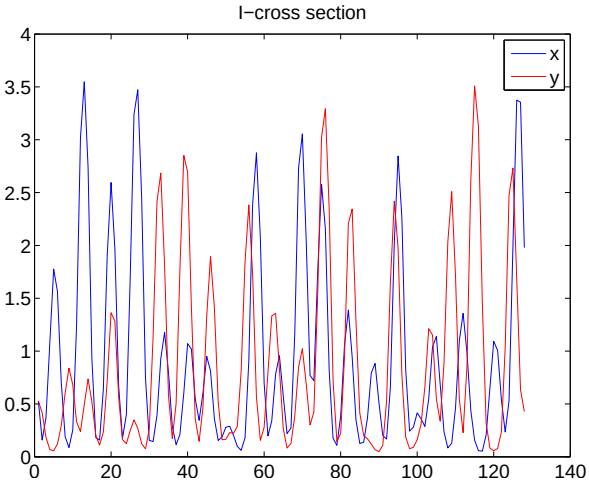

(d)

Figure 3.6: I-solution profiles corresponding to $\beta = 0.3$, (a), this is the initial solution profile of system 3.4 for $t = 0$, (b) is for $t = 1000$, (c) is for $t = 10000$ and (d) is for $t = 100000$. Other parameters are: $R = 0.35,\ \gamma = 0.1,\ r = 0.5,\ \mu = 0.1,\ d_1 = 10,\ d_2 = 1,\ p = 2,\ q = 2$.

In figure 3.6 above, we have the solution profiles for the system 3.4 for $\beta = 0.3$. Initially we have high profiles of fluctuations which is due to the randomness initial data. The profiles look spatially periodic fluctuations which can be compared to the figures in [Alt06]. Although, in that paper, the authors considered the effects of seasonal

transmission and birth rates on the dynamics of inluenza. Our results showed similar profile behaviours of spatially periodic-like fluctuations which we think can be attributed to the Turing instability. However, we did not exploit more on the spatially periodic behaviour in this Chapter since we are more concerned with spatial dynamics. Here, $x = I(:, 1)$ and $y = I(1, :)$.

Now, we increase β to 0.5 to investigate whether other types of spatial patterns can be exhibited by the system.

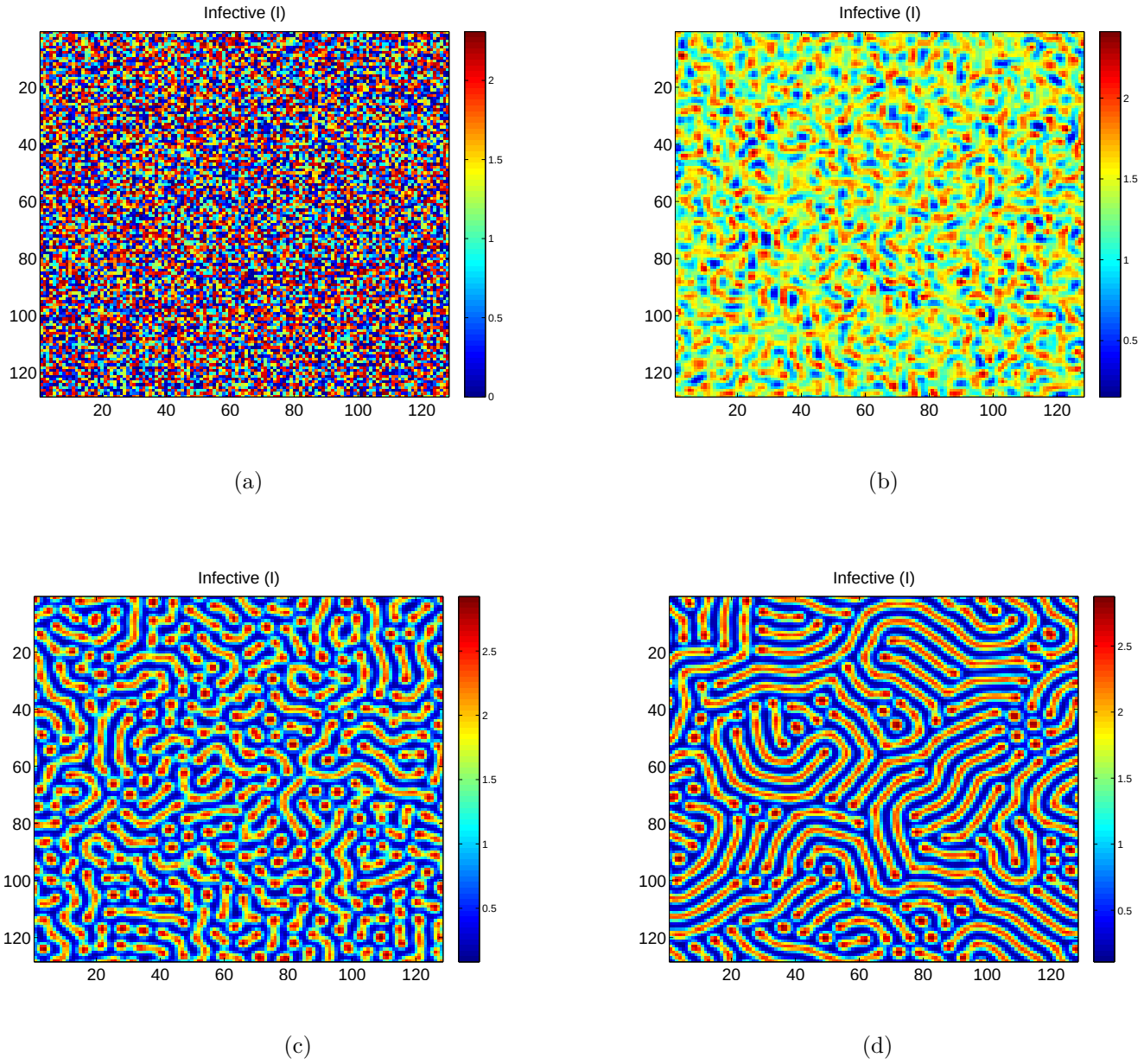

(a) (b)

(c) (d)

Figure 3.7: Time evolution corresponding to $\beta = 0.5$, (a) this is the initial solutions of 3.4 for $t = 0$, (b) is for $t = 1000$, (c) is for $t = 10000$ and (d) is for $t = 100000$. Other parameters are: $R = 0.35,\ \gamma = 0.1,\ r = 0.5,\ \mu = 0.1,\ d_1 = 10,\ d_2 = 1,\ p = 2,\ q = 2$.

In the above simulation we have $\beta = r = 0.5$ (i.e. the transmission rate is equal to the recovery rate), we are interested in these two parameters because of their biological relevant in our model. Figure 3.7 above, illustrates a competition between spots and

stripes, and gradually the spots decay to stripe patterns. Eventually, at $t = 10000$ we have matured stripe (labyrinthine) patterns with few decaying spots.

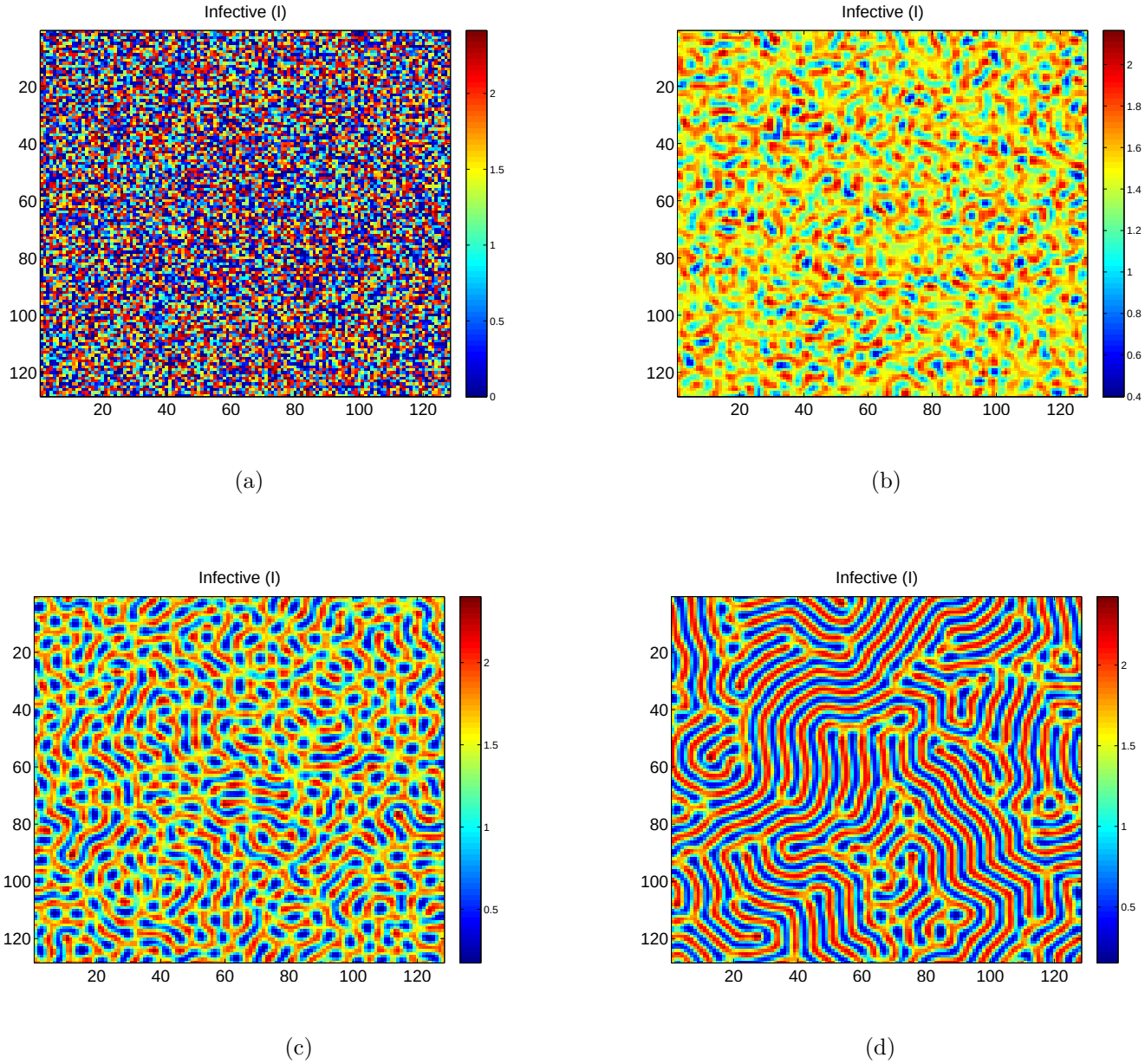

(a) (b)

(c) (d)

Figure 3.8: Time evolution corresponding to $\beta = 0.7$, (a) this is the initial solutions of 3.4 for $t = 0$, (b) is for $t = 1000$, (c) is for $t = 10000$ and (d) is for $t = 100000$. Other parameters are: $R = 0.35$, $\gamma = 0.1$, $r = 0.5$, $\mu = 0.1$, $d_1 = 10$, $d_2 = 1$, $p = 2$, $q = 2$.

In the above experiment, we increase the value of β to 0.7 and all other parameters are

fixed and then we observe the time evolution of the infective individuals. As time evolves the solutions settled on a stable labyrinthine pattern at $t = 100000$. In figures (3.7 and 3.8) above, we have labyrinthine patterns. From epidemic point of view the disease is significant and there is a possibility of epidemic outbreak in these areas.

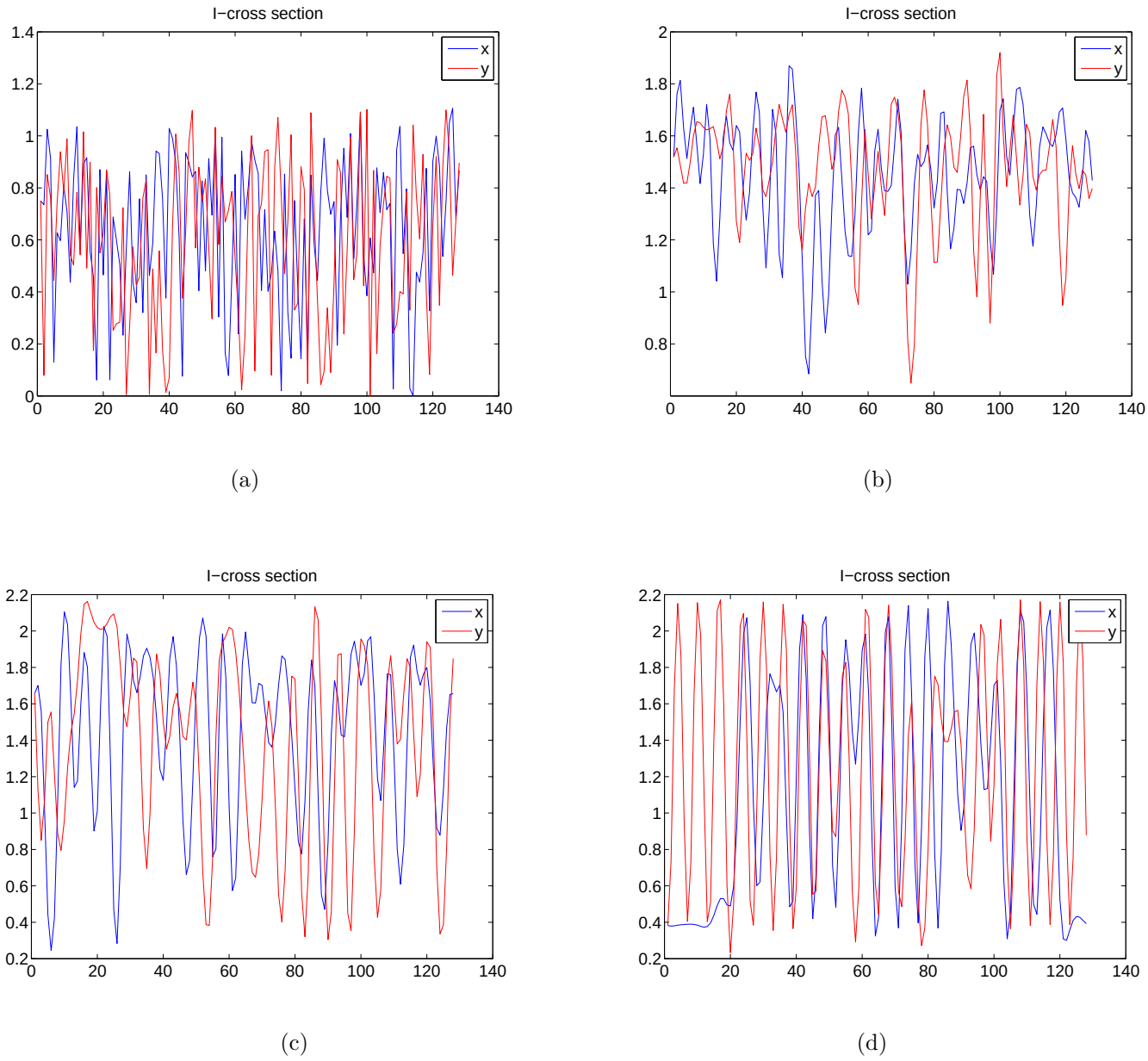

Figure 3.9: I-solution profiles corresponding to $\beta = 0.7$, (a) This is the initial solution profile of system 3.4 for $t = 0$, (b) is for $t = 1000$, (c) is for $t = 10000$ and (d) is for $t = 100000$. Other parameters are: $R = 0.35,\ \gamma = 0.1,\ r = 0.5,\ \mu = 0.1,\ d_1 = 10,\ d_2 = 1,\ p = 2,\ q = 2$.

Again, in figure 3.9 above just like in figure 3.6 before, we showed the solution profiles of the infected individuals. From the figure above we observed spatially periodic-like (choatic) fluctuations. These figures can be compared to the figures in Dushoff et al [Dus04]. Next, we consider an epidemic with high transmission probability (i.e. $\beta = 0.9$).

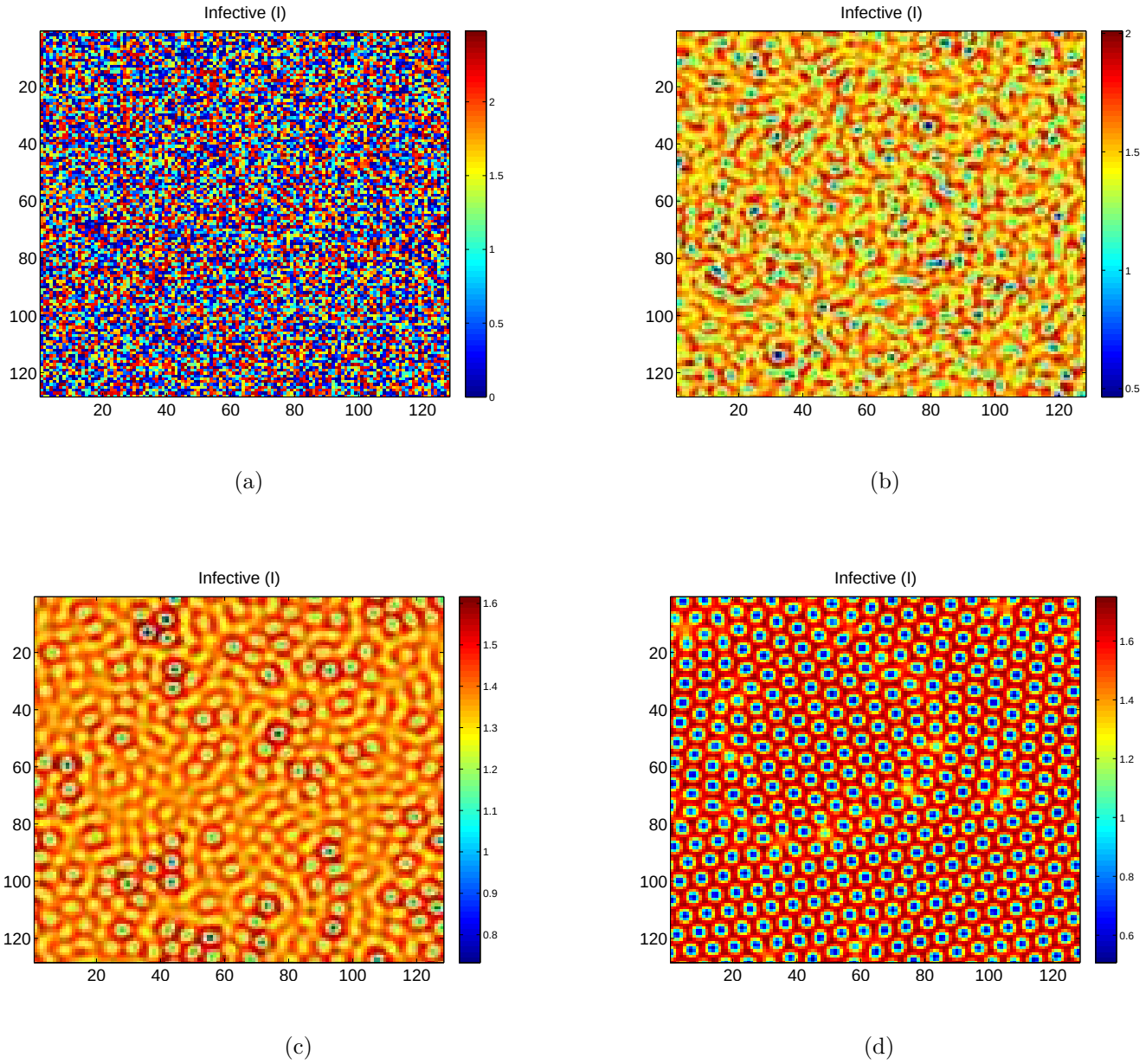

(a) (b)

(c) (d)

Figure 3.10: Time evolution corresponding to $\beta = 0.9$, (a) initial solution for 3.4 for $t = 0,\ \beta = 0.9,\ R = 0.35, \gamma = 0.1, r = 0.5, \mu = 0.1,\ d_1 = 10,\ d_2 = 1,\ p = 2,\ q = 2,$ (b) $t = 1000$ Color plots of stationary solutions of 3.4, (c) $t = 10000$ and (d) $t = 500000$.

In the above experiment, we considered a high transmission rate of 0.9, we were expecting to see stripe pattern but we got spot pattern but they are spots with high concentration. The reason, we were expecting to have stripes is purely biological. We know from biological point-of-view, stable spots can be interpreted to be no outbreak in that region (i.e the infected individuals are isolated regions with low densities) and stripes can be interpreted to be a possibility of epidemic outbreak. Now, because of this and the value of the transmission rate we were certain to have an outbreak in that region. Nevertheless, unlike in figure 3.4 where we had red (hot) spots (red-holes) on a blue background-low density of the infectious I, here we have blue (cold) spots (blue-holes) on a red background-high density of the infectious I. In this case, the infected individuals are isolated in regions with low density, and the other area (red regions), which is larger to the blue-holes area, is of high density. From biological or epidemic view point, this area is not safe because the epidemic is significant. Therefore, under the control of these parameters, we sure of epidemic outbreak in the area. The difference between the two figures is that, in figure 3.4 the red-holes area is smaller than the blue region with low density therefore, one can control the epidemic in this case. While, in figure 3.10, the blue-holes area is smaller than the red region which has high density therefore it is difficult to control the epidemic.

Remark 3.1 (Colour swap in spot patterns)

The biological meaning of colour swap in spot patterns: first we have a change in colour from blue to red which means from low to high densities of the infectious I (Figures 3.4 and 3.10). Secondly, red spots (peaks or hot spots) on blue background means the infectious are isolated zones with high densities of I and disconnected, while blue spots (troughs or cold spots) on red background means the infected individuals are isolated zones with low densities and the infection is significant in the that region. From the view of epidemic dynamics, red (hot/peaks)-spots consist of red (maximum density of I) peaks on a blue (minimum density of I) background, that is, the infectious are isolated zones with high population density, the remainder region is of low density which is larger than

the hot-spots region, which means the epidemic may not break out in the area. In this case, one can see that the diseases' spread is getting smaller with time increasing. In other words, in this case, the area is safe. While, blue(cold/troughs)-spots consist of blue (minimum density of I) troughs on a red (maximum density of I) background, that is, the infectious are isolated zones with low population density, and the remainder region is of high density, which is larger than the cold-spots region. In this case, one can see that the diseases' spread is getting bigger with time increasing.That's to say, under the control of these parameters, the epidemic may break out in the area and therefore, the area is not safe, [Jin14], [Xin14], [Ye14], [Wei12].

In the above experiments (figures 3.4-3.10), we varied β and all other parameters were fixed. In the next two experiments, first we shall vary β and r at the same time to see if r has any effects on the patterns we obtained above and also see if the order of these structures changes as r is varied. Secondly, we will take higher values of the exponent q to see if this has any effect on the dynamical asymptotic behaviour of the system.

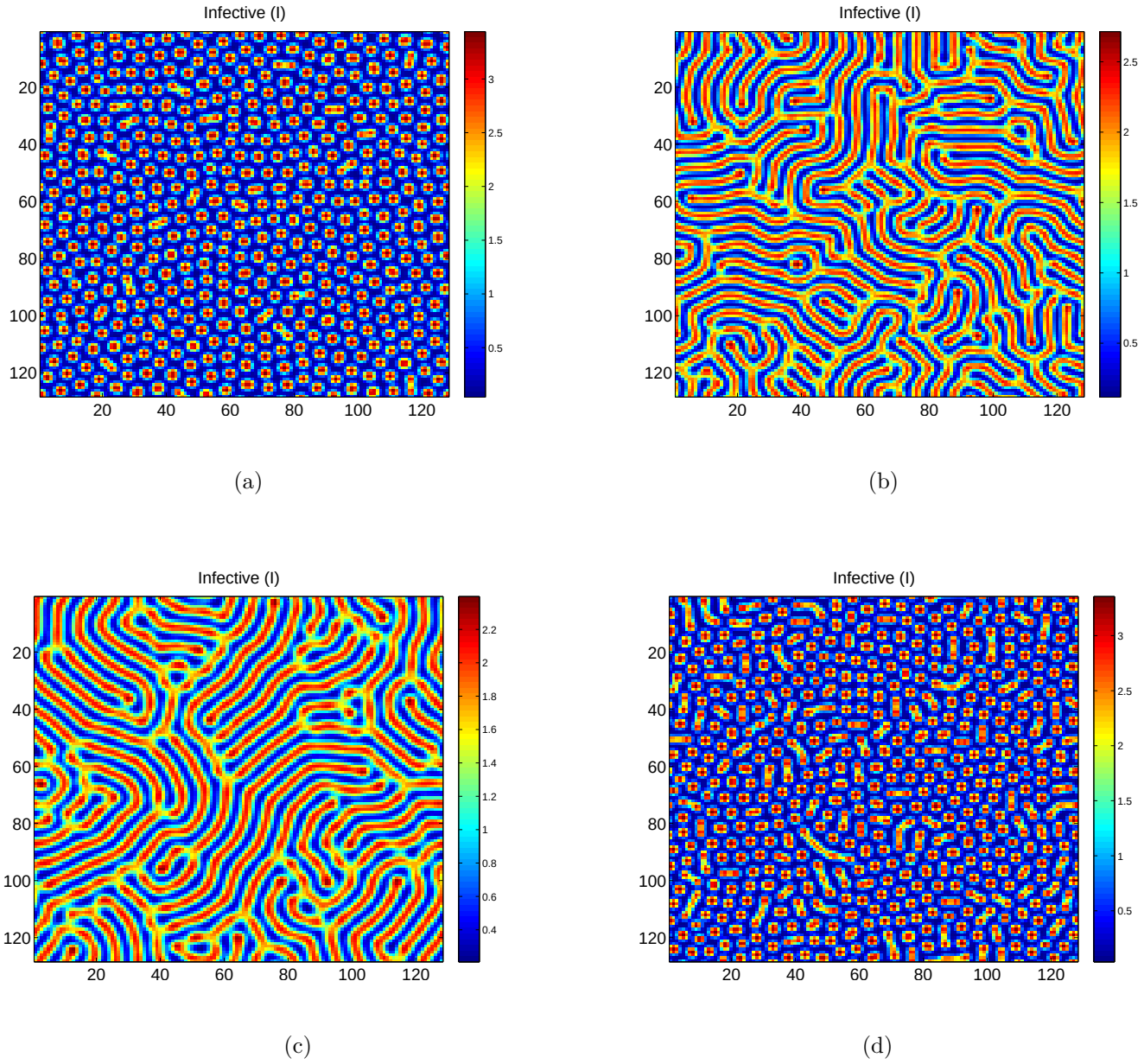

(a) (b)

(c) (d)

Figure 3.11: Time evolution corresponding to different values of β and r, (a) color plots of stationary solutions of 3.4 for $t = 100000,\ \beta = 0.5,\ r = 0.7$, (b) color plots of stationary solutions of 3.4 for $t = 100000,\ \beta = 0.9,\ r = 0.7$, (c) color plots of stationary solutions of 3.4 for $t = 10000,\ \beta = 0.4,\ r = 0.3$, (d) color plots of stationary solutions of 3.4 for $t = 100000,\ \beta = 0.7,\ r = 0.9$. Other parameters are: $R = 0.35,\ \gamma = 0.1,\ \mu = 0.1,\ d_1 = 10,\ d_2 = 1,\ p = 2,\ q = 2$

In the above experiment, we fixed all parameters and varied β and r. In figure (3.11(a)), we take $\beta < r$ i.e. $\beta = 0.5$ and $r = 0.7$, we have spot patterns. This is because $\beta < r$. In

figure (3.11(b)), we take $\beta > r$, i.e. $\beta = 0.9$ and $r = 0.7$, we have stripes this is because $\beta > r$. Again, in figure (3.11(c)), we take $\beta > r$ but all small, i.e. $\beta = 0.4$, with $r = 0.3$, since $\beta > r$ even though β is small we still have stripes. Finally, in figure (3.11(d)), we take $\beta < r$, i.e. $\beta = 0.7$ and $r = 0.9$, and still have spot patterns.
From the above experiment, we observed that whenever $\beta < r$, we have spot patterns and for $\beta \geq r$, we have stripes.

Now, in figure 3.12, we change the value of the exponent q and observe the dynamics of the system.

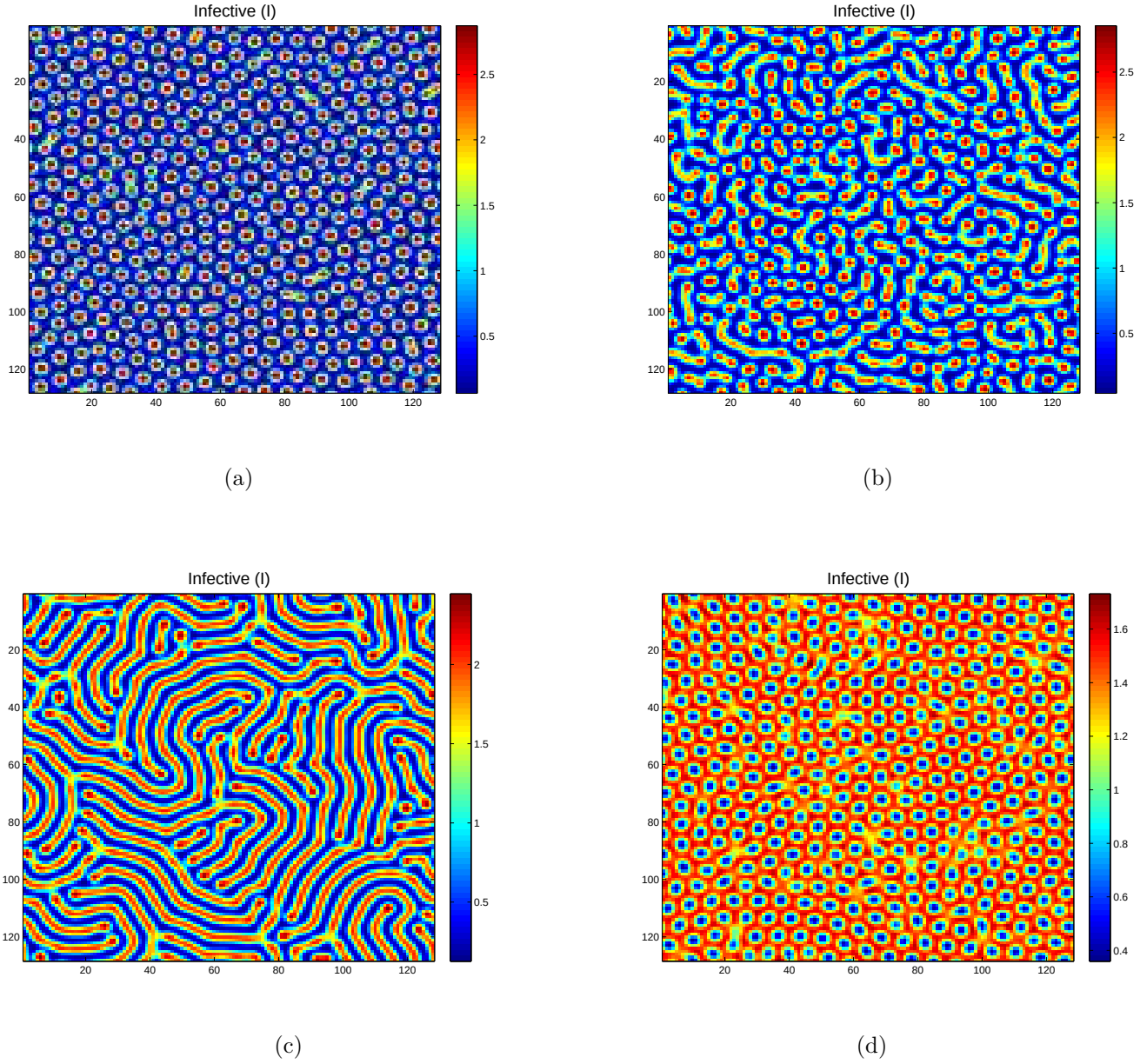

(a) (b)

(c) (d)

Figure 3.12: Time evolution corresponding to different values of β (a) color plots of stationary solutions of 3.4 for $t = 100000,\ \beta = 0.1,$ (b) color plots of stationary solutions of 3.4 for $t = 100000,\ \beta = 0.2,$ (c) color plots of stationary solutions of 3.4 for $t = 10000,\ \beta = 0.3,$ (d) color plots of stationary solutions of 3.4 for $t = 100000,\ \beta = 0.5,$. Other parameters are: $R = 0.35,\ \gamma = 0.1,\ \mu = 0.1,\ r = 0.5,\ d_1 = 10,\ d_2 = 1,\ p = 2, q = 3$

In figure 3.12 above, we take $q = 3$ with $q = 2$, again surprisingly we observed that even at low transmission rate there is a possibility of epidemic outbreak (figure 3.12(b)) and at $\beta = 0.5$ (figure 3.12(d)) epidemic outbreak is certain to occur. This can

be attributed to high contagious effects of the diseases. Also, we have checked for $q = 4$ and $q = 5$, they have similar structures (patterns) to those for $q = 3$ though at different values of the transmission rate. In general, we observed the following sequence of pattern formation for $2 \leq q \leq 5$:
spots(red-holes)→spot-stripe mixtures→stripes→spots(blue-holes).

3.5 Discussion of the results

In this Chapter we derived a spatial SIS reaction-diffusion epidemic model and described the IMEX method that we used in our numerical simulations. We proved conditions for Turing instability of the endemic steady state and performed numerical simulations of the system 3.4. From figures 3.4 to 3.10, we varied β to see the dynamical behaviour for the system 3.4. For small values of the transmission rate β that is, low transmission rate, we have spot patterns (see figures 3.4 and 3.5). For intermediate values of β, we observed a spot-stripe mixture (see figure 3.7). For high values of β that is, high transmission rate, we have striped patterns (see figure 3.8).
In figure 3.11, we varied the bifurcation parameter β and treatment or recovery rate r to see if r has any effects on the above aforementioned dynamics and on the overall dynamical behaviour of the system 3.4. Surprisingly, as we varied the recovery rate r, the dynamical behaviour of the system changed and the patterns ordering also changed! In figure 3.12, we checked the effects of higher values of q on the dynamics of the system.

From the point-of-view of epidemic dynamics, for instance in figures 3.4 and 3.5, there we observed spot patterns-the infected populations are isolated and the area has high density, the remaining area is bigger to the spots area which has low population density, this implies in this region there is no epidemic breakout. Therefore, this region is safe. In the case of figure 3.7, we observed spot-stripe mixture with the spots decaying. Initially, the infected populations are isolated in areas with high density but gradually, the spots decay to stripes. This means there is a possibility of an outbreak in this case. In figure 3.8, we have fully matured stripes patterns and therefore in this case the epidemic

is significant. In figure 2.12, we observed that the infected populations are also isolated in areas with low density, and the other area, which is bigger to the blue-holes area, is of high density. This implies here we may have an epidemic outbreak in the area.

Also, in figures 3.6 and 3.9 we have shown that is possible to have spatially periodic-like (chaotic) fluctuations in the solution profiles of the infective individuals and these results can be compared to those results in [Alt06] and [Dus04] on the seasonality of infectious diseases. These figures showed a possibility of having spatially periodic outbreak of epidemic in that region.

Now, in figure 3.11, we varied both β and r, we found out that whenever $\beta < r$, we have spot patterns and for $\beta \geq r$, we have stripes (see figure 3.7 for $\beta = r = 0.5$). This means whenever the transmission rate β is strictly less than the recovery rate r, the system 3.4 will always have stable spot patterns. And whenever $\beta \geq r$, the solution to the model 3.4 will always settle on stable stripe patterns. Biologically or epidemiological speaking, what this means is that whenever $\beta < r$ there is no epidemic outbreak and whenever $\beta \geq r$ there will always be an epidemic outbreak. Finally, in figure 3.12, we increased the value of the exponent q to 3, and we observed changes in the pattern ordering. For low values of the transmission rate β we have a possibility of epidemic outbreak (see figure 3.12(b)) and for intermediate values of β we certain to have epidemic outbreak (see figure 3.12(d)). Other higher values of q have similar effects on the dynamics of the system. This tells us that as we increase q we have different dynamics from view point of epidemics not pattern formation.

More generally, if the data in our numerical simulations were taken for example from hantavirus, then to explain spatial patterns arising from the spatial epidemic model 3.4 in the real life, we discuss some observations of the spatial and temporal dynamics of hantavirus pulmonary syndrome of the 1990s. Ostfeld et al [Ost05], showed spatial patterns of location of hantavirus pulmonary syndrome in southwestern USA. The patterns we presented in this section in particular figures 3.7 and 3.8 can be compared with the pictures in [Ost05]. Also, figures 3.8 and 3.8 can be compared with the pictures in Gubler [Gub02] on dengue hemorrhagic fever. In general, modelling the diseases using reaction-

diffusion system can help to understand the distribution and dynamics of epidemics in both time and space.

Though, many authors have considered pattern formation in SIR models, the results presented here are unique because we combine both analytical and numerical methods to prove the stability of the steady states. In [Jin08] the authors considered the formation of spatial patterns in epidemic models and found only stripe patterns. In [Sun07] the authors fixed the exponents $p+q = 1$ and found spots and chaotic patterns. While, in [Sun12(a)] the author in the stability analysis fixed the exponents $p = 1$ and $q = 2$ and found spot and stripes patterns. In [Wan11] the authors considered pattern selection with both self and cross diffusion. They found only spots. Also, in [Cai11] the authors found spots, spot-stripe mixture and holes. Also, in [Liu86], [Liu87] and [Het91] the authors studied the dynamical behaviours of models with nonlinear incidence rate of the form $\beta I^q S^p$ and independently concluded that the dynamics of the system depend mainly on the transmission rate β and the exponent q.

In this Chapter, we extended and generalised the results in the papers [Sun07], [Wan11], [Cai11] and [Sun12(a)] by performing the stability analysis for general p and q and to the best of my knowledge this is the first time such analysis is performed. We found different types of spatial patterns in the Turing space. These include spots (red-holes, figures 3.4 and 3.5), spot-stripe mixtures (figure 3.7), stripes (figure 3.8), and spots (blue-holes, figure 3.10). In our numerical simulations we consider the cases $(p = 2, q = 2)$ and $(p = 2,\ q = 3)$ which have not been done before now. In the former case (i.e. for $p = 2, q = 2$), we found spots (red-holes), spot-stripe mixtures, stripes and spots (blue-holes). We can see that it is obvious the sequence of our patterns is different from the ones obtained in [Sun07] and [Sun12(a)]. Unlike in all the above mentioned papers, we have discovered for the first time that the patterns do not depend only on β and q but also on r. In fact, r is the main determinant of the type of pattern we get for any values of β and q. This is one of our main results because for the first time we have shown that the dynamical behaviour of an SIS epidemic model is depended on the recovery rate. In the latter case (i.e. for $p = 2,\ q = 3$) we found a surprising result, that is, even with low

transmission rate there is a possibility of epidemic outbreak.

Also, we compared some of our results with those in [Ost05] and [Gub02] on hantavirus pulmonary syndrome and dengue hemorrhagic fever, respectively. The results in this Chapter revealed that the model 3.4 with appropriate parameter estimates can capture key features of the disease and can give good prediction of the distribution of infected individuals and the dynamics of the disease in both time and space. Hence, the model can be used to study the dynamics of many SIS epidemics. In summary, biologically speaking, what we have discovered in this analysis and in this Chapter is that, for an infectious disease, for instance, influenza even with its high contagious effect and even when the transmission probability is high, we can still eradicate the disease or manage the spread by controlling r. Then, the question is, what is r biologically and how does varying r help to control epidemics? In our model, r is the treatment or recovery rate, and what it means biologically is any form of intervention taken to combat the disease (use of antiviral drugs, quarantine and vaccination strategies). So if $\beta < r$ it means there are more interventions in place and, therefore, it is certain that every infected individual will get treatment and eventually get recovered. Also, in our numerical simulations we assumed that the natural and disease-induced death rates are smaller than the treatment rate. Finally, we used the spatial patterns to explain this distribution of infected individuals in the spatial domain.

Hence, our results generalised the ones in [Sun07], [Wan11], [Cai11], [Sun12(a)] by proving for the first time permanence and invariance principle for any $p, q \in \mathbb{Z}^+$ when N is not constant. Furthermore, we extended the results in [Liu86], [Liu87], [Het91] by showing again for the first time that the recovery rate r is the main determinant of the dynamical behaviour of the system.

Chapter 4

Delayed SIR model with latency and temporary immunity

In mathematical models of physical, engineering and biological systems it is often important to consider temporal delays intrinsic to the problem. Adding time lags in these models allows one to develop more realistic models of phenomena under consideration, thus gaining a better insight into their dynamics [Coo82]. This Chapter presents an SIR model which incorporates two time delays representing latency period and a temporary immunity from a disease. In mathematical modelling of infectious diseases, time delays may be caused by many factors, such as the incubation period or the latent period of infection. For many diseases, some periods of time must elapse before the condition of the infection can change, as is the case, for instance, for tuberculosis and influenza. Although time delays provide more biological realism to epidemic models, they also make the analytical and numerical analysis more challenging [Tak10].

Latent or infectious periods describe the period of time during which individuals are infected but not yet infectious. During this period of time the infected individuals cannot transmit the disease, as the disease in them is not active enough for them to transmit it to susceptible individuals. After this latent period they become infectious and then can infect the S-class on adequate contact with a constant probability rate β. We know that

latency or incubation can be modelled by incorporating it as a time delay effect (delayed SIR models) [Coo79], or by introducing an exposed class ($SEIR$ models) [Het81]. In [Kad10], the authors compared a delayed SIR model and its corresponding $SEIR$ model in terms of local stability. They Showed that when $1/\sigma = \frac{(e^{\mu\tau}-1)}{\mu}$ the delayed SIR model and the $SEIR$ model generate identical local asymptotic behaviour. Here, $1/\sigma$ is the mean latent period. Also, the authors compared the two models numerically using the threshold parameter $\mathcal{R}_0$ and computed the error. They showed that the two models have the same value of the basic reproduction number $\mathcal{R}_0$ when $\mu\tau$ is close to zero, where μ is the natural death rate and τ is the latent period. This means there is no difference between a delayed SIR model and an $SEIR$ model from the local stability point-of-view.

Some infections provide recovered individuals with a short or long immunity against re-infection. This means that it is important to include the effects of immunity into the mathematical models in order to better represent the actual dynamics of epidemic spread and predict future outbreaks. In epidemiology, immunity means that after the infected individuals have recovered, they have a period of immunity, after which they return to the susceptible class. A common disease with such behaviour is influenza, that is, after recovery there is a temporary period after which the individuals move back to the susceptible compartment. There are many diseases which confer temporary immunity, for instance, *Chlamydia trachomatis* but this disease has a short immune period and a high re-infection rate. Other examples include non-plague yersiniosis, salmonella, respiratory syncytial infection[Kyr05].

We introduce latency in the system by incorporating it in the term $I(t-\tau_1)$ and temporary immunity in the $I(t-\tau_2)e^{-\gamma\tau_2}$ term. Here τ_1 and τ_2 are the latency and temporary immunity periods, respectively. The term $e^{-\gamma\tau_2}$ signifies that after recovering the individuals must have survived natural death within the τ_2-period after which they can return to the susceptible class [Coo96], [Bly10]. We ignore the term $e^{-\gamma\tau_1}$ because we assume that the force of infection at time t is given by $\beta S(t)I(t-\tau_1)$, where β is the average number of contacts per infective per day, and $\tau_1 > 0$ is a fixed time during which the infectious individuals develop the disease, and it is only after that time that

the infected individuals can infect the susceptible individuals. Here, we neglect the term $e^{-\gamma\tau_1}$ because we assume that the latent period is short and by expanding the term $e^{-\gamma\tau_1}$ for small τ_1, we have

$$e^{-\gamma\tau_1} \approx 1-\gamma\tau_1+\frac{1}{2}\gamma^2\tau_1^2-.... = 1, \text{ for } |\tau_1| << 1$$

. There are many diseases with short latent period, for instance, influenza (2-3 days), whooping (7-10 days), tetanus (4-21 days), measles (about 10 days), chicken pox (10-21 days). Some authors added this term to their models ([Xue13], [Tch12], [Ber11]) while some neglected the term like in our case ([Rih12], [Kad10], [Wan02]). In general, from the literature by comparing the models which included the term $e^{-\gamma\tau_1}$ and those that did not include the term, we observe that both have the same qualitative dynamical behaviours in terms of stability analysis.

The model we will study here is an SIR delay epidemic model which incorporates two time lags and a bilinear incidence rate. All newborns are assumed to be susceptible, the natural clearance rate is constant in all the compartments and assumed to be equal, and also disease-induced death is constant in the infectious class. We also assume constant periods of latency and temporary immunity given by τ_1 and τ_2, respectively. To analyse the model equilibria, we will consider five distinct cases: first, a case of epidemic that both the latency and immunity periods are set to zero (i.e.$\tau_1 = \tau_2 = 0$), in which case we will prove local and global asymptotic stability, (subsection 4.2). Secondly, for a disease with only latency and immunity period set to zero (i.e. $\tau_1 > 0,\ \tau_2 = 0$), we will establish the existence of a stable endemic steady state for all parameter values, (subsection 4.3.1). Third, for a disease with only immunity and latency period set to zero (i.e. $\tau_1 = 0,\ \tau_2 > 0$), we will prove the existence of periodic solutions arising from Hopf bifurcation of the endemic steady state, (subsection 4.3.2). In the case when latency and immunity are identical (i.e. $\tau_1 = \tau_2 = \tau > 0$), we prove that the system is always stable for any parameter regime see subsection 4.3.3, and finally, we consider the case when both latency and temporary immunity periods are present and unequal

(i.e. $\tau_1 > 0, \tau_2 > 0 \ \ \tau_1 \neq \tau_2$). In this case, the system has rich dynamics, as discuss in subsection 4.3.4. It is worth mentioning that there are many ways to make these kind of models more realistic and more meaningful biologically, but here we chose to add time delays because of our interest in periodic solutions arising from the Hopf bifurcation.

4.1 Derivation of the Delayed SIR Model

Before proceeding with the model derivation we make the following assumptions.

(i.) there is a bilinear incidence rate βSI;

(ii.) there is a latent or infectious period with a fixed length τ_1, after which infected individuals become infectious;

(iii.) there is a temporary immunity period with a fixed length given by τ_2, from which recovered individuals return to the susceptible compartment;

(iv.) there is a natural death rate γ, constant and the same for all compartments;

(v.) there is an additional disease-induced death rate μ, in the I-class;

(vi.) recruitment into the population is only through birth in the S-class at a constant rate b and newborns are assumed to be susceptible.

Let $S(t)$, $I(t)$, $R(t)$ be the population densities at time t of the Susceptible, Infected and Recovered respectively. From these assumptions, we derive the following SIR delay epidemic model that incorporates two time delays (for details see [Wan02], [Coo96], [Mei11], [Kyr05], [Bly10]):

$$\left.\begin{aligned} S_t(t) &= b - \beta S(t)I(t-\tau_1) - \gamma S(t) + rI(t-\tau_2)e^{-\gamma\tau_2} \\ I_t(t) &= \beta S(t)I(t-\tau_1) - (\mu + r + \gamma)I(t) \\ R_t(t) &= rI(t) - rI(t-\tau_2)e^{-\gamma\tau_2} - \gamma R(t) \end{aligned}\right\} \tag{4.1}$$

with given non-negative initial conditions:

$$\begin{aligned} &S(0) > 0 \\ &I(s) \geq 0,\ s \in [-\tau, 0] \quad \text{and} \\ &R(0) \geq 0 \end{aligned}$$

where $\tau = \max\{\tau_1, \tau_2\}$.
The model parameters are defined as follows: b the recruitment constant, β is the transmission rate, γ is the natural death rate, μ is the disease-induced death rate from the I-class, r is the recovery rate, τ_1 and τ_2 are the latent and immune periods, respectively.

Since the first two equations in the model (4.1) above are independent of the R variable, we can ignore the third equation without loss of generality. Therefore, the model 4.1 becomes:

$$\begin{aligned} S_t(t) &= b - \beta S(t) I(t-\tau_1) - \gamma S(t) + r I(t-\tau_2) e^{-\gamma \tau_2}, \\ I_t(t) &= \beta S(t) I(t-\tau_1) - (\mu + r + \gamma) I(t), \end{aligned} \tag{4.2}$$

with the above initial conditions and $S+I = N$. From now on we concentrate in our analysis on model 4.2.

4.1.1 Positivity of Solutions

Since the system 4.2 represents a model of human population, it is important to show that all solutions are non-negative $\forall t > 0$. All we need to show is, the solution to the system 4.2 will always be nonnegative $\forall t > 0$, whenever we start with positive initial data. See Li and Kuang [Li00] for details of the proof.

Theorem 4.1

Let $S_0 > 0$, $I_0(s) > 0$ be the initial data for the model 4.2, $\forall s \in [-\tau; 0)$ and $I_0(0) > 0$. The solutions $S(t)$ and $I(t)$ of the model 4.2 at time $t > 0$ are always positive.

Proof:

We will only sketch the proof of the above theorem here, for details see [Li00]. The proof proceeds by contradiction. First, we assume there exists a first time t_1 when product of $I(t_1)$ and $S(t_1)$ is equal to zero. If we assume $I(t_1)$ is zero, this implies $S(t) \geq 0$, $\forall t \in [0; t_1]$. Therefore,

$$\frac{dI(t)}{dt}\Big|_{t_1} = \underbrace{\beta S(t_1)}_{>0}\underbrace{I(t_1-\tau_1)}_{>0} - \underbrace{(\gamma+r+\mu)I(t_1)}_{=0}. \tag{4.3}$$

Also, when $t \in [0; t_1]$, and since $I(0) > 0$ for $I(t_1) = 0$, we have:

$$\frac{dI(t)}{dt}\Big|_{t_1} < 0,$$

which contradicts 4.3. Following the same logic, we can also show that $S(t)$ is also non-negative. Let us assume by contradiction that $S(t)$ can become negative. Again denote by t_1 the first time when the product of $S(t)$ and $I(t)$ is equal to zero. If we assume that $S(t_1)$ is zero, this gives $I(t)$ to be greater or equal to zero, $\forall t \in [0; t_1]$. We have by the S equation of the model 4.2 thus:

$$\frac{dS(t)}{dt}\Big|_{t_1} = \underbrace{b}_{>0} - \underbrace{\beta S(t_1)I(t_1-\tau_1)}_{=0} - \underbrace{\gamma S(t_1)}_{=0} + \underbrace{rI(t_1-\tau_2)e^{-\gamma\tau_2}}_{\geq 0} > 0. \tag{4.4}$$

And since $S(0) > 0$, to become negative at $t = t_1$, we require

$$\frac{dS(t)}{dt} < 0,$$

which contradicts 4.4 and hence the proof. ■

The model 4.2 has a trivial steady state $E^0 = (S^0, I^0) = (b/\gamma, 0)$ and for $\mathcal{R}_0 > 1$, the non-trivial solution E^* exists and is unique, where,

$$\mathcal{R}_0 = \frac{b\beta}{\gamma(\mu+r+\gamma)} \tag{4.5}$$

$$\begin{aligned} S^* &= \left(\tfrac{(\mu+r+\gamma)}{\beta}\right), \\ I^* &= \tfrac{b-\frac{\gamma(\mu+r+\gamma)}{\beta}}{(\mu+\gamma)+re^{-\gamma\tau_2}} = \tfrac{b-\gamma S^*}{\beta S^*-re^{-\gamma\tau_2}}. \end{aligned} \tag{4.6}$$

4.2 Linear stability analysis without time delays

Here, we analyse the equilibria without time delays (i.e. $\tau_1 = \tau_2 = 0$). We will analyse both the trivial and the nontrivial steady states of the system (4.2). Throughout this section, our analysis will be based on the ODE model that is the case when both the latency and temporary immunity periods are set to zero ($\tau_1 = \tau_2 = 0$). We will analyse the model equilibria both locally and globally using both Routh-Hurwitz criterion and Lyapunov direct approach.

Linearising the system (4.2) near the steady state $E^* = (S^*, I^*)$, we have the following characteristic equation:

$$\begin{aligned} \Delta(\lambda) = \lambda^2+\lambda[\gamma+(\gamma+r+\mu)+\beta I^*-\beta S^*]+(\gamma+r+\mu)(\gamma+\beta I^*)+ \\ -\beta\gamma S^*-\beta r I^*. \end{aligned} \tag{4.7}$$

Introducing the notation

$$\begin{aligned}
\hat{p}_0 &= (\mu+r+2\gamma)+\beta I^*, \\
\hat{p}_1 &= -\beta S^*, \\
\hat{q}_0 &= (\mu+r+\gamma)(\gamma+\beta I^*), \\
\hat{q}_1 &= -\beta\gamma S^* \text{and} \\
\hat{q}_2 &= -\beta r I^*,
\end{aligned} \tag{4.8}$$

the characteristic equation becomes:

$$\lambda^2+\lambda(\hat{p}_0+\hat{p}_1)+(\hat{q}_0+\hat{q}_1+\hat{q}_2) = 0. \tag{4.9}$$

This section presents and analyses the system's equilibria for the ODE model that is, for the case when both the latency and temporal immunity periods are set to zero from a disease. We present the following conditions which will be proved later:

$$\hat{p}_0+\hat{p}_1 > 0 \tag{A1}$$

$$\hat{q}_0+\hat{q}_1+\hat{q}_2 > 0 \tag{A2}$$

We will prove that conditions A1 and A2 hold and are valid throughtout this chapter. The following theorem forms the basis for the analysis and we follow the ideas from [Kyr05], [Rua99].

Lemma 4.1

The characteristic equation 4.9 has eigenvalues with negative real parts, and the following properties are true:

(i.) for $\mathcal{R}_0 < 1$, the disease-free steady state E^0 is locally asymptotically stable and,

(ii.) for $\mathcal{R}_0 > 1$, the non-trivial state E^* exists and is locally asymptotically stable.

Proof:

We begin the proof by recalling the characteristic equation 4.9

$$\lambda^2+\lambda(\hat{p}_0+\hat{p}_1)+(\hat{q}_0+\hat{q}_1+\hat{q}_2) = 0. \tag{4.10}$$

It is enough to show that the assumptions A1−A2 are satisfied, that is, to show that the coefficients $(\hat{p}_0+\hat{p}_1)$ and $(\hat{q}_0+\hat{q}_1+\hat{q}_2)$ are non-negative, which would then imply that the roots of 4.10 have negative real part. To see this, we proceed as follows.

(i.) At the disease-free steady state $E^0 = (S^0, I^0) = (R/\gamma, 0)$, we have thus:

$$\begin{aligned} \hat{p}_0+\hat{p}_1 &= (\mu+r+2\gamma)+\beta I^0-\beta S^0 = (\mu+r+2\gamma)(1-\mathcal{R}_0) > 0 \\ \text{if} \quad & \mathcal{R}_0 < 1 \end{aligned}$$

and

$$\begin{aligned} \hat{q}_0+\hat{q}_1+\hat{q}_2 &= (\mu+r+\gamma)(\gamma+\beta I^0)-\beta\gamma S^0-\beta r I^0 \\ &= \gamma(\mu+r+\gamma)(1-\mathcal{R}_0) > 0 \\ \text{if} \quad & \mathcal{R}_0 < 1. \end{aligned}$$

(ii.) At the endemic steady state E^*, we have:

$$\begin{aligned} \hat{p}_0+\hat{p}_1 &= (\mu+r+2\gamma)+\beta I^*-\beta S^* \\ &= (\mu+r+2\gamma)+\tfrac{\gamma(\mu+r+\gamma)}{\mu+\gamma}(\mathcal{R}_0-1) > 0 \\ \text{if} \quad & \mathcal{R}_0 > 1 \end{aligned}$$

and

$$\begin{aligned} \hat{q}_0+\hat{q}_1+\hat{q}_2 &= (\mu+r+\gamma)(\gamma+\beta I^*)-\beta\gamma S^*-\beta r I^* \\ &= \gamma(\mu+r+\gamma)(\mathcal{R}_0-1) > 0 \\ \text{if} \quad & \mathcal{R}_0 > 1. \end{aligned}$$

From the Routh-Hurwitz principle, we know that all eigenvalues of 4.10 will have negative real parts, and by implication, the disease-free steady state is locally asymptotically stable if $\mathcal{R}_0 < 1$. From the same argument it follows that the endemic steady state E^* is locally asymptotically stable for $\mathcal{R}_0 > 1$. Hence, the proof. ■

4.2.1 Global stability of the disease-free steady state

Here we present global stability analysis of E^0 in $\mathbb{D}$ using Lyapunov direct method, by combining composite quadratic and linear functions.

Theorem 4.2

Let $\mathcal{R}_0$ be defined as in 4.5, then the disease-free steady state E^0 of model 4.2 is globally asymptotically stable if $\mathcal{R}_0 < 1$, and unstable for $\mathcal{R}_0 > 1$.

Proof:

Define $U_1 : (S, I) \in \mathbb{D} : S > 0, I > 0 \to \mathbb{R}$ by

$$U_1(S, I) = \frac{1}{2}\left[(S-S^0)+I\right]^2+\frac{(\mu+2\gamma)}{\beta}I,$$

$U_1(S, I) \geq 0 \in \mathbb{D}$. Then U_1 is C^1 on the interior of $\mathbb{D}$, E^0 is the global minimum of U_1 on $\mathbb{D}$, and $U_1(S^0, I^0) = 0$. The time derivative of the functional U_1 can be computed along solutions of 4.2 as follows

$$\begin{aligned}\frac{dU_1}{dt} &= [(S-S^0)+I]\left(\tfrac{dS}{dt}+\tfrac{dI}{dt}\right)+\tfrac{(\mu+2\gamma)}{\beta}\tfrac{dI}{dt},\\ &= [(S-S^0)+I]\,(b-\gamma(S+I)-\mu I)+\tfrac{(\mu+2\gamma)}{\beta}(\beta SI-(\gamma+r+\mu)I),\end{aligned}$$

which $b = \gamma S^0$, can be transformed into

$$\begin{aligned}\frac{dU_1}{dt} &= [(S-S^0)+I](\gamma S^0-\gamma(S+I)-\mu I)+\tfrac{(\mu+2\gamma)}{\beta}(\beta SI-(\gamma+r+\mu)I)\\ &= -\gamma(S-S^0)^2-(\mu+\gamma)I^2-(\mu+2\gamma)\left(\tfrac{(\gamma+r+\mu)}{\beta}-S^0\right)I\\ &= -\gamma(S-S^0)^2-(\mu+\gamma)I^2-\tfrac{(\mu+2\gamma)(\gamma+r+\mu)}{\beta}(1-\mathcal{R}_0)I.\end{aligned}$$

We can see from the above that whenever $\mathcal{R}_0 < 1 \implies \dot{U}_1 \leq 0$, with $\dot{U}_1 = 0$ only if $S = S^0$ and $I = I^0$. Now by LaSalle's invariant principle, the disease-free solution E^0, is globally asymptotically stable. See appendix 5.2 for the details of LaSalle's principle and [Las76] [Shi07], [Las60], [Mez10], [Cru09] for more details. ■

4.2.2 Global stability of the endemic steady state

It has already been established that when $\mathcal{R}_0 > 1$, the system 4.2 has a unique endemic steady state E^*. Now, using Lyapunov direct method by combining linear and composite functions, we shall show that E^* is globally asymptotically stable.

Theorem 4.3

For $\mathcal{R}_0 > 1$, the endemic equilibrium is globally asymptotically stable.

Proof:

We define a Lyapunov functional

$$U_2 : (S, I) \in \mathbb{D} : S > 0 \to \mathbb{R}, \tag{4.11}$$

as follows

$$U_2(S, I) = \frac{1}{2}[\nu_1 + \nu_2]^2 + \frac{(\mu + 2\gamma)}{\beta}\left(\nu_2 - I^* \ln \frac{I}{I^*}\right), \tag{4.12}$$

where,

$$\nu_1 = S - S^*, \;\; \nu_2 = I - I^*.$$

Then U_2 is C^1 on the interior of $\mathbb{D}$, E^* is the global minimum of U_2 on $\mathbb{D}$, and $U_2(S^*, I^*) = 0$.

Now differentiating U_2 with respect to time, we have

$$\begin{aligned}\frac{dU_2}{dt} &= [\nu_1+\nu_2]\left(\frac{dS}{dt}+\frac{dI}{dt}\right)+\frac{(\mu+2\gamma)}{\beta}\frac{\nu_2}{I}\left(\frac{dI}{dt}\right)\\ &= [\nu_1+\nu_2](R-\gamma(S+I)-\mu I)+\frac{(\mu+2\gamma)}{\beta}\frac{\nu_2}{I}(\beta SI-(\gamma+r+\mu)I),\end{aligned}$$

using $R=\gamma(S^*+I^*)+\mu I^*$ and $\beta S^*=(\gamma+r+\mu)$, we have

$$\begin{aligned}\frac{dU_2}{dt} &= [\nu_1+\nu_2]\{-\gamma[\nu_1+\nu_2]-\mu\nu_2\}+(\mu+2\gamma)\nu_1\nu_2\\ &= -\gamma(\nu_1+\nu_2)^2-\mu\nu_1\nu_2-\mu\nu_2^2+2\gamma\nu_1\nu_2+\mu\nu_1\nu_2\\ &= -\gamma\nu_1^2-(\gamma+\mu)\nu_2^2\end{aligned}$$

Therefore, $\dot{U}_2 \leq 0$, $\dot{U}_2 = 0$ only if $S = S^*$ and $I = I^*$. By applying LaSalle's invariant principle [Las76], [Cru09], this means the endemic steady state is globally asymptotically stable within $\mathbb{D}$. ■

In summary, we have proved that the system equilibria (both disease-free and endemic) of the model 4.2 are globally stable using the Lyapunov functions for the case when there are no time delays, i.e. $\tau_1 = \tau_2 = 0$. The remaining part of this chapter will be devoted to analysing the model 4.2 when the time delays are present in the system.

Remark 4.1

We have proved that conditions $(A1)$ *and* $(A2)$ *hold always for* $\tau_1 = \tau_2 = 0$ *and valid throughout this chapter. These two assumptions guarantee that the characteristic equation 4.9 will always have roots with negative real parts.*

4.3 Stability and bifurcation analysis with time delays

In this section, we will analyse model 4.2 when there are time delays present. In the previous section we proved that the steady states are globally asymptotically stable when $\tau_1 = \tau_2 = 0$. Here, we want to prove the same but when $\tau_1 \geq 0,\ \tau_2 \geq 0$. Again, model 4.2 has a disease free steady state $E^0 = (S^0, I^0) = (b/\gamma, 0)$ and a unique endemic state $E^*_\tau = (S^*_\tau, I^*_\tau)$ where

$$\begin{aligned} S^*_\tau &= \left(\tfrac{\mu+r+\gamma}{\beta}\right) = \tfrac{b}{\gamma \mathcal{R}_0}. \\ I^*_\tau &= \tfrac{b - \frac{\gamma(\mu+r+\gamma)}{\beta}}{(\gamma+\mu)+r(1-e^{-\gamma\tau_2})} = \tfrac{b\left(\frac{\mathcal{R}_0-1}{\mathcal{R}_0}\right)}{(\gamma+\mu)+r(1-e^{-\gamma\tau_2})}. \end{aligned} \tag{4.13}$$

From now on, we will perform bifurcation analysis with time delays, concentrating on the endemic steady state $E^*_\tau = (S^*_\tau, I^*_\tau)$. Linearising the system 4.2 about the endemic steady state $E^*_\tau = (S^*_\tau, I^*_\tau)$, we have the following characteristic quasipolynomial:

$$\begin{aligned} \Delta(\lambda) = \lambda^2 + \lambda[\gamma + (\gamma+r+\mu) + \beta I^*_\tau - \beta S^*_\tau e^{-\lambda\tau_1})] + (\gamma+r+\mu)(\gamma+\beta I^*_\tau) + \\ -\beta\gamma S^*_\tau e^{-\lambda\tau_1} - \beta r I^*_\tau e^{-\tau_2(\gamma+\lambda)}, \end{aligned} \tag{4.14}$$

introducing

$$\begin{aligned} p_0 &= \gamma + (\gamma+r+\mu) + \beta I^*_\tau, \\ p_1 &= -\beta S^*_\tau, \\ q_0 &= (\gamma+r+\mu)(\gamma+\beta I^*_\tau), \\ q_1 &= -\beta\gamma S^*_\tau \quad \text{and} \\ q_2 &= -\beta r I^*_\tau, \end{aligned}$$

the characteristic equation can be written as

$$\lambda^2 + (\lambda p_0 + q_0) + (\lambda p_1 + q_1)e^{-\lambda\tau_1} + q_2 e^{-\tau_2(\lambda+\gamma)} = 0. \tag{4.15}$$

4.3.1 Analysis of the system with only latency

This subsection presents analysis of the system 4.2 when there is only latency (i.e. $\tau_1 > 0$) in the model and immune period is set to zero (i.e. $\tau_2 = 0$). We state the following condition, and later show that it is true

$$\begin{aligned} &p_1^2 - p_0^2 + 2(q_0+q_2) < 0 \text{ and } (q_0+q_2)^2 - q_1^2 > 0 \\ &\text{or } [p_1^2 - p_0^2 + 2(q_0+q_2)]^2 < 4[(q_0+q_2)^2 - q_1^2] \end{aligned} \tag{A3}$$

Now consider the characteristic equation 4.15 with $\tau_2 = 0$:

$$\lambda^2 + (\lambda p_0 + q_0 + q_2) + (\lambda p_1 + q_1)e^{-\lambda\tau_1} = 0. \tag{4.16}$$

Theorem 4.4

Assumption A3 holds always for any parameter values, and the endemic steady state E_τ^* is locally asymptotically stable for all $\tau_1 > 0$.

Proof:

When $\tau_1 = 0$, the result follows from Theorem 4.1 as all eigenvalues have negative real part. To prove the theorem we have to show that when τ_1 increases, the roots of the characteristic equation 4.16 never cross the imaginary axis into a right complex half-plane. Let $\lambda = i\xi$ ($\xi > 0$) be a purely imaginary root of the quasi-polynomial 4.16. It suffices to seek solutions with $\xi > 0$, since complex roots occur in conjugate [Coo82], then ξ satisfies the following equation:

$$-\xi^2 + i\xi(p_0 + p_1(\cos\xi\tau_1 - i\sin\xi\tau_1)) + q_0 + q_1(\cos\xi\tau_1 - i\sin\xi\tau_1) + q_2 = 0. \tag{4.17}$$

Separating real and imaginary sides of equation 4.17 gives

$$\begin{aligned} \xi^2 - q_0 - q_2 &= \xi p_1 \sin\xi\tau_1 + q_1\cos\xi\tau_1 \\ \xi p_0 &= q_1\sin\xi\tau_1 - \xi p_1\cos\xi\tau_1 \end{aligned} \tag{4.18}$$

Squaring and adding the two equations in 4.18 yields

$$\xi^4-[p_1^2-p_0^2+2(q_0+q_2)]\xi^2+(q_0+q_2)^2-q_1^2=0. \tag{4.19}$$

Denoting $z=\xi^2$ we have:

$$z^2-[p_1^2-p_0^2+2(q_0+q_2)]z+(q_0+q_2)^2-q_1^2=0. \tag{4.20}$$

In terms of our model parameters, we have the following:

$$\begin{aligned}
p_1^2-p_0^2+2(q_0+q_2) &= \beta^2(S_\tau^*)^2-[\beta^2(I_\tau^*)^2+2(\mu+r+2\gamma)\beta I_\tau^*+(\mu+r+2\gamma)^2] \\
&+2[(\mu+r+\gamma)(\gamma+\beta I_\tau^*)-\beta r I_\tau^* \\
&= (\gamma+r+\mu)^2-[\gamma^2+2\gamma(\gamma+r+\mu)+2(\gamma+r+\mu)\beta I_\tau^*+2\gamma\beta I_\tau^*+(\gamma+r+\mu)^2+\beta^2(I_\tau^*)^2] \\
&+2\gamma(\gamma+r+\mu)+2(\gamma+r+\mu)\beta I_\tau^*-2r\beta I_\tau^* \\
&= -\gamma^2-2\gamma\beta I_\tau^*-\beta^2(I_\tau^*)^2-2r\beta I_\tau^* \\
&= -(\gamma+\beta I_\tau^*)^2-2r\beta I_\tau^* < 0,
\end{aligned} \tag{4.21}$$

where we have used the fact that $\beta S^*=(\mu+r+\gamma)$. In a similar manner,

$$\begin{aligned}
(q_0+q_2)^2-q_1^2 &= [(\gamma+r+\mu)(\gamma+\beta I_\tau^*)-r\beta I_\tau^*]^2-(-\gamma\beta S_\tau^*)^2 \\
&= \gamma^2(\gamma+r+\mu)^2+2\gamma(\gamma+r+\mu)^2\beta I_\tau^*+(\gamma+r+\mu)^2\beta^2(I_\tau^*)^2-2\gamma(\gamma+r+\mu)r\beta I_\tau^* \\
&-(\gamma+r+\mu)r\beta^2(I_\tau^*)^2+r^2\beta^2(I_\tau^*)^2-\gamma^2\beta^2(S_\tau^*)^2 \\
&= 2\gamma(\gamma+r+\mu)^2\beta I_\tau^*+(\gamma+r+\mu)^2\beta^2(I_\tau^*)^2-2\gamma(\gamma+r+\mu)r\beta I_\tau^* \\
&-(\gamma+r+\mu)r\beta^2(I_\tau^*)^2+r^2\beta^2(I_\tau^*)^2 \\
&= 2\gamma(\gamma+r+\mu)(\gamma+\mu)\beta I_\tau^*+(\gamma+r+\mu)(\gamma+\mu)\beta^2(I_\tau^*)^2+r^2\beta^2(I_\tau^*)^2 > 0.
\end{aligned} \tag{4.22}$$

This means that the assumption A3 is satisfied for any parameter values, and therefore both roots of the equation 4.19 are either negative or have negative real part. It is im-

possible to find real values for $\xi_{\pm}$, and therefore, the steady state E^*_τ is always stable. ■

In summary, theorem (4.4) shows that assumption A3 always holds, which means that the transcendental equation 4.16 has solutions with negative real parts. Then, following [Rua99] and using Rouche's theorem, we conclude that the transcendental equation 4.16 has roots with negative real part. Hence, the endemic steady state E^*_τ is locally asymptotically stable $\forall \tau_1 \geq 0$. This result is in agreement with those in [Xue13] and [Kad10].

4.3.2 Analysis of the system with only temporary immunity

In this subsection we consider the situation when there is temporary immunity, i.e. $\tau_2 > 0$, but the duration of latency is negligibly small: $\tau_1 = 0$. This particular case was considered by Kyrychko et al [Kyr05], they proved global stability of the endemic steady state. In this subsection, we will extend the results in [Kyr05] by finding the conditions that will guarantee that the endemic steady state is stable when τ_2 is less than some critical values, unstable when τ_2 exceeds the critical values and undergoes a Hopf bifurcation when τ_2 takes the critical values. Unlike in [Kyr05], we will show that the system's endemic steady state undergoes κ-switches from stability to instability to stability if certain conditions are satisfied. In this case, linearisation around the endemic steady state results in the following characteristic equation:

$$\lambda^2+\lambda(p_0+p_1)+q_0+q_1+q_2e^{-\tau_2(\lambda+\gamma)} = 0. \tag{4.23}$$

In order to understand how the characteristic eigenvalues determined as roots of the characteristic equation (4.23) depend on the time delay associated with temporary immunity τ_2, it is instructive do distinguish the following cases

$$2(q_0+q_1)-(p_0+p_1)^2 < 0 \text{ and } (q_0+q_1)^2-q_2^2 \geq 0, \tag{A4}$$

and

$$[2(q_0+q_1)-(p_0+p_1)^2]^2 < 4[(q_0+q_1)^2-q_2^2]. \tag{A5}$$

Theorem 4.5

In the case $\tau_1 = 0$ and $\tau_2 > 0$, if the condition (A4) or (A5) holds for all $\tau_2 > 0$, the endemic steady state E_τ^* is locally asymptotically stable for all $\tau_2 > 0$. Otherwise, there exists a positive integer n such that the endemic steady state is stable if

$$\tau_2 \in [0, \tau_c^+) \cup (\tau_c^-, \tau_{2,1}^+) \cup ... \cup (\tau_{2,n-1}^-, \tau_{2,n}^+),$$

and unstable when

$$\tau_2 \in [\tau_c^+, \tau_c^-) \cup (\tau_{2,1}^+, \tau_{2,1}^-) \cup ... \cup (\tau_{2,n}^+, \infty),$$

where

$$\tau_{2,n}^{\pm} = \frac{1}{\xi_\pm} \arctan\left\{\frac{(p_0+p_1)\xi_\pm}{\xi_\pm^2-(q_0+q_1)}\right\} + \frac{2n\pi}{\xi_\pm} \quad (n = 0, 1, 2, ...)$$

$$\xi_\pm^2 = \frac{1}{2}\left[2(q_0+q_1)-(p_0+p_1)^2\right] \pm \left\{\frac{1}{4}[2(q_0+q_1)-(p_0+p_1)^2]^2 - [(q_0+q_1)^2-q_2^2 e^{-\gamma\tau_{c,n}^{\pm}}]\right\}^{1/2}. \tag{4.24}$$

At $\tau_2 = \tau_{2,n}^{\pm}$, the endemic steady state undergoes Hopf bifurcation.

Proof:

In the proof of this Theorem we follow the ideas presented in Ruan (1999) [Rua99]. If we take $\lambda = i\xi$ ($\xi > 0$) to be a purely imaginary root of the transcendental characteristic equation (4.23), then ξ satisfies the following equation

$$-\xi^2 + i\xi(p_0+p_1) + q_0 + q_1 + q_2 e^{-\gamma\tau_2}(\cos\xi\tau_2 - i\sin\xi\tau_2) = 0. \tag{4.25}$$

Separating real and imaginary parts of equation (4.25) yields

$$\begin{aligned} \xi^2-(q_0+q_1) &= q_2 e^{-\gamma\tau_2}\cos\xi\tau_2, \\ (p_0+p_1)\xi &= q_2 e^{-\gamma\tau_2}\sin\xi\tau_2. \end{aligned} \tag{4.26}$$

Squaring and adding the two equations in (4.26) gives a single equation connecting the Hopf frequency ξ and the time delay τ_2:

$$\xi^4-[2(q_0+q_1)-(p_0+p_1)^2]\xi^2+(q_0+q_1)^2-q_2^2e^{-\gamma\tau_2}=0. \tag{4.27}$$

Introducing an auxiliary variable $z=\xi^2$, this equation can be rewritten as follows

$$z^2-A_\tau z+B_\tau=0, \tag{4.28}$$

where

$$A_\tau=[2(q_0+q_1)-(p_0+p_1)^2], \quad B_\tau=(q_0+q_1)^2-q_2^2e^{-\gamma\tau_2}.$$

Hence, one can find the Hopf frequency as

$$\xi_\pm=\sqrt{\frac{1}{2}A_{\tau_\pm}\pm\sqrt{\frac{1}{4}A_{\tau_\pm}^2-B_{\tau_\pm}}}. \tag{4.29}$$

Dividing the two equations in (4.26) allows one to find critical values of the time delay τ_2 implicitly as a function of the Hopf frequency ξ

$$\tau_{c,n}^{\pm}=\frac{1}{\xi_\pm}\arctan\left\{\frac{(p_0+p_1)\xi_\pm}{\xi_\pm^2-(q_0+q_1)}\right\}+\frac{2n\pi}{\xi_\pm} \quad (n=0,1,2,...). \tag{4.30}$$

If the condition (A4) holds for all $\tau_2>0$, this implies that $A_\tau<0$ and $B_\tau\geq 0$, and hence from (4.29) it follows that both values of $\xi_\pm$ are always purely imaginary. This implies that there does not exist a Hopf frequency $\xi>0$ satisfying equation (4.29), and,

therefore, the endemic steady state E_τ^* is stable for all $\tau_2 > 0$.

In a similar way, if the condition (A5) holds, this implies $A_\tau^2 < 4B_\tau$, which, according to (4.29), means that both values of $\xi_\pm$ are always complex, and, therefore, the endemic steady state E_τ^* is stable for all $\tau_2 > 0$.

In all other cases, the endemic steady state E_τ^* may undergo a Hopf bifurcation at the critical values of time delay determined as solutions of the system (4.24), which also provides the value of the associated Hopf frequency.

■

It is noteworthy that although the above **Theorem** provides conditions for stability and Hopf bifurcation of the endemic steady state E_τ^*, the conditions (4.24) actually form a system of equations that has to be solved in order to find a critical value of the time delay τ_2.

Next we investigate how the stability of endemic steady state changes in the (τ_2, β) plane as γ varies (note that this was not done in [Kyr05]). The colour in the figures below corresponds to the real part of the leading eigenvalue of the characteristic quasi-polynomial. The numerical simulations in this subsection and the next are carried out using *TraceDDE*, a toolbox in Matlab for computing the characteristic roots and stability charts for linear autonomous systems of delay differential equations with discrete and distributed time delays [Dim09]. Then, we export the data to gnuplot to generate the figures for the stability boundaries, see figure 4.1 below. Note that the endemic steady state $E^* = (S^*, I^*)$ depends on τ_2.

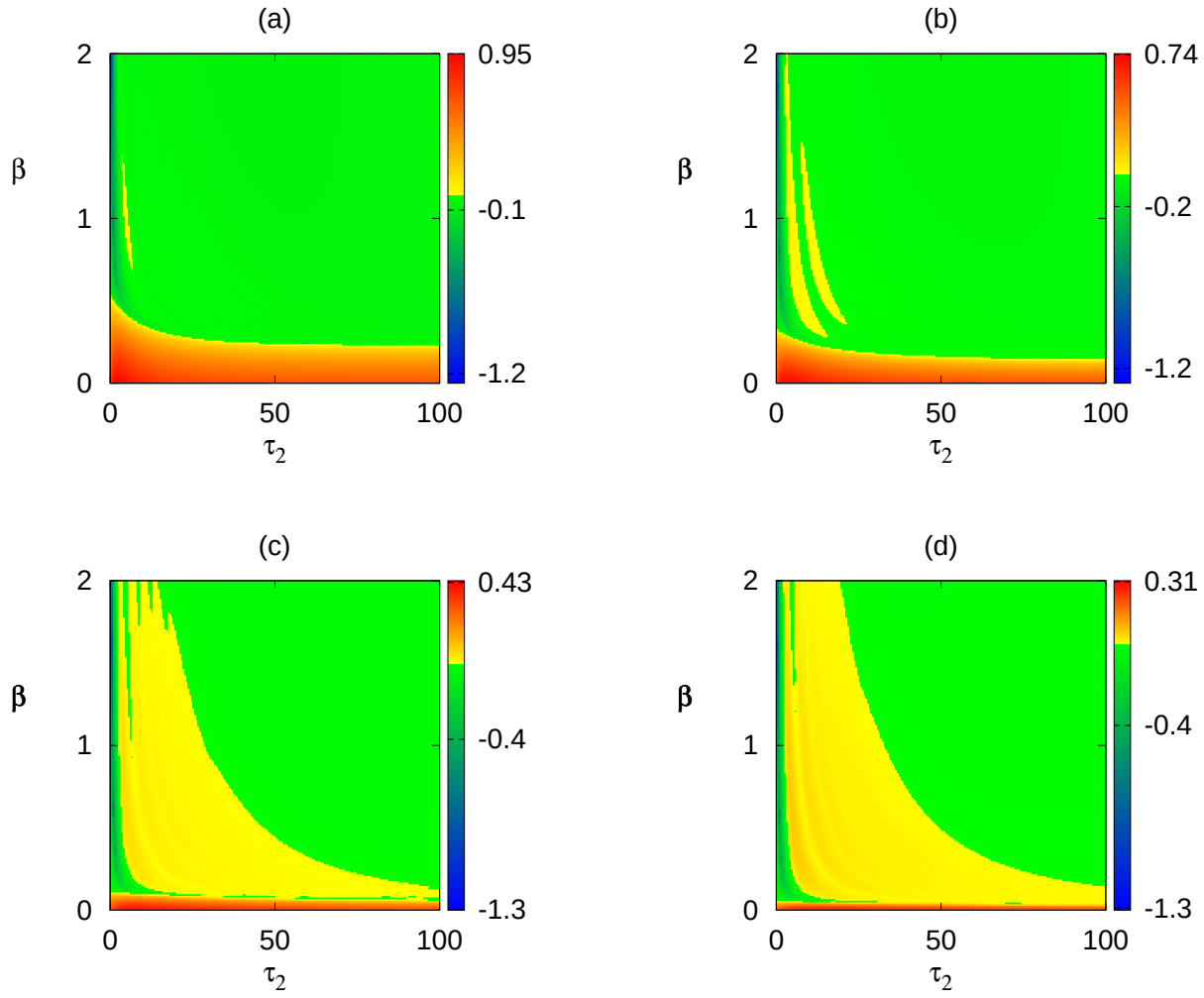

Figure 4.1: Stability charts for the endemic steady state E^*: (a) $\gamma = 0.1$, (b) $\gamma = 0.05$, (c) $\gamma = 0.01$, (d) $\gamma = 0.005$, other parameters are: $b = 0.1, r = 5, \mu = 3, \tau_1 = 0$. The color in the figures corresponds to the real part of the leading eigenvalue of the characteristic quasi-polynomial.

From the above figure we can see how regions of (in)stability of the endemic steady state change in the (τ_2, β) plane. This figure suggests that as the natural death rate decreases the parameter region of instability of the endemic steady state increases. From the above figure, we observe that the natural death rate γ play an important role in the stability and instability of the endemic steady state. Biologically, if we consider a case of an infectious disease, with a transmission probability $\beta \in [0\ 2]$, a temporary immunity $\tau_2 \in [0\ 100]$, a recovery rate $r = 5$ and a disease-induced death rate $\mu = 3$. The mean

values of $\mathcal{R}_0$ are; figure 4.1(a) $\mathcal{R}_0 = 0.1852$, figure 4.1(b) $\mathcal{R}_0 = 0.3727$, figure 4.1(c) $\mathcal{R}_0 = 1.8727$, and figure 4.1(d) $\mathcal{R}_0 = 3.7477$. We conclude that for sub-figures (a) and (b) the epidemic will die out and for sub-figures (c) and (d) the epidemic will persist in the population because $\mathcal{R}_0 \in [1.8727\ 3.7477]$.

Note: $\mathcal{R}_0$ refers to the average of the numerical values for $\mathcal{R}_0$ for β in the interval [0 2] and $\tau \in [0\ 100]$ for each γ, see [Cob09] for details on the mean values of the threshold parameter $\mathcal{R}_0$.

In this subsection, we have shown that the endemic steady state of model 4.2 for the case $\tau_1 = 0$ and $\tau_2 > 0$ have different dynamical asymptotic behaviours if A4, and A5 are satisfied. From figure 4.1, we have seen that biologically there are regions for epidemic safety where the endemic steady state is stable and regions for epidemic significant (outbreak) in the (τ_2, β) parameter plane. These figures (subfigures) tell us when to expect endemic epidemic outbreak and we choose our parameter's values such that we control $\mathcal{R}_0$ which we can use to predict the new rate of infection in the population.

4.3.3 Stability analysis for identical periods of latency and temporary immunity

This subsection deals with the analysis of system (4.2) when the temporal delays are identical, i.e. $\tau_1 = \tau_2 = \tau > 0$. As in the analysis presented above, we will state some conditions and later show that they are true. Then we prove the result that guarantees that the characteristic equation 4.15 will have no root with positive real parts for all $\tau > 0$. We state the following condition:

$$\begin{aligned} &(p_1^2 - p_0^2 + 2q_0) < 0 \text{ and } q_0^2 - (q_1 + q_2)^2 > 0, \\ &\text{or } [p_1^2 - p_0^2 + 2q_0]^2 < 4[q_0^2 - (q_1 + q_2)^2] \end{aligned} \tag{A6}$$

Now let $\tau > 0$, then the linearisation of the model 4.2 around the endemic steady

state has the following characteristic equation:

$$\lambda^2+(\lambda p_0+q_0)+(\lambda p_1+q_1)e^{-\lambda\tau}+q_2e^{-\tau(\lambda+\gamma)} = 0. \tag{4.31}$$

Theorem 4.6

Let $\tau > 0$. Then assumption A6 holds for any values of system parameters and the endemic steady state E^*_τ is locally asymptotically stable $\forall\tau \geq 0$.

Proof:

The proof of this theorem is similar to the proofs of theorems in previous sections, therefore, we will only sketch the proof. If we take $\lambda = i\xi$ ($\xi > 0$) to be a purely imaginary root of the characteristic equation 4.31, then ξ satisfies:

$$-\xi^2+i\xi p_0+q_0+(i\xi p_1+q_1)[\cos(\xi\tau)-i\sin(\xi\tau)]+q_2e^{-\gamma\tau}[\cos(\xi\tau)-i\sin(\xi\tau)] = 0 \tag{4.32}$$

Separating equation 4.32 into real and imaginary parts leads to

$$\begin{aligned} \xi^2-q_0 &= \xi p_1\sin(\xi\tau)+(q_1+q_2e^{-\gamma\tau})\cos(\xi\tau) \\ \xi p_0 &= (q_1+q_2e^{-\gamma\tau})\sin(\xi\tau)-\xi p_1\cos(\xi\tau). \end{aligned} \tag{4.33}$$

Squaring and adding these two equations yields

$$\xi^4-[p_1^2-p_0^2+2q_0]\xi^2+q_0^2-(q_1+q_2e^{-\gamma\tau})^2 = 0. \tag{4.34}$$

By letting $z = \xi^2$ we have the following:

$$z^2-[p_1^2-p_0^2+2q_0]z+q_0^2-(q_1+q_2e^{-\gamma\tau})^2 = 0. \tag{4.35}$$

Now, we show that the equation 4.35 can only have roots with negative real parts.

In terms of model parameters, we have the following:

$$\begin{aligned} p_1^2-p_0^2+2q_0 &= (-\beta S_\tau^*)^2-[\gamma+(\gamma+r+\mu)+\beta I_\tau^*]^2+2[(\gamma+r+\mu)(\gamma+\beta I_\tau^*)]^2 \\ &= \beta^2(S_\tau^*)^2-[\gamma^2+2\gamma(\gamma+r+\mu)+(\gamma+r+\mu)^2+2\gamma\beta I_\tau^*+2(\gamma+r+\mu)\beta I_\tau^*+\beta^2(I_\tau^*)^2] \\ &+2\gamma(\gamma+r+\mu)+2(\gamma+r+\mu)\beta I_\tau^* \\ &= -\gamma^2-2\gamma\beta I_\tau^*-\beta^2(I_\tau^*)^2 \\ &= -(\gamma+\beta I^*)^2 < 0, \end{aligned} \tag{4.36}$$

where we have used the fact that $\beta S^* = (\gamma+r+\mu)$. In a similar manner,

$$\begin{aligned} q_0^2-(q_1+q_2e^{-\gamma\tau})^2 &= [(\gamma+r+\mu)(\gamma+\beta I_\tau^*)]^2-[(-\gamma\beta S_\tau^*)+(-\beta r I_\tau^*)e^{-\gamma\tau})]^2 \\ &= (\gamma+r+\mu)^2[\gamma^2+2\gamma\beta I_\tau^*+\beta^2(I_\tau^*)^2]-[\gamma^2\beta^2(S_\tau^*)^2+2\gamma r(\beta S_\tau^*)\beta I_\tau^* e^{-\gamma\tau}+r^2\beta^2(I_\tau^*)^2e^{-2\gamma\tau}] \\ &= 2\gamma(\gamma+r+\mu)^2\beta I_\tau^*+(\gamma+r+\mu)^2\beta^2(I_\tau^*)^2-2\gamma r(\gamma+r+\mu)\beta I_\tau^* e^{-\gamma\tau}-r^2\beta^2(I_\tau^*)^2e^{-2\gamma\tau} \\ &= 2\gamma(\gamma+\mu)[(\gamma+\mu)+r(1-e^{-\gamma\tau})]\beta I_\tau^*+[(\gamma+\mu)^2+2r(\gamma+\mu)+r^2(1-e^{-2\gamma\tau})]\beta^2(I_\tau^*)^2 > 0. \end{aligned} \tag{4.37}$$

This implies that $(p_1^2-p_0^2+2q_0)$ is always negative, and $q_1^2-(q_1+q_2e^{-\gamma\tau})^2$ is always positive. Hence it is impossible to have real values for $\xi_\pm$, and therefore the steady state E_τ^* is always locally asymptotically stable. Computations in 4.36 and 4.37 show the conditions of assumption A6 always hold for any parameter values. ■

In the above case when the time delays are identical, we found that the endemic steady state is always stable for any values of τ. Biologically, the case corresponds to when the latency period and the temporary immunity are the same. That is, it takes the same period of time for the infected individuals to become infectious and to recover from the disease. Biologically, we cannot say exact why this is true.

4.3.4 Analysis of the system for non-zero latency and temporary immunity periods

This subsection is concerned with analysis of the model in the case when both latency and temporary immunity are present. The presence of these two time delays in the model makes the stability analysis more complicated. Several approaches have been proposed to analyse stability in models with two or multiple time delays [[Gu05], [Rua99], [Bly08]]. This case is the most important because we have the two time delays in the system and are not identical.

We will follow the idea and method proposed in Gu et al [Gu05]. As a first step, we rewrite the characteristic equation 4.15 as follows:

$$a(\lambda, \tau_1, \tau_2) = a_0(\lambda) + a_1(\lambda)e^{-\lambda\tau_1} + a_2(\lambda)e^{-\tau_2(\lambda+\gamma)}. \tag{4.38}$$

For convenience we will use the parametrization of stability boundary with two time delays in the delay parameter region as initially proposed by Gu et al [Gu05], and see Blyuss et al [Bly08] for details. We rewrite the trnscendental characteristic equation 4.38 as follows:

$$1 + \alpha_1(\lambda)e^{-\lambda\tau_1} + \alpha_2(\lambda)e^{-\tau_2(\lambda+\gamma)} = 0, \tag{4.39}$$

where,

$$\begin{aligned} \alpha_1 &= \frac{a_1(\lambda)}{a_0(\lambda)} = \frac{\lambda p_1 + q_1}{\lambda^2 + \lambda p_0 + q_0} \\ \alpha_2 &= \frac{a_2(\lambda)}{a_0(\lambda)} = \frac{q_2}{\lambda^2 + \lambda p_0 + q_0}. \end{aligned} \tag{4.40}$$

The p_i, q_i are defined previously and note that all coefficients depend on τ_2. We denote by Λ the crossing-set, which contains all values of ξ with the possibility that some zero(s) of $a(\lambda, \tau_1, \tau_2)$ can move across from left-right plane at $\lambda = i\xi$ [Gu05]. Given any $\xi \in$

Λ, $a_j(i\xi) = 0,\ j = 0, 1, 2$, we can find the following parameterization of the critical curves (τ_1, τ_2) satisfying 4.39

$$\begin{aligned} \tau_1 &= \tau_1^{p\pm}(\xi) = \tfrac{\text{Arg }\alpha_1(i\xi)+(2p-1)\pi\pm\phi_1}{\xi} \geq 0, \quad p = p_0^{\pm}, p_0^{\pm}+1, p_0^{\pm}+2, ... \\ \tau_2 &= \tau_2^{q\pm}(\xi) = \tfrac{\text{Arg }\alpha_2(i\xi)+(2q-1)\pi\mp\phi_2}{\xi} \geq 0, \quad q = q_0^{\pm}, q_0^{\pm}+1, q_0^{\pm}+2, ... \end{aligned} \tag{4.41}$$

where $\phi_1, \phi_2 \in [0, \pi]$ can be found as follows

$$\begin{aligned} \phi_1 &= \arccos\left(\tfrac{1+|\alpha_1(i\xi)|^2-|\alpha_2(i\xi)|^2}{2|\alpha_1(i\xi)}\right) \\ \phi_2 &= \arccos\left(\tfrac{1+|\alpha_2(i\xi)|^2-|\alpha_1(i\xi)|^2}{2|\alpha_2(i\xi)}\right). \end{aligned} \tag{4.42}$$

and $p_0^+, p_0^-, q_0^+, q_0^- \in \mathbb{Z}$ such that $\tau_1^{p_0^+}, \tau_1^{p_0^-}, \tau_2^{q_0^+}, \tau_2^{q_0^-}$, are nonnegative. Please observe that $p_0^+ \leq p_0^-, q_0^+ \geq q_0^-$.
Let $\mathcal{T}^+_{\xi,p,q}$ and $\mathcal{T}^-_{\xi,p,q}$ be the singletons defined by

$$\mathcal{T}^{\pm}_{\xi,p,q} = \left(\tau_1^{p\pm}(\xi), \tau_2^{q\pm}(\xi)\right) \tag{4.43}$$

and define

$$\mathcal{T}_\xi = \left(\bigcup_{p\geq p_0^+, q\geq q_0^+} \mathcal{T}^+_{\xi,p,q}\right) \cup \left(\bigcup_{p\geq p_0^-, q\geq q_0^-} \mathcal{T}^-_{\xi,p,q}\right)$$

Then $\mathcal{T}_\xi$ is the set of all (τ_1, τ_2) such that $a(\lambda, \tau_1, \tau_2)$ has a zero at $\lambda = i\xi$ [Gu05], [Bly08].
Note: Even though we derived the formulas 4.41 and 4.42, the coefficients $\alpha_i,\ i = 1, 2$ depend on τ_2 and this makes the closed form calculations impossible.

In the figures below, we illustrate the above stability results and numerically compute the real part of the leading eigenvalue of the characteristic equation 4.15 using *TraceDDE* suite in MATLAB. Then we save the data and export to gnuplot to generate the stability regions. By varying the disease transmission rate we investigate how stability changes in the (τ_1, τ_2)-plane, and we also study the effects of the natural death rate γ, and the disease-induced death rate μ on the dynamics of the system.

In Figure 4.2 below, we vary β in the interval $[1-4]$ and observe the dynamical behaviour of the system. Note that the color in the figure corresponds to the real part of the leading eigenvalue of the characteristic quasi-polynomial 4.15. We fixed all other parameters and varied β as it is one of the most biologically relevant parameters, as it represents the rate at which new infections occur through contacts between infected and susceptible individuals. In the second figure (4.3), we will fix β, r, b and vary other parameters like the natural death rate γ and the disease-induced death rate μ. Numerically we observed that when β is decreased and becomes very small the endemic steady state is always stable.

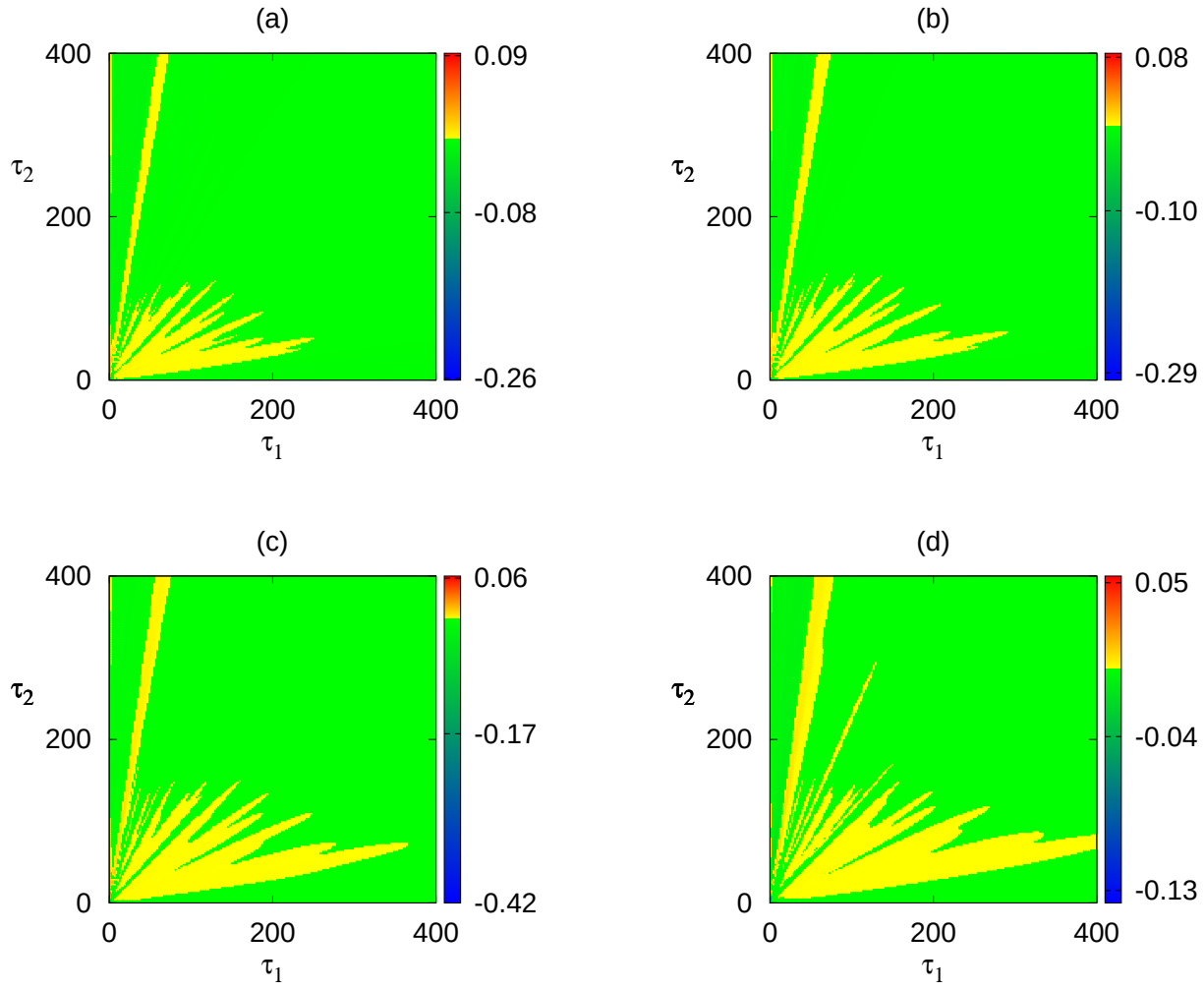

Figure 4.2: Stability charts for the endemic steady state E^*: (a) $\beta = 1$, (b) $\beta = 2$, (c) $\beta = 3$, (d) $\beta = 4$, other parameters are: $b = 0.1, r = 5, \gamma = 0.01, \mu = 3$. The color in the figures corresponds to the real part of the leading eigenvalue of the characteristic quasi-polynomial.

From figure 4.2 we can see that β played an important role in the dynamical behaviour of the system 4.2. As β increases, the regions of instability of the endemic steady state and associated periodic behaviours occupy a larger part of the (τ_1, τ_2) parameter plane. Now if we assume that each infected individual (I) transmits the disease with probability β to each susceptible individual (S) they encounter. The number of susceptible individuals decreases as the incidence (i.e., the number of individuals infected per unit time)

increases. The severity of the epidemic and the initial rate of increase depend upon the value of the basic reproduction number ($\mathcal{R}_0$). Then biologically, we know that as the transmission rate increases the region of instability of the endemic steady state increases. Also, this can be seen as we increased the transmission rate β, the basic reproduction number $\mathcal{R}_0$ increased as well. In (a) $\mathcal{R}_0 = 1.2484$, (b) $\mathcal{R}_0 = 2.4969$, (c) $\mathcal{R}_0 = 3.7453$ and in (d) $\mathcal{R}_0 = 4.9938$. In both sub-figures we can see that there is tendency of disease persistent since $\mathcal{R}_0 > 1$. This is because as β increased, $\mathcal{R}_0$ increased too and the number of infected individuals increased as well. Hence we have less stability as the transmission parameter increased in the τ_1, τ_2 parameter plane. These values of the basic reproduction ratio $\mathcal{R}_0$ can be compared to those in Coburn et al (2009) [Cob09]. Hence, we conclude from this analysis that with appropriate choice of parameter's values, our model can be used to forcast the future occurrence and prevalence of some epidemics.

In Figure 4.3 below, we fixed $\beta,\ r,\ b$ and varied the natural death rate γ and the diesase-induced death rate μ to see if this affects the (in)stability regions in the (τ_1, τ_2)-parameter plane. Since from the above analysis, we can see that the transmission has effects on the dynamical behaviour of the system's equilibria. Then in the next experiment we will fix all parameters and vary γ (sub-figures 4.3(a) and 4.3(b)). Also, in sub-figures 4.3(c) and 4.3(d) we will fix all parameters and vary μ. It is noteworthy that the choice of these parameters is purely because of their biological relevant in our model. Just like in the previous figures, we numerically compute the real part of the leading eigenvalue of the characteristic equation 4.15 using *TraceDDE* suite in MATLAB. Then we save the data and export to gnuplot to generate the stability regions. The color in the figure below corresponds to the real part of the leading eigenvalue of the characteristic equation. From the above analysis, we conclude that the dynamical asymptotic behaviour of the system is richer when we have the two time delays in the system (c.f., figures 4.2 and 4.3).

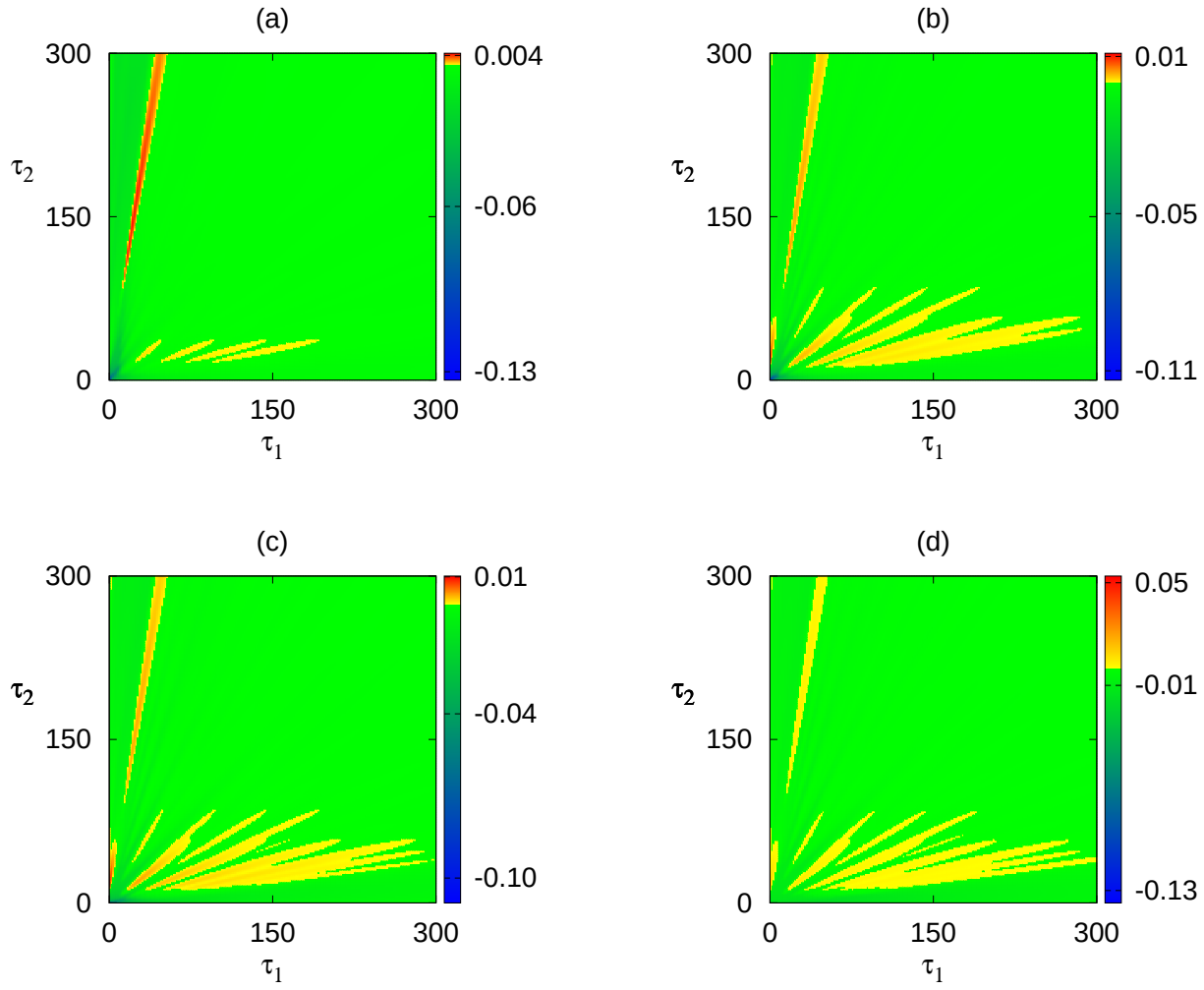

Figure 4.3: Stability charts for the endemic steady state E^*: (a) $\gamma = 0.02$ and (b) $\gamma = 0.01$ with $\mu = 0.1$, (c) $\mu = 0.05$, (d) $\gamma = \mu = 0.01$ with $\gamma = 0.01$. Other parameters are $\beta = 10, r = 0.5, b = 0.003$. The color in the figures corresponds to the real part of the leading eigenvalue of the characteristic quasi-polynomial.

In figure 4.3 above, we fixed β, r, b and varied the natural death rate γ and the disease-induced death rate μ which are important from biological point of view. In (a) and (b) we fixed all parameters and varied γ and in (c) and (d) we varied μ. In sub-figure 4.3(a), we take $\gamma = 0.02$, $\mu = 0.1$ we can see that there are regions of instability for the endemic steady state in the (τ_1, τ_2)-parameter plane. In sub-figure 4.3(b), we decreased γ to 0.01 with μ fixed at 0.1, we observed that the parameter regions of instability of the endemic steady state increased. In sub-figure 4.3(c), we took $\mu = 0.05$ with fixed

$\gamma = 0.01$ and we observed that the regions of instability of the endemic steady state have increased dramatically. Then, in sub-figures 4.3(c) and 4.3(d), we fixed γ at 0.01 and took μ to be 0.05 and 0.01 respectively. It can be seen from 4.3(c) and 4.3(d) as we decreased μ, we observed wider parameter regions of instability of the endemic steady state. So, this means decreasing γ or μ or both increases the parameter regions of instability of the endemic steady state in the (τ_1, τ_2) plane. From the parameter values chosen we observed that the severity of the epidemic is high because the values of the basic reproduction ratio $\mathcal{R}_0$ increased as we decreased γ or μ. The $\mathcal{R}_0$ are: 4.3(a) $\mathcal{R}_0 = 2.4194$, 4.3(b) $\mathcal{R}_0 = 4.9180$, 4.3(c) $\mathcal{R}_0 = 5.3571$ and in 4.3(d) $\mathcal{R}_0 = 5.7692$.

4.4 Numerical simulations

This section presents the results of the numerical simulations of the model 4.2 using *dde23* suite in Matlab. These simulations will support the theoretical results of the previous sections and also illustrate temporal dynamics of the system in different parameter regimes. We have four cases to consider: in the first case, we will show that the solution is always stable for all $\tau_1 > 0,\ \tau_2 = 0$. In the second case, we will show that the system approaches a stable endemic steady state when A4 is satisfied, possesses periodic solutions arising from a Hopf bifurcation at $\tau = \tau_0$ when A5 holds, and can undergo k stability switches otherwise. For the third case, the endemic steady state is always stable for any parameter values which is similar to the first case. The fourth case is the most important because here we have both latency and temporary immunity periods in the system. We will show that if $\tau < \tau_c$) the endemic steady state E^* is stable, unstable if $\tau > \tau_c$) and undergoes Hopf bifurcation if $\tau = \tau_c$).

4.4.1 There is latency but no temporary immunity in the system

In this subsection, through numerical simulation we confirm the analytical results in subsection 4.3.1. We will show that the characteristic equation 4.16 has roots with negative real parts if condition A3 is satisfied and therefore, the endemic steady state is always stable for any parameter values. Here, $\tau_1 > 0$ and $\tau_2 = 0$ and we consider an infectious disease with the following parameter estimates $\beta = 0.9$, $r = 0.5$,$\gamma = 0.1$, $b = 0.35$, $\mu = 0.1$, $\tau_1 = 1.5$.

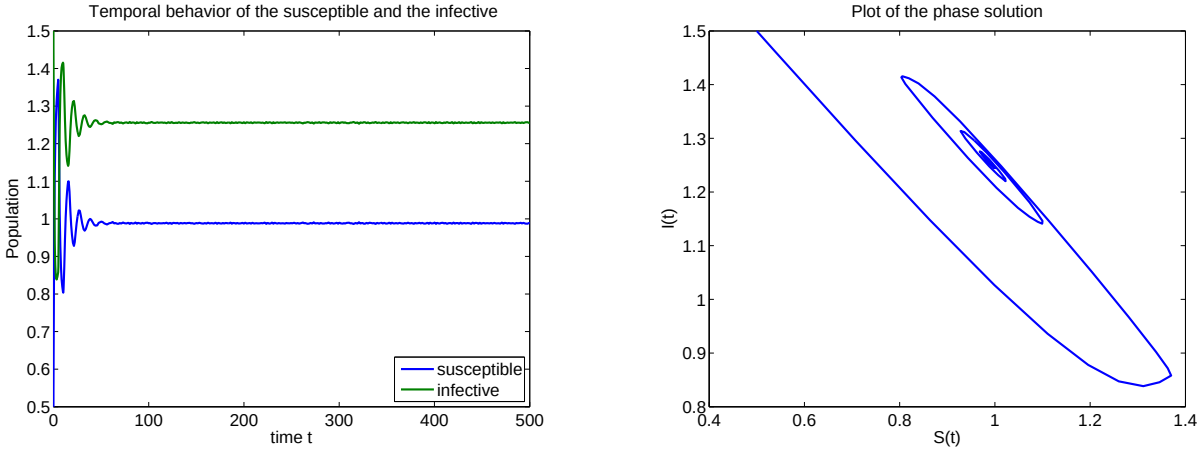

(a) (b)

Figure 4.4: Solutions profile for the system 4.2 , parameter values are: $\beta = 0.9,\ r = 0.5,\ \gamma = 0.1,\ b = 0.35,\ \mu = 0.1,\ \tau_1 = 1.5,\ \tau_2 = 0.$

From figure 4.4 above, we observed that the system approaches a stable endemic steady state for all $\tau_1 \geq 0$ and this confirm our analytical results in subsection 4.3.1. Also, for the case when $\tau_1 = \tau_2 = \tau$, we have similar dynamics as in figure 4.4 above, the system's steady state is always stable for all $\tau \geq 0$. Therefore, we omitted the figure for that case because it has the same dynamics as figure 4.4 above. Even though, the results in these two cases are consistent with those in [Xue13] and [Kad10], we could not understand from biological point of view why in both cases the endemic steady state E^* is always stable for any parameter's values.

4.4.2 There is only temporary immunity in the system

In this subsection, we consider the case for a disease with only temporary immunity and latency period set to zero ($\tau_2 > 0$ and $\tau_1 = 0$). As an example to test our results, we consider an infectious disease with short immunity period. Example of such diseases are chlamydia infection and influenza. Now for sufficiently short period of immunity, the endemic steady state is stable if condition A4 or A5 is satisfied, otherwise it undergoes

Hopf bifurcation when the period of immunity τ_2 takes the critical value τ_c as described by Theorem 4.6 in subsection 4.3.2 see figures 4.5 and 4.6 below.

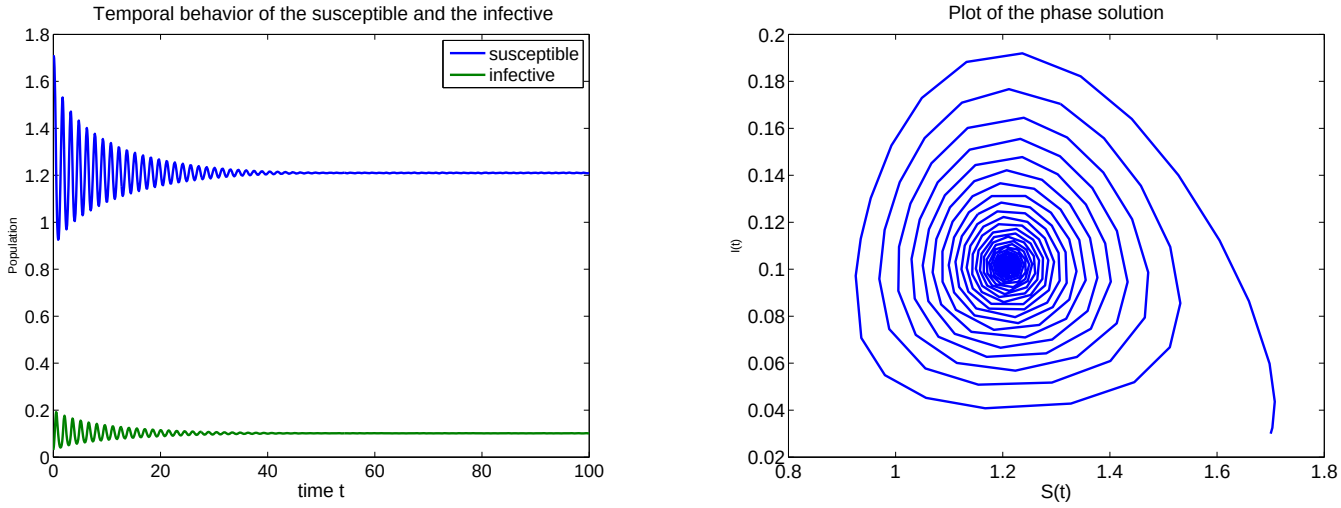

(a) (b)

Figure 4.5: Solutions profile for the system 4.2 , parameter values are: $\beta = 10,\ b = 0.7,\ r = 7,\ \gamma = 0.1,\ \mu = 5,\ \tau_2 = 0.9,\ \tau_1 = 0$

In figure 4.5 above the system approaches a stable endemic steady state $(S^*_\tau, I^*_\tau) = (1.2100, 0.1015)$ for a short period of temporary immunity $\tau_2 = 0.9$. This showed that with the above parameter's values, the condition A4 is satisfied. Next, we allow τ_2 to take the critical values τ_c.

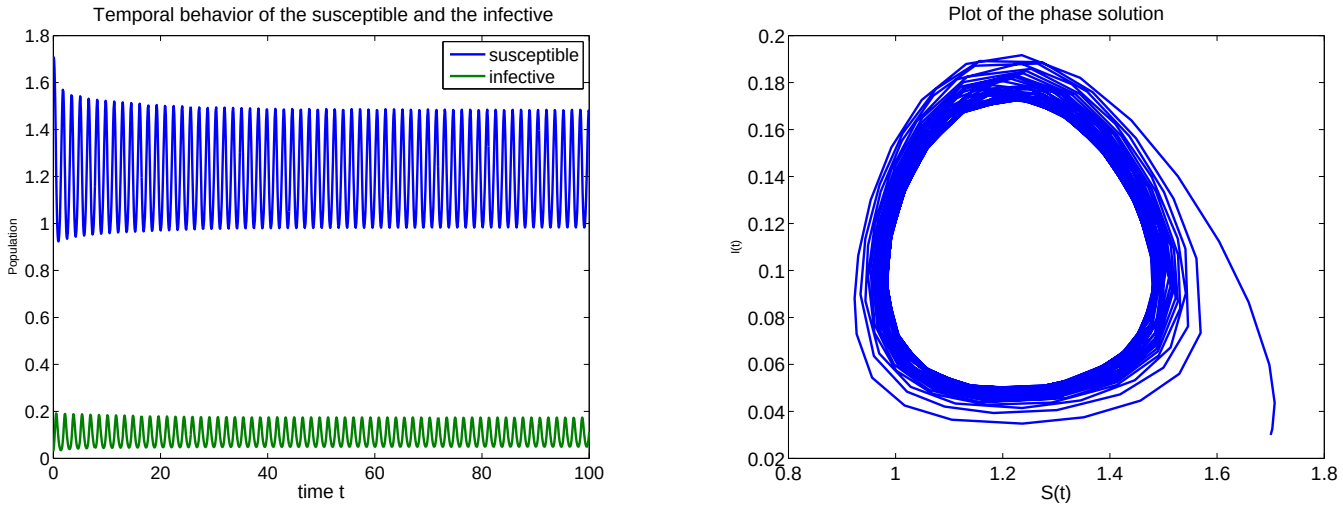

(a) (b)

Figure 4.6: Solutions profile for the system 4.2 , parameter values are: $\beta = 10,\ b = 0.7,\ r = 7,\ \gamma = 0.1,\ \mu = 5,\ \tau_2 = 1,\ \tau_1 = 0$

In figure 4.6 above we have Hopf bifurcation at $\tau_2 = 1$ and this means we will have periodic outbreak of epidemic. Our results can be compared to those in for instance [Kyr05].

4.4.3 There is both latency and immunity

In this subsection we consider the case when the two time delays are presence in the model 4.2 (i.e. $\tau_1 > 0,\ \tau_2 > 0$). We will show temporal behaviour of both the susceptible and infected individuals and also the phase trajectories of the system. We consider an instance of an infectious disease with short periods of latency and immunity, a good example of such disease is chlamydia infection but with very high rates of reinfection.

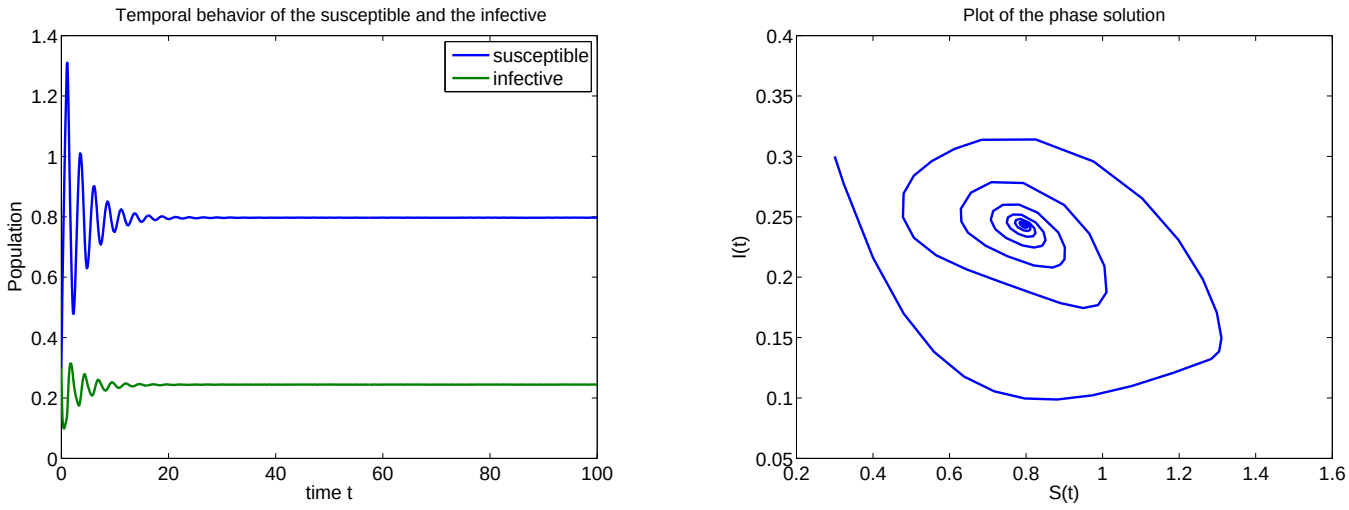

(a) (b)

Figure 4.7: Solutions profile for the system 4.2 , parameter values are: $\beta = 2,\ r = 5,\ \gamma = 0.1,\ b = 0.35,\ \mu = 0.1,\ \tau_1 = 1,\ \tau_2 = 2$

In figure (4.7) above, we have stable endemic steady state for $\beta = 2$, $\tau_1 = 1$ and $\tau_2 = 2$. The phase trajectories illustrate stable spirals.

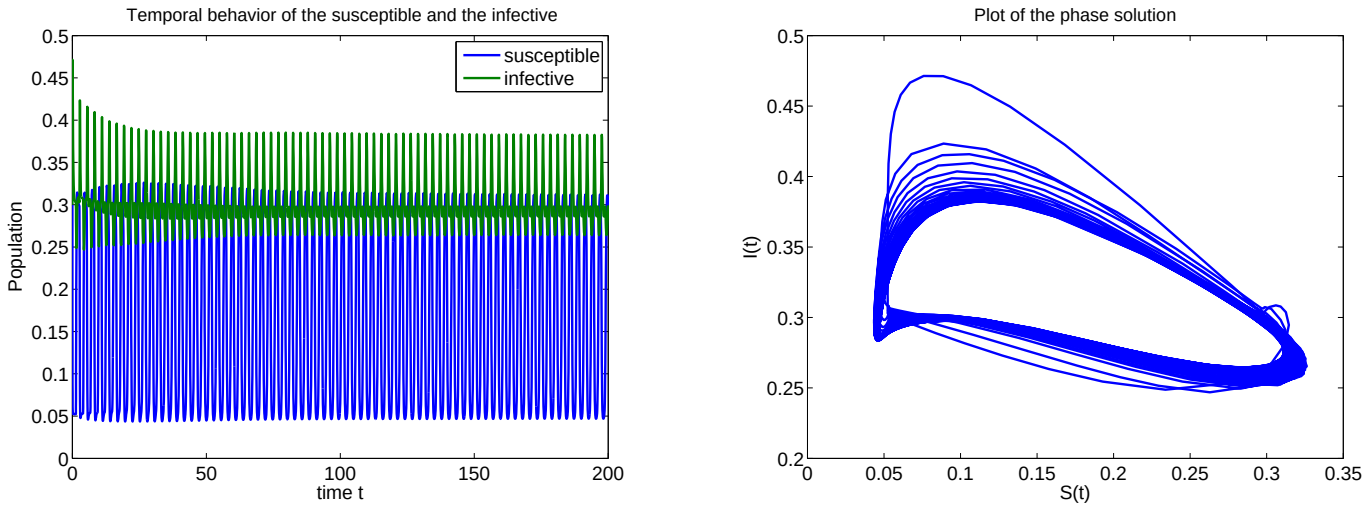

(a) (b)

Figure 4.8: Solutions profile for the system 4.2 , parameter values are: $\beta = 10,\ b = 0.3,\ r = 5,\ \gamma = 0.1,\ \mu = 0.1,\ \tau_1 = 1.323,\ \tau_2 = 2.133$

In figure 4.8 above, we clearly have periodic epidemic outbreak.

4.5 Conclusion from the Chapter

In this chapter, we have derived and analysed a delayed SIR epidemic model with two time delays. We proved both local and global stability of the system equilibria for the case when $\tau_1 = \tau_2 = 0$. In the presence of the time delays we proved the existence of periodic solutions arising through a Hopf bifurcation of an endemic steady state. We found the system's endemic steady state is always stable for any parameter values for the case when there is only latency in the system. When there is temporary immunity in the model, we found that when $\tau_2 < \tau_c$ the endemic steady state is stable, if $\tau_2 > \tau_c$ the endemic steady state is unstable, and at $\tau_2 = \tau_c$ the endemic steady state undergoes Hopf bifurcation. For the case when there is both latency and immunity ($\tau_1 > 0$, $\tau_2 > 0$) in the model, we found large regions of instability of the endemic steady state in the

(τ_1, τ_2) parameter plane. The most interesting results in this Chapter are the analysis in subsections 4.3.2 and 3.5 for the cases when we have immunity and when we have both latency and immunity in the system. The results we presented in those subsections showed interesting regions of (in)stability for the endemic steady state in different parameter regimes. We studied the effects of the transmission rate β, the natural death rate γ and the disease-induced death rate μ on the (in)stability of the endemic steady state. We found that increasing β always increases the regions of instability while decreasing γ and/or μ, increased the regions of instability of the endemic steady state of the model 4.2. We found that the dynamics of the system is richer when we have the two time delays in the model (c.f., figures 4.2 and 4.3). The choice of β, γ and μ were purely because of their biological importance in our model. Also, we computed the basic reproduction number $\mathcal{R}_0$ which we found to be a plausible range. We have also shown that our model can be a good predictor for infectious diseases through numerical simulations. All our numerical results agreed well with the analytical results. It is noteworthy to mention that even though our choice of parameter values were not exact for these infectious diseases but they showed comparable results to those on real data. We did not pay much attention to getting real data from the initial stage of this research because our main goal was to derive more general models that can describe a few number of epidemics rather than focusing on one epidemic for the entire research.

Chapter 5

Summary and conclusion

5.1 Summary

In this research work, we have considered two mathematical models; a spatial SIS reaction-diffusion epidemic model with a nonlinear incidence rate, which we modelled by two-component reaction-diffusion system in two spatial dimensions; and an SIR delayed epidemic model with two time delays and a bilinear incidence rate. For each of the models, we performed rigorous numerical and analytical analysis of the models equilibria. For the spatial SIS model 3.4, we are interested on the effects of space on the dynamical behaviour of the system as the model parameters vary. Therefore, we studied Turing instability (bifurcation) conditions in the parameter space. For the delayed SIR model, we are interested in Hopf bifurcation and therefore, we studied periodic solutions arising from Hopf instability and temporal behaviour in different parameter regimes.

In the first part of the thesis, we introduced the concept of mathematical modelling of infectious diseases (chapter 1). We reviewed some related literature both spatial and delay models. In chapter 2, we derived the SIS non-spatial model and introduced a nonlinear incidence rate $\beta S^p I^q$ to account for multiple exposure and high contagion of some infectious diseases like influenza. We proved positivity, boundedness, invariant principle and permanence for the model 3.4 for the general exponents $p, q \in \mathbb{Z}^+$ and for

a non-constant population N. And well-posededness was achieved from a mathematical and physical point-of-view. The model 2.1 has two equilibria, a disease-free steady state and a unique endemic state exists if $\mathcal{R}_0 > 1$. Local stability of the system's equilibria was proved using the idea of Routh Hurwitz principle. We found that the disease-free steady state E^0 is locally asymptotically stable for the general phenomenological and unconditionally stable at $q = 1$. Also, we found that the endemic steady state E^* exists for $\mathcal{R}_0 > 1$ and is conditionally stable if $pI > qS$. An effort was made to define and derive the basic reproductive number $\mathcal{R}_0$ using the idea of *next generation matrix operator*. $\mathcal{R}_0$ is a necessary and sufficient threshold parameter in proving stability of the system equilibria. And it's one of the most important threshold quantity in medicine and epidemiology which tells how epidemics grow. An explicit expression was derived for $\mathcal{R}_0$ for the model 2.1. We used the basic reproduction number in Chapters 3 and 4 to study the prevalence of the disease. Finally, we presented some numerical results in one space dimension.

In Chapter 3, we modified the model 2.1 by incorporating space. Then, the resulting spatial model which is a system of two-components reaction-diffusion equations that modelled the interaction of susceptible and infected individual populations in their physical environment was analysed. Finding a correct numerical method to approximate a reaction-diffusion system like model 3.4 is a not an easy task. The simplest and commonest numerical methods for approximating differential equations are the so-called *finite differences*. In solving non-linear and semi-linear systems like model 3.4, these methods suffer from stability issues and can be very slow and are expensive to implement because of the restriction on the time steps (for explicit schemes) and for having to solve system of equations at every time step (for implicit schemes). Initially, we tested our model with finite differences and we suffered from the restriction on time steps which inexorably slow our numerical computations. For this reason, the quest for more reliable, more effective and more stable methods intensified. Then, we found a method that is faster and stable. The method is the so-called Implicit-Explicit (IMEX) scheme and similar to the splitting methods and more of predictor-corrector methods. In this method, we divided

the problem into linear and nonlinear parts and each was approximated with a different numerical scheme. We solved the linear (diffusion) terms implicitly in Fourier space and the nonlinear (reaction) terms explicitly in real space. This made our numerical computations faster and more reliable. To be sure that the IMEX method actually solved our model 3.4, we benchmarked the problem by solving a modified version of model 3.4 with a known exact solution. We computed the experimental order of convergence (EOC) and found that the method converged with correct order one. Also, we went further to compute the error in L^2, H^1 and L^∞ norms and we obtained small error of order 10^{-5} on average which is good for our case (chapter 3).

In the presence of diffusion, the spatial model 3.4 was linearised around the non-trivial steady state E^* and we performed linear stability analysis. We derived Turing instability conditions that guaranteed the existence of spatial patterns in Turing space. We used pattern formation to explain the spread and control of the epidemics over a course of time. Turing instability conditions are established and analysed for the model 3.4 to exhibit patterns. The spatial patterns revealed that the susceptible and infected populations behave in the same way. In some cases, these populations are in isolation which means we can easily control the epidemic. We showed that the model 3.4 has rich dynamics of patterns for different values of the bifurcation parameter β and the treatment rate r located in the Turing space (see figure 3.3.1). In figures 3.4−3.12, numerically, we showed four types of spatial patterns showing the distribution of the infective I for system 3.4. The spatial patterns are due to the randomness from our initial data for different values of the bifurcation β. The four categories of the patterns are: spots with low density which consists of red (maximum proportion of I) hexagons with blue (minimum proportion of I) background, this means, the infectious are in isolated areas which has low population proportion, we called them 'red-holes', spots with high density which consists of blue (minimum proportion of I) hexagons with red (maximum proportion of I) background, we called them 'blue-holes', spot-stripe mixture, and the fourth category is stripe patterns.

From figures 3.4−3.11, we can see that for a fixed r, when we increase the bifurcation

parameter β, we obtain the following sequence of patterns 'spots' (red-holes) to 'spot-stripe' mixture to 'stripes' to 'spot-holes' (blue-holes). From the viewpoint of epidemic dynamics, in figures 3.4 & 3.5, we observed spot patterns and the infected I are isolated in areas with high proportion, the other area has low proportion but bigger than the spots area, this implies in this region there is no epidemic breakout. Therefore, for this case, the region is safe. For figure 3.7, we observed spot-stripe mixture with the spots decaying. Initially, the infectious individuals are isolated in areas which have high proportion but gradually, the spots decay to stripes. This means there is a possibility of an outbreak in this case. In figure 3.8, we have fully matured stripes patterns and therefore in this case the epidemic is significant. In figure 2.12, we observed that the infected populations are isolated in areas which have low proportion, and the remaining area, which has high proportion is bigger than the blue-holes (blue-hexagons or spots with red-background) area. This implies, there will be an epidemic breakout in this region. Therefore, from figures 3.4−3.10, we can observe that as we varied the transmission rate β, we obtained rich dynamics of the system 3.4. Now, in figure 3.11, we varied both β and r, we found that whenever $\beta < r$, we have spot patterns and for $\beta \geq r$, we have stripes. This means whenever the transmission rate β is strictly less than the recovery rate r, the system 3.4 will always have stable spot patterns. And whenever $\beta \geq r$, the solution to the model 3.4 will always be stable stripe patterns. Biologically or epidemiologically speaking, whenever $\beta < r$ there is no outbreak and whenever $\beta \geq r$ there will always be an outbreak.

In the second part of the thesis, we derived and analysed a delayed $SIRS$ epidemic model that described diseases with latency (τ_1) and temporary immunity (τ_2) periods and bilinear incidence rate. In modelling infectious diseases, it is important and necessary to capture or incorporate these two features of diseases (latency & temporary immunity). Also, it is sometimes important to take into consideration of temporal delays inherent in the problem. Adding delays explicitly in the models is often a way of simplification or idealisation that is introduced because in most cases a detailed description of the underlying processes may be too complicated to be modelled mathematically , and in some cases details of the underlying processes are unknown. To analyse the stability of

the model equilibria, we considered five special cases first, for a case $\tau_1 = \tau_2 = 0$) and in this case we found the model equilibria are globally asymptotically stable. This was proved using the famous technique of Lyapunov direct approach. Secondly, for a disease with only latency, that is, $\tau_1 > 0$, and $\tau_2 = 0$, we found that the steady state solution is always stable for any parameter values. Thirdly, for a disease with immunity but latency period set to zero (i.e. $\tau_1 = 0,\ \tau_2 > 0$), we have conditional stability, periodic solutions arising from Hopf bifurcation whenever $\tau_2 = \tau_0$ and instability whenever $\tau_2 > \tau_0$. Fourth, when there are latency and immunity and both are identical (i.e. $\tau_1 = \tau_2 = \tau > 0$), we found that the steady state solution is always stable. And finally, we considered the case when there are both latency and temporary immunity periods and they are distinct (i.e. $\tau_1 > 0, \tau_2 > 0\ \ \tau_1 \neq \tau_2$), for certain parameter values the nontrivial solution is stable, but for some values of the time delays it undergoes Hopf bifurcation giving rise to periodic solutions and for certain parameter regime the system is unstable. Analytical results are supported with extensive numerical simulations, illustrating behaviour of the system in different dynamical regimes.

5.2 Conclusion

In this thesis, we made an effort to analyse the spatio-temporal dynamics of two epidemic models (spatial SIS and delay SIR), the former with nonlinear incidence rate and the later with bilinear incidence rate. The contribution of this research work lies in the following aspects.

For the first model, we presented rigorous and thorough numerical and analytical analysis of the model equilibria. We were able to prove that the system equilibria are locally asymptotically stable. The analysis of spatial or Turing patterns revealed that model 3.4 has rich and complex dynamics in the parameter space. We showed that the model 3.4 has four categories of spatial patterns in the parameter regime. We then used these spatial structures to study and explain how epidemics spread in space. From these structures, we can establish confidently the parameter regimes in which we can have

safety or epidemic outbreak in our spatial domain. Again, from numerical simulations, we found that the speed at which the epidemics spread increase dramatically as the bifurcation or transmission parameter β increases. We have proved that model 3.4 has diffusion-driven pattern formation not just spot and stripe patterns but also, spot-stripe and stripe-spot (holes) mixtures of patterns. More interestingly, we found that when we varied both the transmission rate β and the treatment rate r, the ordering of the spatial patterns aforementioned changed. We observed numerically that whenever $\beta < r$ the model 3.4 will always have spot patterns and whenever $\beta \geq r$, we have stripe patterns. This means whenever $\beta < r$ there is no epidemic outbreak and whenever $\beta \geq r$ there is always an outbreak for the model 3.4. Biologically speaking, this means when the interventions are in place and administered at the right time then no matter the stage of the epidemic it may still be controlled. But when the interventions are less than the speed of the epidemic no matter how small it may be, there is always a possibility of an outbreak. Therefore, to keep an epidemic under control we keep $\beta < r$. Finally, the question of pattern selection, i.e. whether stripes or spots are preferred for particular values of parameters in the system 3.4 is investigated. These results can answer the question of Which is preferred, isolation or not from the infective? And we have showed that, isolation is better. Also, these results will enrich the research into spatial patterns in epidemic models. The results obtained extend well the findings of pattern formation in epidemic models and may have direct implications for the study of disease spread and control and perhaps the mechanistic impact of public health interventions on epidemics. Finally, we have seen from our results that the spatial model can be used to model diseases like influenza and chlamydia infection.

For the second part of the thesis, we derived and analysed an $SIRS$ epidemic model for disease transmission with two time delays (latency and temporary immunity periods). We prove both global and local stability of the system equilibria in the case when there are no time delays, i.e. both the latency and temporary immunity periods are set to zero. We found that the steady state is aways stable for cases; when there is only latency and when the two time delays are identical in the system. For the cases; when there

is temporary immunity but no latency and when there are both latency and temporary immunity in the system, we found periodic solutions arising from a Hopf bifurcation. In the last two cases, we found rich dynamics when the transmission, the natural death rate and disease-induced death rate were varied. We observed that varying these parameter increased the regions of instability of the endemic steady state (c.f, figures 4.1, 4.2, 4.3). We conclude that the dynamical behaviour of the system is richer when we have the two time delays in the model. Finally, to show the biological and epidemiological relevant of this research we have related our results to some known epidemics and our results showed that the models considered in this research can be used to model infectious diseases.

Bibliography

[Het81] H.W. Hethcote, H.W. Stech, P. Van den Driessche, *Periodicity and stability in epidemic models: A survey, in: S.N. Busenberg, K.L. Cooke (Eds.), Differential Equations and Applications in Ecology, Epidemics, and Population Problems*, Academic Press, New York, pp. 65-82, 1981.

[Coo79] K.L. Cooke, *Stability analysis for a vector disease model*, Rocky Mt. J. Math., 9(1), pp. 31-42, 1979.

[Alf12] B.O. Alfonso, D. Kay, and K. Burrage, *Fourier spectral methods for fractional in space reaction diffusion equations*, Journal of Computational Physics, 2012.

[Alt06] Sonia Altizer, Andrew Dobson, Parviez Hosseini, Peter Hudson, Mercedes Pascual and Pejman Rohani, *Seasonality and the dynamics of infectious diseases*, Ecology Letters,9: 467-484, 2006.

[Ari06] J. Arino, and P. van den Driessche, *Time delays in epidemic models: modeling and numerical considerations*, In: Arino, O., Hbid, M.L., Ait Dads, E. (Eds.), Delay Differential Equations and Applications, pp. 539-578. Springer, Berlin, 2006.

[Ari04] J. Arino, K.L. Cooke, van den Driessche, P., and J. Velasco-Hernandez, *An epidemiology model that includes a leaky vaccine with a general waining function*, Discrete Contin. Dyn. Syst. B 2, 479-495, 2004.

[Bal04] W.M. van Ballegooijen, and M.C. Boerlijst, *Emergent trade-offs and selection for outbreak frequency in spatial epidemics*, PNAS 101 (52) (2004) 18246.

[Ban10] M. Banerjee, *Self-replication of spatial patterns in a ratio-dependent predator-prey model*, Mathematical and Computer Modelling, 51(1-2), 2010.

[Bel89] E. Beltrami, *Mathematics for dynamic modeling*, Academic Press, N.Y,1989.

[Bel59] B. P. Belousov, *A periodic reaction and its mechanism*, Compilation of Abstracts on Radiation Medicine, 147:145, 1959.

[Ben11] M. Bendahmane, and M. Saad, *Mathematical analysis and pattern formation for a partial immune system modeling the spread of an epidemic disease*,Acta Appl. Math. 115 17-42, 2011.

[Ben93] D. E. Bentil and J. D. Murray, *On the mechanical theory for biological pattern formation*, Physica D: Nonlinear Phenomena, 63(1-2), 1993.

[Ber11] Edoardo Beretta, *An SEIR eidemic model with constant latency time and infectious period*, Mathematical Biosciences and Engineering Volume 8, Number 4, October 2011.

[Ber02] E. Beretta, and Y. Kuang, *Geometric stability switch criteria in delay differential systems with delay dependent parameters*, SIAM J. Math. Anal. 33 1144-1165, 2002.

[Ber01] E. Beretta, and Y. Kuang, *Convergence results in SIR epidemic models with varying population sizes*, Nonlinear Analysis, 28 (1997) 1909-1921.

[Bly10] K.B. Blyuss, and Y.N. Kyrychko, *Stability and Bifurcations in an Epidemic Model with Varying Immunity Period*, Bulletin of Mathematical Biology, 72: 490-505 2010.

[Bly08] K.B. Blyuss, and Y.N. Kyrychko, P. Hövel , and E. Schöll, *Control of unstable steady states in neutral time-delayed systems*, Eur. Phys. J. B 65, 571-576 2008.

[Bol96] B. M. Bolker and B. T. Grenfell, *Impact of vaccination on the spatial correlation and persistence of measles dynamics*, Proc. Natl. Acad. Sci. USA, 93(22):12648-53, 1996.

[Cai11] Y. Cai and W. Wang, *Spatiotemporal dynamics of a reaction diffusion epidemic model with nonlinear incidence rate*, Journal of Statistical Mechanics: Theory and Experiment, 2011.

[Can11] T. Canrong, Z. Ling, and Z. Lin, *Turing pattern formation in a predator prey mutualist system*, Nonlinear Analysis: Real World Applications, 2011.

[Can03] R. Cantrell, and C. Cosner, *Spatial Ecology via Reaction-Diffusion Equations*, Wiley, 2003.

[Cas01] C. Castillo-Chavez, B. Fred, *Mathematical models in population biology and epidemiology*, Berlin: Springer. ISBN 0-387-98902-1.

[Che05] G. Chen, J. Zhou, and S. Celikovsky, *On LaSalle's Invariance Principle and its Application to Robust Synchronization of General Vector Lienard Equations*, Automatic Control, IEEE 869-874, 50 (6) 2005.

[Che95] J. Chen, G. Gu and C.N. Nett, *A new method for computing delay margins of linear delay systems*, Systems and Control Letters 26(2), 107-117, 1995.

[Cob09] Coburn BJ, Wagner BG, Blower S., *Modeling influenza epidemics and pandemics:insights into the future of swine flu (H1N1)*, BMC Med, 7:30, 2009.

[Col07] C. Colijn, and M.C. Mackey, *Bifurcation and bistability in a model of hematopoietic regulation*, SIAM Journal on Applied Dynamical Systems, 378-394 (6), 2007.

[Col06] C. Colijn, A.C. Fowler, and M.C. Mackey, *High frequency spikes in long period blood cell oscillations*, Journal of Mathematical Biology, 499-519 (53), 2006.

[Col05(a)] C. Colijn, and M.C. Mackey, *A mathematical model of hematopoiesis-I: Periodic chronic myelogenous leukemia*, Journal of Theoretical Biology, 117-132 (237), 2005.

[Col05(b)] C. Colijn, and M.C. Mackey, *A mathematical model of hematopoiesis: II. Cyclical neutropenia*, Journal of Theoretical Biology, 133-146 (237), 2005.

[Coo99] K.L. Cooke, P. van den Driessche, and X. Zou, *Interaction of matiration delay and nonlinear birth in population and epidemic models*, J. Math. Biol.39 332-352, 1999.

[Coo97] K.L. Cooke, *Stability analysis for a vector disease model*, Rocky Mount. J. Math. 9 (1979) 253-263.

[Coo96] K.L. Cooke, and P. van den Driessche, *Analysis of an SEIRS epidemic model with two delays*, J. Math. Biol. (1996) 35: 240-260.

[Coo82] K.L. Cooke, and Z. Grossman, *Discrete delay, distributed delay and stability switches*, J. Math. Anal. Appl. 86,1982 592-627.

[Cou02] P. Coullet, *Localized Patterns and Fronts in Nonequilibrium Systems*, World Scientific, 2002.

[Cra06] R.V. CRASTER, *Spectral algorithms for reaction diffusion equations*, Technical Report, 2006.

[Cra91] J.D. Crawford, *Introduction to Bifurcation Theory*, Reviews of Modern Physics 63, 991-1037, 1991.

[Cros06] M. Cross,*Notes on the Turing instability and chemical instabilities*, Lecture note, Beijing Normal University, 2006.

[Cru09] V.D. Cruz, *Constructions of Lyapunov Functions for Classics SIS, SIR and SIRS Epidemic model with Variable Population Size*, Revista Electronica Foro Red Mat, 26, 2009.

[Cru99] I. Cruickshank, W. Gurney, A. Veitch, and T. Su, *The characteristics of epidemics and invasions with thresholds*, Theor. Popu. Biol. 56 (3) (1999) 279-292.

[Dav08] D.J.B. Lloyd and B. Sandstede *Localized hexagon patterns of the planar Swift Hohenberg equation*, University of Surrey e-publications, 2008.

[Die00] O. Diekmann, and J.A.P. Heesterbeek, *Mathematical Epidemiology of Infectious Diseases*, Model Building,Analysis and Interpretation, Wiley, New York, 2000.

[Dim09] B. Dimitri, S. Maset, and R. Vermiglio, *TRACE-DDE: a Tool for Robust Analysis and Characteristic Equations for Delay Differential Equations*,Springer Berlin Heidelberg: Lecture Notes in Control and Information Sciences Volume 388, 2009, pp 145-155

[Doe06] E. J. Doedel, B. Krauskopf, and H. M. Osinga, *Global Bifurcations of the Lorenz Manifold*, Nonlinearity 19, 2947-2972, 2006.

[Dri02] P. van den Driessche, and J. Watmough, *Reproduction numbers and subthreshold endemic equilibria for compartmental models of disease transmission*, Mathematical Biosciences, 180(1), 2002.

[Dri70] R. D. Driver, *Ordinary and Delay Differential Equations*, Springer-Verlag, New York, 1977.

[Dus04] Dushoff, J., Plotkin, J.B., Levin, S.A., Earn, D.J.D., *Dynamical resonance can account for seasonality of influenza epidemics*, Proc. Natl. Acad. Sci. 101, 16915-16916, 2004.

[Els73] L.E El'sgol'ts and S.B Norkin, *An introduction to the theory and application of differential equations with deviating arguments*, Academic press, New York, 1973.

[Ena12] Y. Enatsu, *Lyapunov functional techniques on the global stability of equilibria of SIS epidemic models with delays*, Research Institute for Mathematical stress recorded, 1792, 118-130..

[Fer01] N.M. Ferguson, C.A. Donnelly, and R.M. Anderson, *The foot-and-mouth epidemic in Great Britain: pattern of spread and impact of interventions*, Science 292 (5519) (2001) 1155.

[Fes07] N.V. Festenberg, T. Gross, and B. Blasius, *Seasonal forcing drives spatio-temporal pattern formation in rabies epidemics*, Math. Model. Nat. Phen. 2 (4) (2007) 63-73.

[Fil04] J.A.N. Filipe, and M.M. Maule, *Effects of dispersal mechanisms on spatio-temporal development of epidemics*, J. Theoret. Biol. 226 (2) (2004) 125-141.

[Fun05] G. Funk, V. Jansen, S. Bonhoeffer, and T. Killingback, *Spatial models of virus-immune dynamics*, J. Theoret. Biol. 233 (2) (2005) 221-236.

[Gie72] A. Gierer and H. Meinhardt, *A theory of biological pattern formation*, Biological Cybernetics, 12(1):30-39, 1972.

[Gre01] B.T. Grenfell, O.N. Bjornstad, and J. Kappey, *Travelling waves and spatial hierarchies in measles epidemics*, Nature 414 (6865) (2001) 716-723.

[Goc06] M.M. Gockenbach, *Understanding and Implementing the Finite Element Method*, SIAM, 2006.

[Gu05] K. Gu, S. Niculescu, and J. Chen, *On stability crossing curves for general systems with two delays*, mathematical analysis and applications, 2005.

[Gu03] K. Gu, V.L. Kharitnov, and J. Chen, *Stability of Time-Delay Systems*,Birkhauser, Boston, 2003.

[Gub02] Duane J. Gubler, *Epidemic dengue/dengue hemorrhagic fever as a public health, social and economic problem in the 21st century*, TRENDS in Microbiology Vol.10 No.2, 2002.

[Guc83] J. Guckenheimer and P. Holmes, *Nonlinear Oscillations, Dynamical Systems and Bifurcations of Vector Fields*, volume 42 of Applied Mathematical Sciences (Springer-Verlag, New York Inc., USA, 1983).

[Hai10] H. Brezis, *Functional Analysis,Sobolev Spaces and Partial Differential Equations*, Springer, 2010.

[Hal09] J.K. Hale, *Ordinary Differential Equations*, Dover Publications, USA, 2009. 79.

[Hal93] J.K. Hale, and W. Huang, *Global geometry of the stable regions for two delay differential equations*, J. Math.Anal. Appl. 178, (1993) 344-362.

[Hal69] J.K. Hale, *Ordinary Differential Equations*, John Wiley & Sons, New York, 79, 1969.

[Han09] Hanens Uecker, *A short ad hoc introduction to spectral methods for parabolic PDE and the Navier-Stokes equations*,Lecture given at the International Summer School Modern Computational Science Oldenburg Germany, August 16-28, 2009

[Has81] B.D. Hassard, N. D. Kazarinoff, and Y. N. Wan, *Theory and Application of Hopf Bifurcation, London Mathematical Society Lecture Notes Series*, Cambridge University Press, Cambridge, 1981.

[He03] D. He, and L. Stone, *Spatio-temporal synchronization of recurrent epidemics*, Proc. R. Soc. Lond. B 270 (1523) (2003) 1519-1526.

[Het00] H. W. Hethcote, *The mathematics of infectious diseases*, SIAM Review, 599-653(4), 2000.

[Het95] H.W Hethcote, and P. van den Driessche, *An SIS epidemic model with variable population size and a delay*, J. Math. Biol. 34, 177-194, 1995.

[Het91] H.W. Hethcote and P. van den Driessche, *Some epidemiological models with nonlinear incidence*, J. Math. Biol. 29:271-287, 1991.

[Hil07] F.M. Hilker, M. Langlais, S.V. Petrovskii, and H. Malchow, *A diffusive SI model with Allee effect and application to FIV*, Math. Biosci. 206 (1) (2007) 61-80.

[Hol94] E.E. Holmes, M.A. Lewis, J.E. Banks, and R.R. Veit, *Partial differential equations in ecology: spatial interactions and population dynamics*, Ecology 75 (1994) 17-29.

[Hos95] Y. Hosono, and B. Ilyas, *Traveling waves for a simple diffusive epidemic model*, Math. Model. Method. Appl. Sci. 5 (1995) 935-966.

[Ign12] R. Ignacio, *Topics in the Stability of Localized Patterns for some Reaction-Diffusion Systems*, PhD Thesis, The University Of British Columbia, 2012.

[Jam97] M.H. James, and J. Li, *Behaviour changes in SIS STD models with slective mixing*, Society for Industrial and Applied Mathematics, 1997.

[Jia09] L. Jiangguo, and S. Tavener, *Semi Implicit Spectral Collocation Methods for Reaction Diffusion Equations on Annuli*, Wiley Online Library (wileyonlinelibrary.com),2009.

[Jin14] Li Jing, Sun Gui-Quan and Jin Zhen, *Pattern formation of an epidemic model with time delay*, Physica A: Statistical Mechanics and its Applications, 403(100-109), 2014.

[Jin08] Q. Liu and Z. Jin, *Formation of spatial patterns in an epidemic model with constant removal rate of the infectives*, Journal of Statistical Mechanics: Theory and Experiment, 2008.

[Joh06] B. John, and E. Knobloch, *Localized states in the generalized Swift Hohenberg equation*, PHYSICAL REVIEW E 73, 2006

[Jon05] E.F. Jonathan, *Delay Differential Equation Models in Mathematical Biology*, PhD thesis, www.math.utah.edu/ forde/research/JFthesis/, 2005.

[Jor99] D.W. Jordan, and P. Smith, *Nonlinear Ordinary Differential Equations. An Introduction to Dynamical Systems*, (Oxford University Press, oxford, UK, 1999), 3rd edition. 317.

[Kad11] Abdelilah Kaddar, Abdelhadi Abta, Hamad Talibi Alaoui, *A comparison of delayed SIR and SEIR epidemic models*, Nonlinear Analysis: Modelling and Control, Vol. 16, No. 2, 181-190, 2011.

[Kad10] A. Kaddar, *Stability analysis in a delayed SIR epidemic model with a saturated incidence rate*, Nonlinear Analysis: Modelling and Control, Vol. 15, No. 3, 299-306, 2010.

[ker27] W.O. Kermack, and A.G. McKendrick, *A Contribution to the Mathematical Theory of Epidemics*, Proc. of Royal Soc., 1927.

[kha02] H. Khalil, *Nonlinear Systems*, Prentice Hall, Englewood Cliffs, NJ, 2002, 3rd edition.

[kim08] A.R Kimbir, and H.K Oduwole, *A mathematical model of HIV/AIDS transmission dynamics considering counselling and antiretroviral therapy*, J. of Modern maths. and statistic, 2(5) 2008.

[Kon95] S. Kondo, and R. Asai, *A reaction-diffusion wave on the skin of the marine angelfish pomacanthus*, Nature, 376:765-768, 1995.

[Kra63] N.N. Krasovskii, *Problems of the Theory of Stability of Motion*, Stanford University Press, Stanford, CA, 1963.

[kun93] Y. Kuang, *Delay Differential Equations with Applications in Population Biology*, Academic Press, New York,1993.

[Kuz04] Y.A. Kuznetsov, *Elements of Applied Bifurcation Theory*, volume 112 of Applied Mathematical Sciences (Springer-Verlag, New York, USA, 2004), 3rd edition.

[Kyr05] Y.N. Kyrychko, and K.B. Blyuss, *Global properties of a delayed SIR model with temporary immunity and nonlinear incidence rate*, Nonlinear Analysis: Real World Applications, 6 (2005) 495-507.

[Las76] J.P. LaSalle, *The Stability of Dynamical Systems*, SIAM, Philadelphia, PA, 1976.

[Las60] J.P. LaSalle, *Some Extensions of Liapunov's Second Method*, IRE Transactions on Circuit Theory CT-7, 520-527 1960. 324

[Li08] G. Sun, Z. Jin, Q. Liu and and L. Li, *Chaos induced by breakup of waves in a spatial epidemic model with nonlinear incidence rate*, Journal of Statistical Mechanics: Theory and Experiment, 2008

[Liu07] Q. Liu, and Z. Jin, *Formation of spatial patterns in an epidemic model with constant removal rate of the infectives* , J. Stat. Mech. 2007 P05002.

[Liu06] Q. Liu, and Z. Jin *Formation of spatial patterns in an epidemic model with constant removal rate of the infectives*, Journal of Statistical Mechanics: Theory and Experiment, 2006.

[Li00] B. Li, and Y. Kuang, *Simple food chain in a chemostat with distinct removal rates*, J. Math. Anal. Appl. 242 (2000) 75-92.

[Liu87] W. Liu, H.W. Hethcote, and S.A. Levin, *Dynamical behaviour of epidemiological models with nonlinear incidence rate*, J. Math. Biol. 25 (1987) 359-380.

[Liu86] W. Liu, S.A. Levin, and Y. Iwasa, *Influence of nonlinear incidence rates upon behaviour of SIRS epidemiological models*, J. Math. Biol. 23 (1986) 187-204.

[Llo04] A.L. Lloyd, and V.A. Jansen, *Spatiotemporal dynamics of epidemics: synchrony in metapopulation models*, Math. Biosci. 188 (1-2) (2004) 1-16.

[Lou01] J. Louisell, *A matrix method for determining the imaginary axis eigenvalues of a delay system*, IEEE Trans. Autom. Control 12, 2001.

[Ma09] Z. Ma, Y. Zhou, and J. Wu, *Modeling and Dynamics of Infectious Diseases*, Higher Education Press, Beijing, 2009.

[Mal08] H. Malchow, S.V. Petrovskii, and E. Venturino, *Spatiotemporal Patterns in Ecology and Epidemiology-Theory, Models, and Simulation*, in: Mathematical and Computational Biology Series, Chapman & Hall/CRC, Boca Raton, 2008.

[Mei11] Y. Jiang, L. Mei, and X. Song, *Global analysis of a delayed epidemic dynamical system with pulse vaccination and nonlinear incidence rate*, Applied Mathematical Modelling (35) 4865-4876, 2011.

[Mei09] H. Meinhardt, *The algorithmic beauty of sea shells*, Springer Verlag, 2009.

[Mez10] F. Mazenc, and M. Malisoff, *Strict Lyapunov Function Constructions Under LaSalle Conditions With an Application to Lotka-Volterra Systems*, Automatic Control, IEEE Transactions on 55, 841-854 2010.

[Min42] N. Minorsky,*Self-excited in dynamical systems possessing retarded actions*, J. Appl. Mech. 9, 1942.

[Mog02] S.M. Moghadas, and A.B. Gumel, *Global stability of a two-stage epidemic model with generalized non-linear incidence rate*, Math. Comput. Simulation 60 (2002) 107-118.

[Mul07] G. Mulone, B. Straughan, and W. Wang, *Stability of epidemic models with evolution*, Studies in Appl. Math. 118 (2) (2007) 117-132.

[Mur03] J.D. Murray, (2003). *Mathematical Biology: II: Spatial Models and Biomedical Applications*. Berlin: Springer.

[Mur02] J.D. Murray, *Mathematical Biology: I. An introduction*, third ed., Springer, 2002.

[Mur93] J. D. Murray, *Mathematical biology*, Springer-Verlag, New York, 1993.

[Mur81] J. D. Murray, *A pre-pattern formation mechanism for animal coat markings*, Journal of Theoretical Biology, 88(1), 1981.

[Mur75] G. D. Murray and A. D. Cliff, *A stochastic model for measles epidemics in a multi-region setting*, Trans. Inst. Brit. Geog., 2:158-174, 1975.

[Nag07] C. Nagaiah, *Adaptive Numerical Simulation of Reaction-Diffusion systems* Thesis Otto-von-Guericke University Magdeburg Germany, 2007.

[Neu01] C. Neuhauser, *Mathematical challenges in spatial ecology*, Notices Amer. Math. Soc. 48 (11) (2001) 1304-1314.

[Nic05] S. Niculescu,P. Fu, and J. Chen, *Stability switches and reversals of linear systems with commensurate delays: a matrix pencil characterization*, IFAC 2005 World Congress, Praha, Czech republic, 2005.

[Nic01] S. Niculescu, *Delay effects on stability: A robust control approach*, Lecture notes in control and information sciences No. 269, Springer, 2001.

[Nob74] J. V. Noble, *Geographic and temporal development of plague*, Nature, 250:726-728, 1974.

[Oku01] A. Okubo, and S Levin, *Diffusion and Ecological Problems*, Modern Perspectives, second ed., Springer, New York, 2001.

[Ost05] Ostfeld, R.S., Glass, G.E., Keesing, F., *Spatial epidemiology: an emerging (or re-emerging) discipline*, Trends Ecol. Evol. 20, 328-336, 2005.

[Pas05] M. Pascual, and F. Guichard, *Criticality and disturbance in spatial ecological systems*, TREE 20 (2) (2005) 88-95.

[Pie00] M. Pierre, and D. Schmitt, *Blowup in Reaction-Diffusion Systems with Dissipation of Mass*, SIAM, 2000.

[Pri68] I. Prigogine, and R. Lefever, *Symmetry breaking instabilities in dissipative systems II*, The Journal of Chemical Physics, 48:1695, 1968.

[Ras03] L. Rass, and J. Radcliffe, *Spatial Deterministic Epidemics*, American Mathematical Society, 2003.

[Ric09] Richard T. Gray, Kenneth W. Beagley, Peter Timms, and David P. Wilson, *Modeling the Impact of Potential Vaccines on Epidemics of Sexually Transmitted Chlamydia trachomatis Infection*, The Journal of Infectious Disseases, 199 1680-1688 (11), 2009.

[Rih12] Fathalla A. Rihan and M. Naim Anwar, *Qualitative Analysis of Delayed SIR Epidemic Model with a Saturated Incidence Rate*,Hindawi Publishing Corporation Int. J. of Dif. Eqn., 2012.

[Rob94] E. Robin, *Modelling Pattern Formation in Reaction-Diffusion Systems*, Master thesis, Copenhagen University, 1994.

[Ros11] R. Ross, *The prevention of malaria*, John Murray, 1911.

[Rua04] S. Ruan, and S.F Rami, *Dynamics of a two-neuron system with discrete and distributed delays*, Physica D 191 (2004) 323-342.

[Rua01] S. Ruan, *Absolute Stability, conditional stability and bifurcation in Kolmogorov-Type predator-prey systems with discrete delays*, Quarterly Journal of Applied mathematics, 2001.

[Rua99] J. Wei, S. Ruan, *Stability and bifurcation in a neural network model with two delays*, Physica D 130,(1999) 255-272.

[Saa11] M. Bendahmane, and M. Saad, *Mathematical analysis and pattern formation for a partial immune system modeling the spread of an epidemic disease*, Acta Appl. Math., 2011.

[Sah12] Sahu, G. P., and Dhar, J., *Analysis of an SVEIS epidemic model with partial temporary immunity and saturation incidence rate*, Applied Mathematical Modelling, 36(3), 908-923, 2012.

[Sai12] A. Said, *Numerical Evolution Methods of Rational Form for Reaction Diffusion Equations*, Ph.D thesis Carleton University, 2012.

[Sch02] A. Scherer, A. McLean, Brit., *Mathematical models of vaccination*, British Medical Bulletin 62 (187-199), 2002.

[Shi07] H. Shim, and J. H. Seo, *Improving LaSalle's Invariance Principle using Geometric Clues*, SICE-ICASE, International Joint Conference 5253-5255 2007.

[Sho08] M. B. Short, M. R. DOrsogna, V. B. Pasour, G. E. Tita, P. J. Brantingham, A. L. Bertozzi, and L. B. Chayes, *A statistical model of criminal behaviour*, Mathematical Models and Methods in Applied Sciences, 18(S1), 2008.

[Sun12(b)] G. Sun, Z. Jin, and L. Li, Mainul Haque and Bai-Lian Li, *Spatial patterns of a predator-prey model with cross diffusion*, Nonlinear Dynamics, 2012.

[Sun12(a)] G. Sun, *Pattern formation of an epidemic model with diffusion*, Nonlinear Dynamics, 2012.

[Sun10] G. Sun, Z. Jin, and L. Li and Bai-Lian Li, *Self-organized wave pattern in a predator-prey model*, Nonlinear Dynamics, 2010.

[Sun09] G. Sun, Z. Jin, Q. Liu, and L. Li, *Spatial pattern in an epidemic system with cross-diffusion of the susceptible*, Journal of Biological Systems, 17 (1) (2009) 1-12.

[Sun08] G. Sun, Z. Jin, Q.X. Liu, L. Li, *Chaos induced by breakup of waves in a spatial epidemic model with nonlinear incidence raten*, J. Stat. Mech. 2008 P08011.

[Sun07] G. Sun, Z. Jin, Q. Liu, and L. Li *Pattern formation in a spatial S-I model with non-linear incidence rates*, Journal of Statistical Mechanics: Theory and Experiment, 2007.

[Str94] S. Strogatz, *Nonlinear Dynamics and Chaos with Applications to Physics, Biology, Chemistry and Engineering*, Persus Books Publishsing LLC, USA, 1994.

[Tak10] G. Huang, Y. Takeuchi, W. Ma, and D. Wei, *Global Stability for Delay SIR and SEIR Epidemic Models with Nonlinear Incidence Rate*, Bulletin of Mathematical Biology, 2010.

[Tch12] Jean M. Tchuenche and Christinah Chiyaka, *Global dynamics of a time delayed SIR model with varying population size*, Dynamical Systems, Vol. 27, , 145-160 No. 2, June 2012.

[Tch09] Jean M. Tchuenche1, and Alexander Nwagwo, *Local stability of an SIR epidemic model and effect of time delay*, Math. Meth. Appl. Sci., 32:2160-2175 2009.

[Tho09] E. Thomas, *Surveys and Tutorials in the Applied Mathematical Sciences*, Springer Science+Business Media, 2009.

[Tri10] T.M. Pryer, *Recovery Methods for Evolution and Nonlinear Problems*, DPhil thesis University of Sussex, 2010.

[Tur52] A.M. Turing, *The Chemical Basis of Morphogenesis*, Biological Sciences, Series B, Philosophical Transactions of the Royal Society of London, 1952.

[Upa08] R.K. Upadhyay, N. Kumari, and V. Rao, *Modeling the spread of bird flu and predicting outbreak diversity*, Nonl. Anal.: RWA 9 (4) (2008) 1638-1648.

[Wan11] W. Wang, Y. Lin, H. Wang, H. Liu, and Y. Tan, *Pattern selection in an epidemic model with self and cross diffusion*, J. Biol. Sys. 19 19-31, 2011.

[Wan08] K. Wang, W. Wang, and S. Song, *Dynamics of an HBV model with diffusion and delay*, J. Theoret. Biol. 253 (1) (2008) 36-44.

[Wan07] K. Wang, and W. Wang, *Propagation of HBV with spatial dependence*, Math. Biosci. 210 (1) (2007) 78-95.

[Wan02] W. Wang, *Global Behaviour of an SEIRS Epidemic Model with Time Delays*, Applied Mathematics Letters (15) 423-428, 2002.

[Wei12] W. Weiming, Y. Cai, Mingjiang Wu, Kaifa Wang and Zhenqing Li, *Complex dynamics of a reaction diffusion epidemic model*, Nonlinear Analysis: Real World Applications, 2012.

[Wei11] W. Weiming, Y. Lin, H. Wang, H. Liu, and Y. Tan, *Pattern selection in an epidemic model with self and cross diffusion*, Journal of Biological Systems, 2011.

[Wei11] Z. Wenjie, and J. Wei, *Stability and Hopf bifurcation in a diffusive predator prey system with delay effect*, Nonlinear Analysis: Real World Applications, 12, 2011.

[Wan09] C. Wan, *Localized Patterns in the Gray Scott Model*, PhD Thesis The University of British Columbia, 2009.

[Wei08] H. Wei, X. Li, and M. Martcheva, *An epidemic model of a vector-borne disease with direct transmission and time delay*, J. Math. Anal. Appl. 342, (2008) 895-908.

[Who04] WHO, *World Health Organization*, World Health Report, 2004.

[Who03] WHO, *World Health Organization*, Fact Sheet 211, 2003.

[Wer02] WER, *Weekly Epidemiological Record*, Record 46, 381, 2002.

[Wod13] Wodarz, D., Z. Sun, J. W. Lau, and N. L. Komarova, *Nearest-Neighbor Interactions, Habitat Fragmentation, and the Persistence of Host-Pathogen Systems*, The American Naturalist 182 :E94-E111, 2013.

[Xin14] Lian Xinze, Lu Guichen and Wang Hailing, *Pattern Formation in a Bacterial Colony Model*, Abstract and Applied Analysis, 2014. http://dx.doi.org/10.1155/2014/149801

[Xu09] R. Xu, and Z. Ma, *An HBV model with diffusion and time delay*, J. Theoret. Biol. 257 (3) 499-509, 2009.

[Xue13] Tiantian Li, Yakui Xue, *Global Stability Analysis of a Delayed SEIQR Epidemic Model with Quarantine and Latent*, Scientific Research: Applied Mathematics, 4, 109-117, 2013.

[Yan10] D. YANKE, and R. XU, *A delayed SIR epidemic model with nonlinear incidence rate and pulse vaccination*, J. Appl. Math. and Informatics, 1089-1099 (5-6), 2010.

[Yan93] K. Yang, *Delay differential equations with applications in population dynamics*, Academic press, Inc, 1993.

[Ye14] Fan Ye, *Pattern formation of an epidemic model with cross diffusion*, Applied Mathematics and Computation, 228(311-319), 2014.

[Yon09] P. Yongzhen, L. Shaoying, G. Shujing, L. Shuping, and L. Changguo, *A delayed SEIQR epidemic model with pulse vaccination and the quarantine measure*, Computers and Mathematics with Applications (58) 135-145, 2009.

[Zha10] J. Zhang, J. Wang, and T. Su, *Bifurcation Analysis of A Delayed SIR Model*, International Conference on Computer Application and System Modeling ICCASM, 2010.

[Zha09] G. Sun, G. Zhang, Z. Jin, and L. Li, *Predator cannibalism can give rise to regular spatial pattern in a predator prey system*, Nonlinear Dynamics, 2009.

[Zha08] T. Zhang, and Z. Teng, *Global behaviour and permanence of SIRS epidemic model with time delay*, Nonlinear Analysis:Real World Applications, 1409-1424 (9), 2008.

[Zhu07] H. Zhu, and L. Huang, *Stability and bifurcation in a tri-neuron network model with discrete and distributed delays*, Applied Mathematics and Computation 188 (2007) 1742-1756.

[Zoh13] A. Zohreh, and S.M. Hosseini, *Numerical solution of two dimensional sine Gordon and MBE models using Fourier spectral and high order explicit time stepping methods*, Computer Physics Communications, 2013.

AppendixA

LaSalle's invariance principle

The LaSalle's invariance principle for global solutions of differential equations is an extension of the well-known Lyapunov's direct method and it's important in proving global stability for discrete and continuous dynamical systems. The method uses the notions of limit and invariance sets to obtain Lyapunov functional in a less restrictive way. For instance, the LaSalle's invariance method or principle removes the strict requirement that every Lyapunov functional U for continuous dynamical systems which are described by autonomous systems of ODEs must have a negative definite time premitive (derivative) for the systems to be asymptotically stable.

Theorem 5.1 (LaSalle's invariance principle)

Suppose the set $\Psi \cup D$ is a compact and positive invariant set with respect to the system of ODEs

$$\dot{y} = f(t).$$

And suppose furthermore that the functional U defined by $U : D \to \mathbb{R}$ is a continuously differentiable function and

$$\dot{U} \leq 0 \quad \text{on} \quad \Psi. \tag{5.1}$$

If $E = \{y \in \Psi : U(y) = 0\}$ and E^* (E^* is the steady state) is the largest invariant set in E, then every solution of the system of ODEs

$$\dot{y} = f(t).$$

that starts in the set Ψ tends E^* as time t tends infinity.

For more details on LaSalle's invariance principle see [Las60],[Las76],[Kra63],[Che05],[Shi07],[Mez10].

AppendixB

Theorem 5.2 (Comparison theorem for differential inequalities)
In the theory of differential equations, comparison theorems assert particular properties of solutions of a differential equation (or of a system thereof) provided that an auxiliary equation/inequality (or a system thereof) possesses a certain property. If

$$\dot{x}(t) \leq c_0 - c_1 x(t),$$

then

$$\lim_{t \to +\infty} \sup x(t) \leq \frac{c_0}{c_1},$$

where c_0 and c_1 are constants.